

# Enhanced Indoor Positioning Utilising Wi-Fi Fingerprint and QR Calibration Techniques

Abd Shukur Ja'afar

A thesis submitted to the  
Lancaster University for degree of  
Doctor of Philosophy

March 2017

# **Abstract**

## **Enhanced Indoor Positioning Utilising Wi-Fi Fingerprint and QR Calibration Techniques**

**Abd Shukur Ja'afar**

Submitted for degree of Doctor of Philosophy

March 2017

The growing interest in location-based services (LBS), due to the demand for its application in personal navigation, billing and information enquiries, has expedited the research development for indoor positioning techniques. The widely used global positioning system (GPS) is a proven technology for positioning, navigation, but it performs poorly indoors. Hence, researchers seek alternative solutions, including the concept of signal of opportunity (SoOP) for indoor positioning. This research planned to use cheap solutions by utilizing available communication system infrastructure without the need to deploy new transmitters or beacons for positioning purposes. Wi-Fi fingerprinting has been identified for potential indoor positioning due to its availability in most buildings. In unplanned building conditions where the available number of APs is limited and the locations of APs are predesignated, certain positioning algorithms do not perform well consistently. In addition, there are several other factors that influence positioning accuracy, such as different path movements of users and different Wi-Fi chipset manufacturers. To overcome these challenges, many techniques have been proposed, such as collaborative positioning techniques, data fusion of radio-based positioning and mobile-based positioning that uses sensors to sense the physical

movement activity of users. A few researchers have proposed combining radio-based positioning with vision-based positioning while utilizing image sensors.

This work proposed integrated layers of positioning techniques, which is based on enhanced deterministic method; Bayesian estimation and Kalman filter utilising dynamic localisation region. Here, accumulated accuracy is proposed with distribution of error location by estimation at each test point on path movement. The error distribution and accumulated accuracy have been presented in graphs and tables for each result.

The proposed algorithm has been enhanced by location based calibration with additional QR calibration. It allows not only correction of the actual position but the control of the errors from being accumulated by utilizing the Bayesian technique and dynamic localisation region. The position of calibration point is determined by analysing the error distribution region. In the last part, modification on Kalman filter step for calibration algorithm did further improve the location error compared to other deterministic algorithms with calibration point. The CDF plots have shown all developed techniques that provide accuracy improvement for indoor positioning based on Wi-Fi fingerprinting and QR calibration.

## **Declaration**

I declare that the material presented in this thesis consists of original work undertaken solely by myself and whenever work by other authors is referred to, it has been properly referenced. The material has not been submitted in substantially the same form for the award of a higher degree elsewhere.

**Abd Shukur Jaafar**

March 2017

## **List of Publications / Contributions:**

### Conferences and Journals:

1. A. S. Jaafar, “Enhanced Positioning Technique with QR Calibration” International Conference on Advances in Information Processing and Communication Technology – IPCT 15, Rome, Italy, April 2015.
2. A. S. Jaafar, G. Markarian, A.A.M. Isa, N. A. Ali, M. Z. A. Aziz, “Enhanced Integrated Indoor Positioning Algorithm Utilising Wi-Fi Fingerprint Technique” Journal of Telecommunication Electronic and Computer Engineering (JTEC) Vol 9, Issue 4, 2017.

## Acknowledgements

First and foremost, I am thankful to God the Almighty, the Beneficent, and the Merciful, without whom nothing is possible. My sincere appreciation and gratitude to my supervisor, Professor Garik Markarian for his invaluable help, guide, understanding, and encourage throughout my PhD study. Without his supervision, this thesis would not have been accomplished. I also greatly appreciate his care and concern not only for my study but also the well-being of my family and myself.

I want to thank Dr. Leila Musavian and Dr. Phillip Benachour for their advice and support during my years of study here. I am very thankful for my lab mates at Infolab21 for being great neighbours during the whole PhD course. Special thanks to P. M. Muhammad Syahrir Johal, Dr. Ivan Manuylov, Azliza, Dr. Song Lee, Cui Jing Jing and Su Bin Bin. I also would like to thank all the School of Computing and Communications staff members who have assisted me throughout my study here.

I also wish to thank my sponsor and my employer, Universiti Teknikal Malaysia Melaka (UTeM), who gave me opportunity to further my studies and also provided financial support.

I owe my deepest thank to my parents and parents-in-law especially my mother Maimunah Abd Kadir and my sister Dr. Nor Haslina Ja'afar who have sacrificed a lot for me during my years in Lancaster, U.K. I would also like to thank my beloved wife, Nur Alisa Ali, my hero M. Eirfan and my two daughters, A. Sofiyah and A. Shahirah who have always been by my side giving endless love, encouragement, and support through my tough times. This thesis is specially dedicated to them.

# Table of Contents

Abstract.....	ii
Declaration.....	iv
List of Publications / Contributions:.....	v
Acknowledgements.....	vi
Table of Contents.....	vii
Lists of Tables.....	x
List of Figures.....	xi
List of Abbreviations.....	xiii
CHAPTER 1: Introduction.....	1
1.1 Location-Based-Services.....	1
1.2 Fundamentals of Location and Positioning Techniques.....	1
1.2.1 Time of Arrival (TOA).....	2
1.2.2 Time Difference of Arrival (TDOA).....	3
1.2.3 Angle of Arrival (AOA).....	3
1.2.4 Signal Strength.....	4
1.2.5 Hybrid Measurement.....	5
1.3 Aims of the Research.....	5
1.4 Contributions of the Thesis.....	6
1.5 Structure of Thesis.....	7
CHAPTER 2: Overview of Positioning Technology.....	9
2.1 Wireless Positioning Technology Classification.....	9
2.1.1 Wireless Positioning System.....	9
2.2 Mobile Positioning System.....	12
2.2.1 Movement Based Positioning System.....	13
2.3 Vision-based Positioning.....	15
2.4 QR Code as Potential in Location Based Services.....	18
2.4.1 Generating Codes.....	19
2.5 Indoor Positioning Technique.....	24
2.5.1 Deterministic Techniques.....	29
2.5.2 Bayesian Estimation.....	31
2.5.3 Kalman Filter.....	33

2.6	Research on Wi-Fi Fingerprint Technique.....	34
2.7	Summary .....	39
CHAPTER 3: Setup and Measurement .....		40
3.1	Introduction .....	40
3.1.1	Building Layout.....	41
3.2	Simulation Tools.....	45
3.2.1	Vistumbler.....	45
3.3	Wi-Fi Deterministic Algorithm .....	47
3.4	Unplanned Environment and Influence Factors .....	49
3.5	Summary .....	57
CHAPTER 4: Indoor Positioning.....		58
4.1	Introduction .....	58
4.2	Bayesian Technique .....	58
4.3	Enhanced Weighted K-Nearest Neighbour (EWKNN).....	62
4.4	Design the Kalman Filter .....	65
4.5	Algorithm Description .....	66
4.6	Direction Movement and Number of Samples .....	72
4.6.1	Movement Direction from Point R to Point S .....	73
4.6.2	Movement Direction from Point S to Point R .....	82
4.7	Overall Results .....	90
4.8	Summary .....	93
CHAPTER 5: Enhanced Indoor Positioning Utilising QR Calibration.....		95
5.1	Introduction .....	95
5.2	Location Based Calibration (LBC).....	95
5.2.1	Algorithm Description .....	98
5.2.2	Results of Location Based Calibration (LBC) .....	102
5.3	Kalman Filter Modification on QR Calibration .....	111
5.3.1	Algorithm Description .....	111
5.3.2	Results of Location Based Calibration (LBC) with Kalman Filter .....	115
5.3.3	Overall Results .....	120
5.4	Summary .....	123
CHAPTER 6: Conclusion.....		124
6.1	Summary .....	124
6.2	Future Work.....	125
6.2.1	Applying Other Distance Calculation with Statistical information.....	126

6.2.2	Integration between Localisation Region and Clustering Techniques.....	126
6.2.3	Integrated Fingerprint with Triangulation Technique Utilising QR Calibration	127
References: .....		128

## Lists of Tables

Table 3.1: Accumulated accuracy for different values of K. ....	53
Table 3.2: Accumulated accuracy for different devices.....	55
Table 3.3: Accumulated accuracy for different path directions. ....	56
Table 4.1: Accumulated accuracy of average estimation vs Bayesian estimation.....	60
Table 4.2: Accumulated accuracy of different algorithms.....	91
Table 5.1: Accumulated accuracy comparison of algorithms with QR calibration. ....	120

## List of Figures

Figure 1.1: User target location using TOA measurements .....	2
Figure 1.2: Position location using TDOA measurements.....	3
Figure 1.3: Final target position using AOA measurements.....	4
Figure 2.1: General process for generating QR code .....	19
Figure 2.2: Data encoding process.....	21
Figure 2.3: QR code function pattern.....	23
Figure 2.4: Placement of data bits [57]. .....	23
Figure 2.5: Potential components for positioning. [60] .....	26
Figure 2.6: Two phases of fingerprinting: a) off-line phase b) on-line phase.....	28
Figure 2.7: Kalman filter algorithm .....	34
Figure 3.1: Layout of B floor, Infolab21, School of Computing and Communication, Lancaster University.....	42
Figure 3.2: Detailed position of APs ( $\emptyset_i$ ), reference points (RPs/ green dot), and direction path movement points (S, R). .....	43
Figure 3.3: RSSIs from different MAC address at one of TP location. ....	44
Figure 3.4: GUI of Vistumbler.....	45
Figure 3.5: Detailed information from the *.CSV file. ....	46
Figure 3.6: Monitoring RSSI level from one of AP available. ....	47
Figure 3.7: Comparison of errors for different distances $q$ . .....	48
Figure 3.8: Phases of Wi-Fi fingerprint deterministic technique: a) off-line phase b) on-line phase. ....	49
Figure 3.9: Direction of movement from point S to point R, and vice versa.....	50
Figure 3.10: Error distribution for nth TPs location for different numbers of K. ....	52
Figure 3.11: Error distribution for different devices based on K-NN algorithm (K=3).....	54
Figure 3.12: Location error estimated for different path directions based on K-NN algorithm (K=3).....	56
Figure 4.1: Average estimation (black dotted) vs. Bayesian estimation (red dotted) for each RSSI sample at TP 17. ....	59
Figure 4.2: Bayesian estimation vs average estimation. ....	60
Figure 4.3: Ratio of processing time for average and Bayesian estimation. ....	61
Figure 4.4: Flow chart of EWKNN.....	63
Figure 4.5: KNN (K=3) vs WKNN (K=3) vs EWKNN. ....	64
Figure 4.6: Indoor positioning concept .....	67
Figure 4.7: Dynamic shape changes in the localisation region depending on prior location. ....	69

Figure 4.8: Flow chart of the proposed algorithm.....	70
Figure 4.9: Error distribution for a Qualcomm Atheros Wi-Fi chipset with 25 RSSI samples. .	75
Figure 4.10: Error distribution for a Qualcomm Atheros Wi-Fi chipset with 50 RSSI samples.	76
Figure 4.11: Average RSSI distribution during offline phase and online phase.....	77
Figure 4.12: Accuracy map on layout building for Qualcomm Atheros chipset. ....	78
Figure 4.13: Error distribution for a Broadcom Wi-Fi chipset with 25 RSSI samples. ....	79
Figure 4.14: Error distribution for a Broadcom Wi-Fi chipset with 50 RSSI samples. ....	80
Figure 4.15: Average RSSI distribution during offline phase and online phase.....	81
Figure 4.16: Accuracy map on layout building for Broadcom chipset. ....	82
Figure 4.17: Error distribution for Qualcomm Atheros Wi-Fi chipset with 25 RSSI samples. ..	83
Figure 4.18: Error distribution for Qualcomm Atheros Wi-Fi chipset with 50 RSSI samples. ..	84
Figure 4.19: Average RSSI distribution during offline phase and online phase.....	85
Figure 4.20: Accuracy map on layout building for Qualcomm Atheros chipset .....	86
Figure 4.21: Error distribution for Broadcom Wi-Fi chipset with 25 RSSI samples.....	87
Figure 4.22: Error distribution for Broadcom Wi-Fi chipset with 50 RSSI samples.....	88
Figure 4.23: Average RSSI distribution during offline phase and online phase.....	89
Figure 4.24: Accuracy map on building layout for Broadcom chipset. ....	89
Figure 4.25: Performance positioning error comparison between proposed algorithm and several location estimation algorithms. ....	92
Figure 5.1: Block diagram of a combination of W-Fi fingerprint technique and QR vision-sensor-based calibration.....	96
Figure 5.2: Building layout and <i>localisation region</i> with QR calibration. ....	97
Figure 5.3: Flowchart of algorithm to enhance Wi-Fi fingerprint with QR calibration.....	100
Figure 5.4: Comparison of EWKNN with Bayesian estimation, basic K-NN and K-NN with Kalman Filter, without QR calibration. ....	103
Figure 5.5: The effect of QR calibration (at point 5) on three different algorithms. ....	104
Figure 5.6: Comparison of EWKNN with Bayesian estimation, basic K-NN and K-NN with a Kalman filter, without QR calibration. ....	105
Figure 5.7: The effect of QR calibration (at point 25) on three different algorithms. ....	106
Figure 5.8: Comparison of EWKNN with Bayesian estimation, basic K-NN and K-NN with Kalman Filter, without QR calibration. ....	107
Figure 5.9: The effects of QR calibration (point 25) on three different algorithms.....	108
Figure 5.10: Comparison of EWKNN with Bayesian estimation, basic K-NN and K-NN with Kalman filter, without QR calibration. ....	109
Figure 5.11: The effects of QR calibration (at point 5) on three different algorithms.....	109
Figure 5.12: Area location of QR code calibration.....	110
Figure 5.13: Kalman filter process with QR calibration. ....	112
Figure 5.14: Flowchart for algorithm enhancement with QR calibration and Kalman filter....	113
Figure 5.15: The effects of QR calibration (at point 5) on four different algorithms. ....	116
Figure 5.16: The effects of QR calibration (at point 25) on four different algorithms. ....	117
Figure 5.17: The effect of QR calibration (at point 25) on four different algorithms.....	118
Figure 5.18: The effect of QR calibration (at point 5) on four different algorithms.....	119
Figure 5.19: Performance positioning error comparison between the proposed algorithm and several location estimation algorithms with QR calibration. ....	122

## **List of Abbreviations**

2D	Two-Dimensional
3D	Three-Dimensional
AOA	Angle of Arrival
AP	Access Point
BS	Base Station
CIR	Channel Impulse Response
CPS	Cellular Positioning System
CPU	Central Processing Unit
DOA	Direction of Arrival
EWKNN	Enhanced Weighted K-Nearest Neighbour
FM	Frequency Modulation
GLONASS	Globalnaya Navigazionnaya Sputnikovaya Sistema
GNSS	Global Navigation Satellite Systems
GPS	Global Positioning System
GSM	Global System for Mobile Communications
GUI	Graphic User Interface
iOT	Internet of Things
K-NN	K-Nearest Neighbours
L&P	Location and Positioning
LBC	Location Based Calibration
LBS	Location-Based-Services
LLS	Linear Least Square
LOS	Line-of-Sight

LTE	Long Term Evolution
MAC	Media Access Control
MS	Mobile Station
MU	Mobile Unit
MBPS	Movement Based Positioning System
MEMS	Micro-machined Electromechanical Systems
NLOS	Non-Line of Sight
pdf	Probability Density Function
PDP	Power Delay Profile
PHY	Physical Layer
QR	Quick Response
RF	Radio Frequency
RFID	Radio Frequency Identification
RP	Reference Point
RSS	Received Signal Strength
RSSI	Received Signal Strength Indicator
SNR	Signal-to-Noise Ratio
SoOP	Signal of Opportunity
SSID	Service Set Identifier
TDOA	Time Difference of Arrival
TOA	Time of Arrival
TP	Test Point
UWB	Ultrawideband
VBP	Vision-Based-Positioning
VBPS	Vision-Based-Positioning System
WiMAX	Worldwide Interoperability for Microwave Access

WKNN	Weighted K-Nearest Neighbours
WLAN	Wireless Local Area Network
WPS	Wireless Positioning System
WSN	Wireless Sensor Network

# **CHAPTER 1: Introduction**

## **1.1 Location-Based-Services**

The increasing commercial interest in location-based services (LBS), especially in indoor environments has led to many developments in positioning techniques. Limitations of Global Positioning System (GPS), due to signal blocking by buildings, has made researchers look for alternative and innovative solutions to support LBS. LBS can be used in a variety of applications, including health services, entertainment, security, and pedestrian navigation.

Various types of communication technologies have been investigated, such as Wi-Fi, Bluetooth, radio frequency identification (RFID), FM radio frequency, cellular communication including GSM, WiMAX and LTE, and the use of sensors utilising magnetic fields. Among these technologies, the Wi-Fi has caught the attention of researcher due to the presence of wireless LAN spread in almost every building. The concern is to find an innovative positioning solution utilising data communication technology that is easy to access which in this case is Wi-Fi positioning. This chapter starts with an elaboration of fundamental concepts of location and positioning techniques.

## **1.2 Fundamentals of Location and Positioning Techniques**

There are a few different types of measurements used to determine user positions, despite the large number of positioning systems. These measurements are output from a measurement layer in hardware sensor devices and can be determined

using various parameters, such as received signal strength indicator (RSSI), time of arrival (TOA), time difference of arrival (TDOA), angle of arrival (AOA) and hybrids of these.

### 1.2.1 Time of Arrival (TOA)

TOA is a time-based method that is widely used in positioning technology. It is based on a trilateration approach [1], whereby the system measures the one-way signal propagation time and uses at least three transmitters to determine a user's position in a coplanar scenario. Here the assumption made is that the positions of all transmitter nodes are known. For a non-planar case, four transmitter nodes are required. Based on measurement of distance, the user's position is localised within a sphere of a certain radius  $R_i$  where  $R_i$  is proportional to the  $\tau_i$  with a receiver at the centre of the sphere. The position of the target user can be calculated by either the transmitter node/base station or user devices.

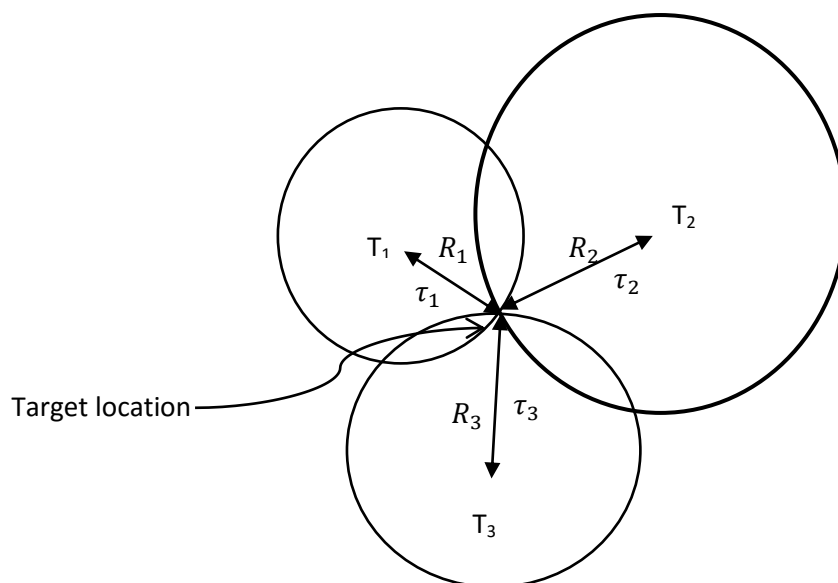


Figure 1.1: User target location using TOA measurements.

### 1.2.2 Time Difference of Arrival (TDOA)

TDOA estimation is a hyperbolic positioning technique that requires the measurement of difference in time between signals arriving from two transmitter nodes. It is similar to the TOA concept, and assumes that the positions of the transmitter or base nodes are known [2]. As illustrated in Figure 1.2, two TDOA measurements are required to localise a target node. The base nodes that first receive a signal from a user are considered as the reference base nodes. All TDOA measurements are made with respect to reference base nodes. A potential target location will be the intersection from two hyperbolae formed from TDOA measurements between (1-2) and (1-3), with reference to the base station.

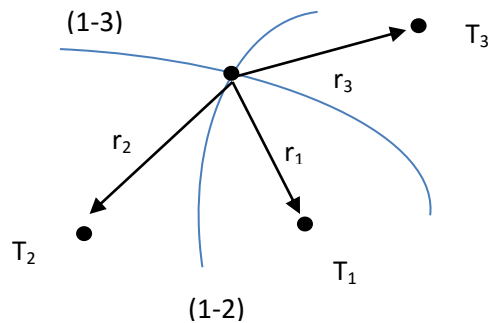


Figure 1.2: Position location using TDOA measurements.

### 1.2.3 Angle of Arrival (AOA)

AOA is basically estimated through the use of antenna arrays at the base station. Each antenna array should be equipped with RF front end components and this makes the system more complex, costly and power hungry. It does similar things to TOA and TDOA measurements so that the position of the transmitter node should be known in

the first stage. To determine the AOA, the main lobe of the antenna array is steered in the direction of the peak incoming energy of the arriving signal [3]. As shown in Figure 1.3 the intersection of directional lines of position (LOPs) defines the position of the target user.

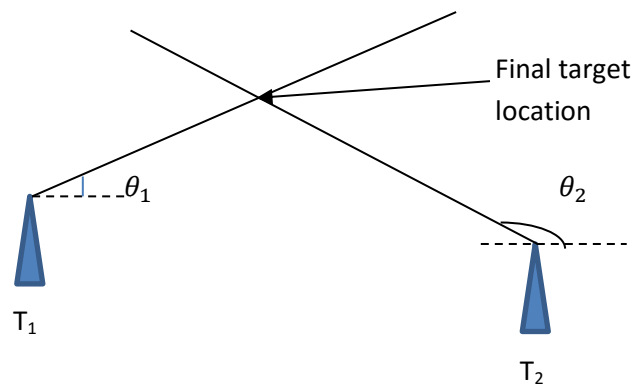


Figure 1.3: Final target position using AOA measurements.

#### 1.2.4 Signal Strength

Received signal strength indicator (RSSI) is a measure of the magnitude of the signal power at the target user's receiver in transmitter node. The strength of received signals indicates the distance travelled by the propagation signal. For many location applications, concerns about cost, hardware complexity and feasibility of the system make an RSSI-based method an attractive choice for positioning location in wireless networks. RSS values are always available in every wireless system without the need for extra hardware or modifications to the current system, making it a popular choice. This technique estimates the distance from transmitter to receiver by calculating path loss due to propagation.

### **1.2.5 Hybrid Measurement**

Each of the positioning measurements mentioned above has their own strengths and weaknesses, depending on where they are applied. To further improve positioning accuracy, being dependent on only one type of positioning measurement is not enough. Two or more related parameters are needed and these can be employed in order to obtain more information about the position target node. These are called the hybrid schemes and include the TOA/AOA [3][4], TOA/RSS [5], TDOA/AOA [6][7], TOA/TDOA [8].

Besides conventional TOA, TDOA, AOA and RSS parameters, and hybrid combinations, there is another scheme for positioning that includes a parameter that involves obtaining a multipath power delay profile (PDP) or channel impulse response (CIR) related to the received signal [8]. This kind of estimation can provide significantly more information, but commonly requires a database consisting of previous PDP/CIR estimates. Hence, the algorithms involved in PDP/CIR estimation usually include a training phase, then position estimation can occur.

## **1.3 Aims of the Research**

The importance of location-based services has caught many researchers' interest in indoor positioning. The purpose of this research is to utilise an existing communication system without spending on extra facilities to provide indoor positioning. Wi-Fi, in particular IEEE 802.11, standards are usually deployed in buildings for Internet access. For this reason, a Wi-Fi signal was chosen as the best possible candidate to perform localisation. The pattern of signal strength level from

various access points was studied and utilised to enhance location estimation accuracy. However, the current algorithm performance is not sufficient in terms of consistency. The scope of the research to improve existing techniques is based on a Wi-Fi fingerprint for indoor positioning. This was achieved by integrating several layers of positioning algorithms to get better consistency in positioning accuracy.

## **1.4 Contributions of the Thesis**

There are many techniques or approaches to determine a user's position, as explained by previous researchers [9][10][11]; however the Wi-Fi fingerprint technique has caught researcher's attention as it produces consistent and better accuracy [12][13]. This thesis focuses on the determination of a user's location, based on a Wi-Fi fingerprint technique and visual based calibration for indoor positioning. The design algorithms were carefully designed to fit and match the QR calibration to improve the whole location accuracy. The contributions made through this thesis are summarised as follows:

- i) Development of several integrated layers of indoor positioning algorithm consisting of dynamic deterministic location estimation (Enhanced Weighted K-NN), Bayesian approach under dynamic localisation region and Kalman filter to improve the effect of movement direction and different Wi-Fi chipset for indoor localisation.
- ii) Based on the algorithm from Part i), the author proposes enhanced integrated indoor positioning algorithm with QR calibration point to reduce accumulated error in indoor path movement.

- iii) Introduction of the accumulated accuracy on error distribution to determine the correct placement of QR calibration point for indoor positioning.
- iv) Proposes novel algorithm by combining previous algorithm from Part ii) with modification on Kalman Filter to suit QR calibration point to further improve accumulated accuracy and CDF for indoor navigation experience.

## **1.5 Structure of Thesis**

Each of the remaining chapters investigates a different aspect of solving the indoor positioning problem, they analyse each technique before drawing a conclusion about the effectiveness of various algorithms.

Generally, in Chapter 2, an overview of work on localisation and positioning that is specific to indoor positioning is given. The chapter gives an overview of basic location and positioning techniques and current solutions to Wi-Fi positioning, especially fingerprint techniques. This section highlights the categorization of general classification positioning based on such technologies as radio-based positioning and mobile-based positioning, and future trends based on vision-based positioning.

Chapter 3 describes the measurement setup and simulation environment. The chapter briefly describes the measurement of Wi-Fi signals, the layout plan and the limitations and assumptions made in this research. The concept of an off-line phase and an on-line phase in Wi-Fi fingerprinting is explained in detail. Furthermore, the terms reference point and test point are also elaborated. Suitable simulation tools for this research are discussed in this chapter on algorithm development and testing.

Then, Chapter 4 discusses basic Wi-Fi deterministic techniques as the first layer of localisation. Comparisons with a different kind of algorithm and additional

improvements to current Wi-Fi deterministic techniques are also presented. In addition, Bayesian estimation is explained in this chapter and the advantages of how implementing it in localisation helps with accuracy improvement. The effect on a number of RSSI samples when implementing Bayesian estimation is also discussed. Moreover, the effects of movement direction, different Wi-Fi chipsets, and algorithms themselves on positioning accuracy are also presented. Kalman filter was introduced into the end layer of localisation. This helps to reduce the presence of noise and instability in RSSI readings from various APs available in the building. Consequently, Kalman filter helped to reduce the differences in positioning estimation from one test point to another.

With a focus on calibration methods, Chapter 5 presents how current Wi-Fi algorithms can be improved via a combination of calibration techniques for dedicated path movement. This chapter starts with a brief introduction on how to generate QR code. The flow process for encoding QR code is briefly explained, and the advantages and popularity of using QR code in everyday life are also discussed. Furthermore, the results of utilising QR code as a calibration point for indoor positioning are also presented in the chapter. A modification algorithms to suit implementation of QR code in localisation is illustrated in detail as well. Simulations were conducted to evaluate the effectiveness of the algorithms proposed.

Finally, Chapter 7 concludes the thesis by summing up contributions of this work and proposes some possible future directions in the field of indoor wireless positioning.

## **CHAPTER 2: Overview of Positioning Technology**

### **2.1 Wireless Positioning Technology Classification**

With the increasing demand for location-based services (LBS), the research field of wireless positioning, specifically mobile positioning has become more active over the past fifteen years. This comprises research applications in various fields such as mobile positioning, vehicle navigation, emergency search and rescue, and tourist guides. In addition, position information becomes an important part of networking as network protocols can utilise this extra information to reduce routing overheads. Meanwhile, on the security side, position information is necessary for encryption and decryption to establish a secure channel. Recent advances in computing technology and sensing have inspired a new generation of integrated positioning systems. For instance, the current smartphones are equipped with many wireless modules and sensors, such as Wi-Fi module, GPS, gyro meter, image sensor and many other. Much of this potential can be utilised for the purpose of positioning. The potential for positioning can be classified into three areas [14]: traditional wireless positioning system (WPS), mobile positioning system, and vision-based positioning.

#### **2.1.1 Wireless Positioning System**

In wireless positioning system (WPS), the system involves a direct wireless network where the radio signal of a user is measured so that the user's position can be estimated by referring to network stations. The WPS includes the global navigation satellite system (GNSS), the well-known Global Positioning System (GPS), cellular

positioning system (CPS) from GSM to LTE network, wireless local area network (WLAN) positioning system, and wireless sensor networks (WSN) positioning system. Both GPS and CPS are suitable for outdoor, while the WLAN positioning system is preferred in indoor environments. WSN positioning system is typically used in an unknown environment where WSN nodes need to deploy before localisation can occur. From all these wireless technologies, which operate on their own dedicated frequency bands, the performance of WPS is entirely dependent on radio signal propagation conditions and environmental conditions. Non-line-of-sight (NLOS) radio propagation is the main cause of large positioning errors in CPS, from metres to hundreds of metres [14]. Furthermore, GPS and CPS signals can be blocked in closed environments, such as buildings, urban canyons and tunnels, which is a huge challenge in the location and positioning field.

A common infrastructure of WPS consists of a user target and beacons/ base stations/ transmitter nodes. User target and base stations measure radio signals within their communication range and the result of measurements are used to determine the distance between two transceivers. One of the early techniques called cell ID [2] is a simple position estimation that treats any position within the base station's communication range.

In WPS, a signal can be measured in term of signal strength, propagation time, and arriving angle of a radio signal. These measurement is needed for advanced location estimation techniques such as time of arrival (TOA) [15], time difference of arrival (TDOA) [16], received signal strength [17], and angle of arrival (AOA) [18], which is more accurate compared to the cell ID. Moreover, hybrid of advanced location estimation methods have been proposed, such as the hybrid TOA/TDOA [8] and hybrid AOA/TDOA [6][7]. Wireless positioning relies purely on radio signal measurement, and the performance of existing WPS depends heavily on signal propagation. The

condition of radio propagation can vary significantly. Two main factors influence positioning accuracy are NLOS propagation [19][20][21] and multipath effect [22]. Experiments on CPS based code-division multiple access have shown that in an urban area, building can cause NLOS and multipath propagation which can result in positioning errors as large as 588.971m [23]. In an indoor environment, NLOS obstacles comprise walls, doors, furniture and human bodies [9]. In WSN, positioning error is 7.0 m when the propagation signal is good but can rise to double positioning error in an NLOS condition [24]. However, it is a different case for ultrawideband (UWB) where it can work better in an NLOS condition. UWB is a radio communications system with a bandwidth more than 500 MHz. This high frequency can penetrate obstacles such as doors and walls, and this makes it possible to measure signals accurately via arriving time (TOA estimation) and arriving angle (AOA estimation). The precision of UWB-based positioning can be within 10 cm but in challenging environments, interference and multipath effects can reduce ranging precision by 12.6% [25]. In contrast, UWB only can be used for short-range communication, such as in indoor and body area networks.

In some cases, an obstacle can block the entire propagation signal between user target and base stations. This condition can happen to GPS and CPS users inside a tunnel or an urban canyon [26][27]. Sometimes GPS and CPS are unable to position a mobile user if the user measures the signal from less than four stations [28] (for 3-D plane) and less than three in a 2-D plane. This problematic condition is called a system outage. Other factors that can influence the performance of WPS based positioning are number of beacons, relative position of the user to beacons, antenna orientation, and time synchronisation.

## 2.2 Mobile Positioning System

To overcome the problems in wireless positioning systems (WPS), alternative positioning systems have recently been developed. These positioning systems do not depend on the measurement of propagation signals, rather they sense physical activity by target users and use physical information for positioning. To get the position of a user, the physical information needed is the user's movements and the surrounding environment. User movements can be measured with a motion sensor and a direction sensor, and this information is then processed through dead reckoning (DR) [29] and inertial navigation (IN) [30]. Compared to traditional WPS, the mobile positioning system has several advantages, as follows:

- Reliable – capable of working in any conditions, especially in places with limited wireless positioning.
- Accuracy – ranging from centimetres to a few metres.

The principles of DR and IN are based on extrapolating previous positions and displacement, including moving direction and distance. IN is grouped under DR methods that utilise inertial sensors to measure displacement in 3-D and 2-D. In 3-D, it is equipped with pitot tubes for space vehicles, while in 2-D it is used by vehicles [31] and pedestrians [32]. Lately, there have been improvements in positioning based on DR and IN. For instance, Liu and Lee [33] developed a simplified DR method and proposed using pseudobeacons that require distance information without common method direction information. J. Bojja et al. used a dead reckoning technique [34] and suggested positioning in 3D space with 3D map matching, where path information from a map is useful in positioning.

### 2.2.1 Movement Based Positioning System

In Movement Based Positioning System (MBPS), the measurement of displacement is done by two types of sensors: direction sensors and motion sensors. Magnetometer is a type of direction sensors that sense the earth's magnetic field, and gyroscopes measure angular frequency, such as magnitude and the speed at which a user changes direction.

A motion sensor includes an odometer, a pedometer and an inertia sensor. An odometer is usually a built-in feature in ground vehicles to measure moving distance. Meanwhile for pedestrians, a pedometer is mounted on the body with step length being estimated based on previous positions. Both an odometer on a ground vehicle and a pedometer mounted on a body use a dead reckoning technique to determine the position.

Another type of motion sensor is the inertial sensor. This positioning system is based on measuring displacement in 3-D and is usually called an inertial navigation system (INS). At the early stage, inertial sensors were mostly used for positioning in advance aviation and military industries [35]. Recent advances in sensors made with micro-machined electromechanical systems (MEMS) technology have successful miniaturised inertial sensors. Current inertial sensors are now widely used on vehicles and smartphones, offering great potential for LBS. By utilising the sensors on smartphones, extensive research is being done on pedestrian localisation and navigation [36],[37],[38],[39].

There are several advantages of utilising DR and IN with MBPS in positioning. MBPS can be used together with the WPS to improve positioning accuracy. Output data from DR and IR systems can reach about 50 to 100 data per second while GPS only updates each epoch, which is a second. For this reason, MBPS is suitable for high-

speed applications like missiles and space vehicles. A combination of GPS and MBPS usually uses data fusion techniques [40],[41],[42], and this can improve accuracy compared to standalone GPS.

Moreover, MBPS can be used in positioning in standalone mode as a backup to the main WPS. In certain scenarios, a user may move into an urban area or tunnel where the wireless signal is totally blocked. In this situation, MBPS will be the main positioning system and replace the WPS for a temporary period, until WPS can operate again. The accuracy of MBPS in standalone mode is influenced by three main factors:

- accuracy of initial position.
- accuracy of the sensor.
- design of data fusion algorithm.

Chen et al. [43],[44] demonstrated the integration of GPS/ INS with a Kalman filter and neural network, this can achieve errors of below 1 metre during a 40-second GPS outage.

Besides the great potential of MBPS for positioning systems, it faces numerous challenges. The first difficulty with MBPS is dealing with measurement errors from data collected by sensors. Measurement errors in MBPS come from two sources: first, the initial position given by WPS; and second, data collected from the sensors themselves. Sensor measurement errors are temporarily stable and bias is almost constant. These errors can accumulate during an iterative process and become large over time. Machine learning has been used to solve this kind of problem by implementing a Kalman filter in a linear condition [45][46]. System model and measurement noise statistics are the basis of a Kalman filter, the process being calculated iteratively. For a non-linear system, an extended Kalman filter (EKF) can be

implemented [47] and some systems use artificial intelligence (AI) technology, such as neural network (NN) or fuzzy logic [48][49][50].

### **2.3 Vision-based Positioning**

The latest positioning system that has caught researchers' intention is the vision-based positioning (VBP). VBP enhances positioning capability by using a vision/image sensor to capture pictures and compare them with the environment previously collected. In VBP, prior knowledge of the environment is crucial and information can be in the form of landmarks, maps and objects that can be used as references in a database. The VBP method captures certain images in a given location and uses image features to establish an environment model. Those image features also contain information about sensor movement, which can be used to compare with the database based on computer-vision theory. Generally, the key part of VBP algorithms is linked to tracking and features matching. Using image sensors, it is possible to get a continuous image that contains some fixed points referred to as feature points.

A Vision Based Positioning System (VBPS) usually consists of an image database and a processing unit for feature analysis to estimate the position. Each reference image is indexed to a location position. When an image from a user is received, it is processed by analyzing a query from an image database that has references images showing similar features. Then, it will return the exact position of the user. Basically VBPS can be grouped into two categories. The first group is called independent VBPS and the second group networked VBPS. The differences between independent VBPS and network VBPS are in the database storage. Independent VBPS keeps all reference images in a local image database while network VBPS relies on

image databases on Web servers. The advantage of independent VBPS is that it can work in standalone mode without any Internet connection, while the constraints of large images databases make them suitable for indoor positioning. Network VBPS utilises the unlimited storage of Web servers. Harlan et al. [51] have shown that by using a smartphone and an independent server, positioning accuracy can achieve up to 5 cm. Their study was limited to an indoor hallway without using any optimization algorithm. There are several advantages of network VBPS:

- the hardware cost on the user's part can be minimised as images are stored on Web servers;
- complex features analysis is run by Web servers instead of using the limited capability of user devices;
- crowdsourcing can be implemented, whereby mobile users can contribute images to Web servers.

Compared to MBPS, VBPS is much simpler because it is not required to use extra sensors, such as body-mounted sensors. It just utilises vision or image sensors already built into the smartphones of mobile users. However, the need to develop image database as references at first make it one of the drawback of VBPS. Several challenges have been highlighted by Liu et al. [14] as follows:

- Searching for images can be time-consuming because of the large number of images in a database;
- Another problem with VBPS is the low recognition rate, due to the absence of moving objects. Moving objects that appear in images could be vehicles, pedestrians or others. The absence of moving objects in the background can

make two images look different even though the images are actually of the same place.

- Image quality can be a problem because of distortion and blur. Continuous camera movement during localisation is often the main cause of blurry images. Matching features in a blurred image can be tough. For distorted images, feature points can be wrongly matched. Some research has been done to correct blurred and distorted images by using heuristic method particle swarm optimization to reverse the effect of motion [52]. These techniques require more time for processing and will not be suitable for VBPS at times.

## **2.4 QR Code as Potential in Location Based Services**

The use of Quick Response code or QR code is quite common at the moment [53]. It was first developed in Japan by Denso-Wave to solve a tracking component issue in the automotive industry. It became popular since it offers fast readability and greater storage-capacity modes: numeric, alphanumeric, binary and kanji. It includes the benefits of other barcodes, including the high data capacity of PDF417, the reduced space printing of Data Matrix and the high-speed reading of MAXI code [54].

QR Code covers a wider range of uses, from inventory control systems like stock maintenance and incoming raw materials to commercial tracking and ticketing, besides extensive use in labelling. Some become familiarised with it in more innovative ways, such as a library with QR code which directs users to download required information, placing giant QR code advertisements on top of buildings so that they can be viewed through Google Maps. Researchers from RMIT University and La Trobe University have used active RFID assisted by QR Code for sighted and blind pedestrian navigation in buildings [55]. RFID tags were placed at entrances, on corners and at selected points to help determine a current user's location. QR code was placed along with RFID tags in entrances and at selected points of interest to help sighted people by giving information for navigation purposes.

### 2.4.1 Generating Codes

Nowadays, QR code can be generated through free or paid websites, and via applications of different sizes depending on information size. It seems easy to produce label code, but there is quite a complex and complete system involved, before black and white square geometry can be used. There are seven levels of information that need to be gone through before it is converted to QR code, as shown in Figure 2.1.

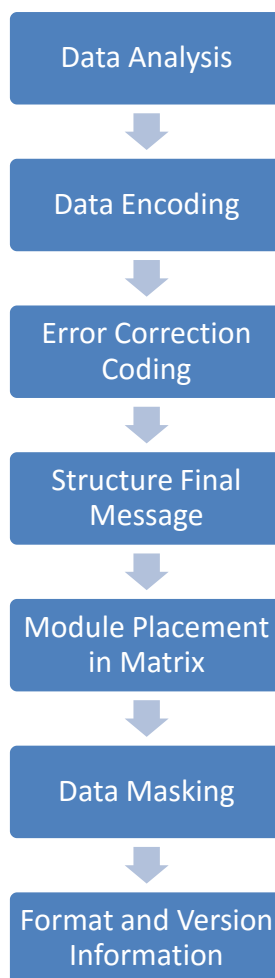


Figure 2.1: General process for generating QR code

## Data Analysis:

The QR code has four modes for encoding the text which are:

- Numeric mode.
- Alphanumeric mode.
- 8-bit byte mode.
- Kanji and kana characters mode.

As the first step, before starting to encode text, data analysis needs to be performed to determine which mode is the most suitable and optimal for text, depending on whether it is in numeric, alphanumeric, byte or kanji mode.

## Data Encoding:

At this stage, data encodings aim to create the shortest possible strings of text characters. A few steps need to be taken before this level. Figure 2.2 shows the data encoding process consists of five stages. The first stage is the error correction level. There are four levels of error correction, which are L: about 7% recovery, M about 15% recovery, Q about 20% recovery and H about 30%. Error correction is based on Reed-Solomon error correction [56] which is used for recovering messages whenever parts of the QR code is dirty or blocked. The number of text characters will determine the size of the QR code, which is called the version. This version runs from 1 to 40, where each version is 4 pixels larger than the previous one. The smallest version is 21 x 21 pixels and the largest 177 x 177 pixels. After that, a four-bit mode indicates whether it is in numeric, alphanumeric, byte or kanji mode and is added to the encoded data. At the end of this stage there is a string of bits that is broken up into 8-bit-long data codewords.

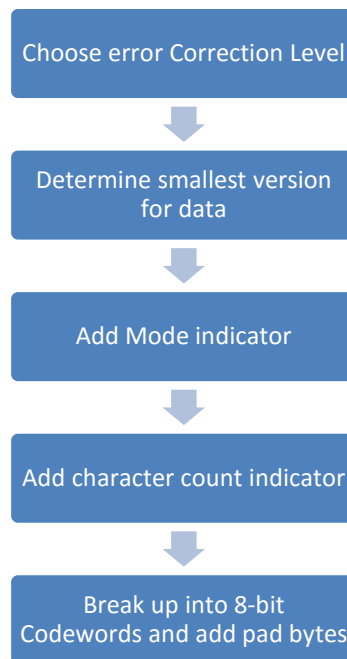


Figure 2.2: Data encoding process.

The next stage is error correction coding. One of the reasons why QR code is so popular is because of its robustness, and error correction coding plays an important role here. After the text has been converted into a string of data bits, these bits are used to generate error correction codewords through a process called Reed-Solomon error correction [56]. During the scanning process, all data codewords of text information and error correction codewords are read by scanners. A scanner can determine whether it has read the information correctly or not by comparing data codewords and error correction codewords. Errors can be corrected if scanners have not read the data correctly, depending on which recovery level was set earlier during QR code encoding. This is important for situations when a QR code label is not in good condition, whether it is dirty, pale or part of the code is blocked during scanning. The higher the recovery level that is set earlier, the less information can be encoded and the more QR code is immune to errors.

For the structure of the final message section, larger data codewords from the previous section need to be broken up into smaller blocks, and at the same time each block needs to have its own error correction codewords. Therefore, data block and error correction codewords must go through an interleaving process according to the QR code specification [57].

After arranging all the data and error correction codewords in the correct sequence, all the bits must be placed in a QR code matrix in a specific way. Before bit placement can occur, the function pattern needs to be given more priority. The function pattern includes:

- A finder pattern which is three blocks in the top right, top left and bottom left corners of the QR code;
- Separate areas of white space alongside the finder pattern;
- Alignment patterns which are used in version 2 and larger;
- A dark module which is a single black module placed beside the bottom left finder pattern.

A detailed explanation on how to set up a function pattern can be found in the previous works [54],[57]. Figure 2.3 shows QR code with four essential function patterns, as explained earlier.

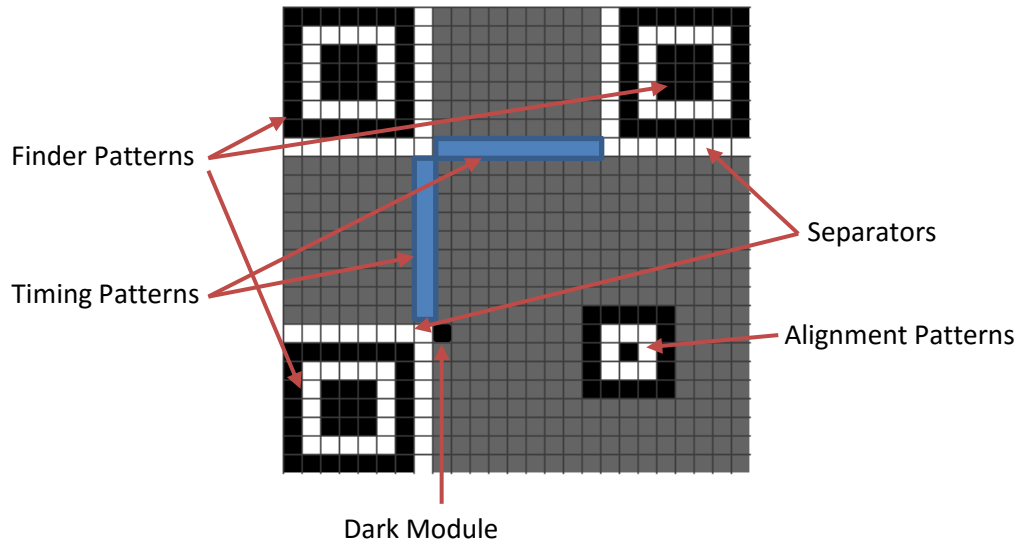


Figure 2.3: QR code function pattern.

After the main function pattern has been placed in a QR code matrix, the data bits can be placed in the empty space remaining by moving upwards and downwards in the columns repeatedly, as depicted in Figure 2.4.

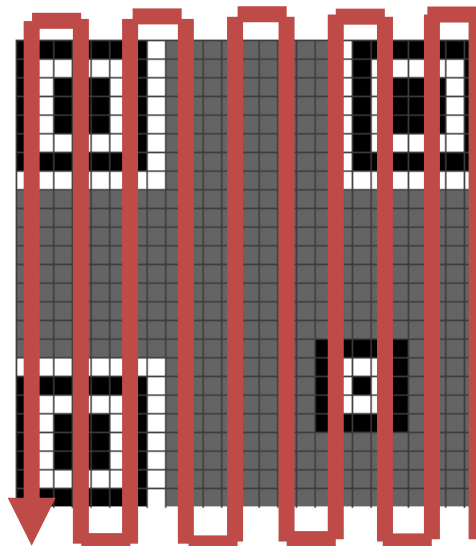


Figure 2.4: Placement of data bits [57].

Now, all the four function patterns, data blocks and error codewords have been placed into a QR code matrix. Certain patterns in QR code matrices are quite difficult to be read by the scanner. To overcome this challenge, the next stage is to perform data masking according to eight types of mask patterns, depending on which is most suitable. This data masking, only of data blocks and error codewords, will change the QR code to a particular pattern. A suitable data masking pattern can be determined by evaluating a masked matrix based on penalty rules. Details on QR code can be referred here [54], [57].

## **2.5 Indoor Positioning Technique**

Recently, indoor location based services (ILBS) has caught the attention of many researchers due to its potential social and commercial value in the future. However, getting a user's position in an indoor environment is a huge challenge for several reasons. A building's complex structure and geometry mean signals are transmitted in a non-line-of-sight (NLOS) condition. In the worst case, it is not possible to depend on the main satellite positioning system (GPS) because the GPS signal is totally blocked by the building's structure. The presence of furniture inside buildings can be a further obstacle to signal propagation and this too contributes to the degradation of positioning accuracy. Even changes to the environment inside a building can lead to different levels of error location. Another challenge is fluctuation in the signal itself and the presence of noise, which is also a challenge when developing an algorithm for indoor positioning. In spite of the many problems mentioned above, indoor positioning needs high accuracy compared to outdoors. Even location error of

just above 5 metres can lead to a different room or space, and this is a challenge to algorithm development in this field.

GPS signal cannot penetrate well in an indoor field, which means researchers look for alternative communication systems. There are some unique solutions for indoor positioning, for example the work which used beacons or an extra transceiver in order to get a user's position [58],[59]. Other systems use body-mounted sensors to calculate stride length in order to improve positioning accuracy. These extra devices are not favoured by customers because there is an extra cost to deploy them. Due to this, the penetration of indoor positioning implementation into society is quite slow and none of the proven indoor positioning techniques has become a standard. Researchers in this field are looking to solve this problem by developing positioning systems that are capable of offering both high indoor positioning accuracy and cheap solutions. To achieve both points mentioned, people look for any possible communication systems that are available, and reliable sensors that can be manipulated to achieve indoor positioning goals.

P.D Groves et al. [27], [60], [61] highlight the potential components of a multisensory integrated navigation system, as shown in Figure 2.5. Besides the potential of components and sensors that could be used for positioning and navigation, they highlighted the context where particular users behave in environments in certain ways. This provides extra information to improve accuracy in positioning and navigation. The third future trend is opportunistic navigation. This refers to signals of opportunity (SoOP) [62], [63] which is a system designed for non-positioning purposes that can be exploited for positioning purposes. These include Wi-Fi signals, broadcast TV signals and magnetic anomalies. Often, SoOP needs a development database to work effectively in positioning. The last point to be highlighted is cooperative positioning between systems where data are shared and exchanged among positioning

systems to help improve positioning accuracy. P.D. Groves [60] has shown all the potential in detail, of components that can be utilised for positioning and navigation to target pedestrian and car navigation.

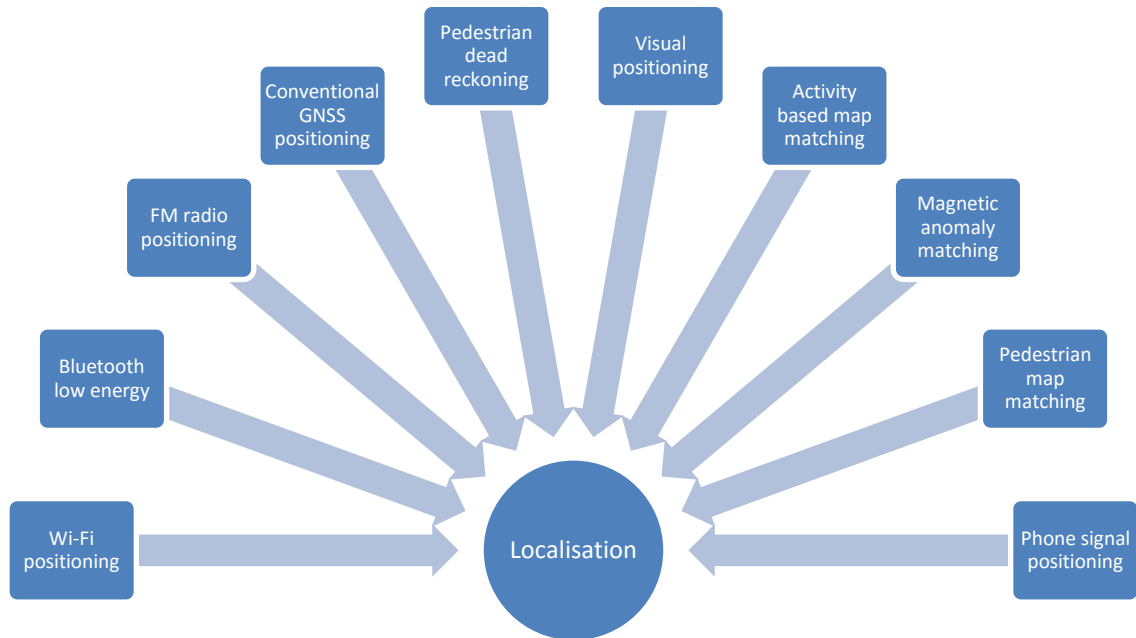


Figure 2.5: Potential components for positioning. [60]

Among the listed potential positioning technologies highlighted in Figure 2.5, Wi-Fi positioning and visual-based positioning is the most interesting, which is more suitable for indoor environment and the combination of these two groups still leaves much to explore. Besides Wi-Fi positioning, many other potential indoor positioning technologies have been explored, including Bluetooth [64],[65], FM radio positioning [66],[63], ultrasound [67], magnetic field [68][69], ultrawideband [70] and RFID [71],[72]. Wi-Fi has caught the attention of many researchers and industries [73] , [74] for these several factors:

- Almost each building is deployed with wireless LAN (WLAN) and most smartphones nowadays are equipped with a Wi-Fi chipset;

- The typical range of a Wi-Fi access point is up to 50 m indoors, unlike other technologies like UWB, Bluetooth and RFID, so this is another reason why it is most suitable for indoor positioning;
- The third reason to implement Wi-Fi positioning is that it is very cost-effective. There is no additional infrastructure, like beacons or transceiver nodes, that needs to be deployed and this makes Wi-Fi positioning the preferred choice.

Conventional techniques for localisation using TOA and DOA are based on trilateration and triangulation and require line-of-sight measurement. Although we can use this conventional technique in an indoor environment, to solve the NLOS condition is complex, with many aspects to consider, such as geometry of the building, materials used, location of furniture and items in the building, and location of Wi-Fi access points themselves [75][76]. In the NLOS condition, the signal might face various phenomena, e.g. reflections, multipath and shadowing. Wi-Fi fingerprinting has become a popular choice where positions are characterised by signal-strength patterns. One reason is because it does not require time or angle measurement, even when the exact location of an access point is not known.

Conventional Wi-Fi fingerprinting consists of two phases: an offline phase (survey) or ‘training phase’ and a second phase called the online phase (query) or ‘positioning’ phase. During the offline phase, a site survey is conducted to build a radio map of vectors of received signal strength indicators (RSSI) from all access points (AP) available at a certain known reference position (RP). All the RSSI, RP, location and AP information is then stored in a database for reference in the online phase. In the online phase, a user in a certain location will query their location by collecting samples of RSSI and comparing them with data in the database; then, the closest ‘match’ will

return the position of the user. Figure 2.6 depicts the whole process of Wi-Fi fingerprinting.

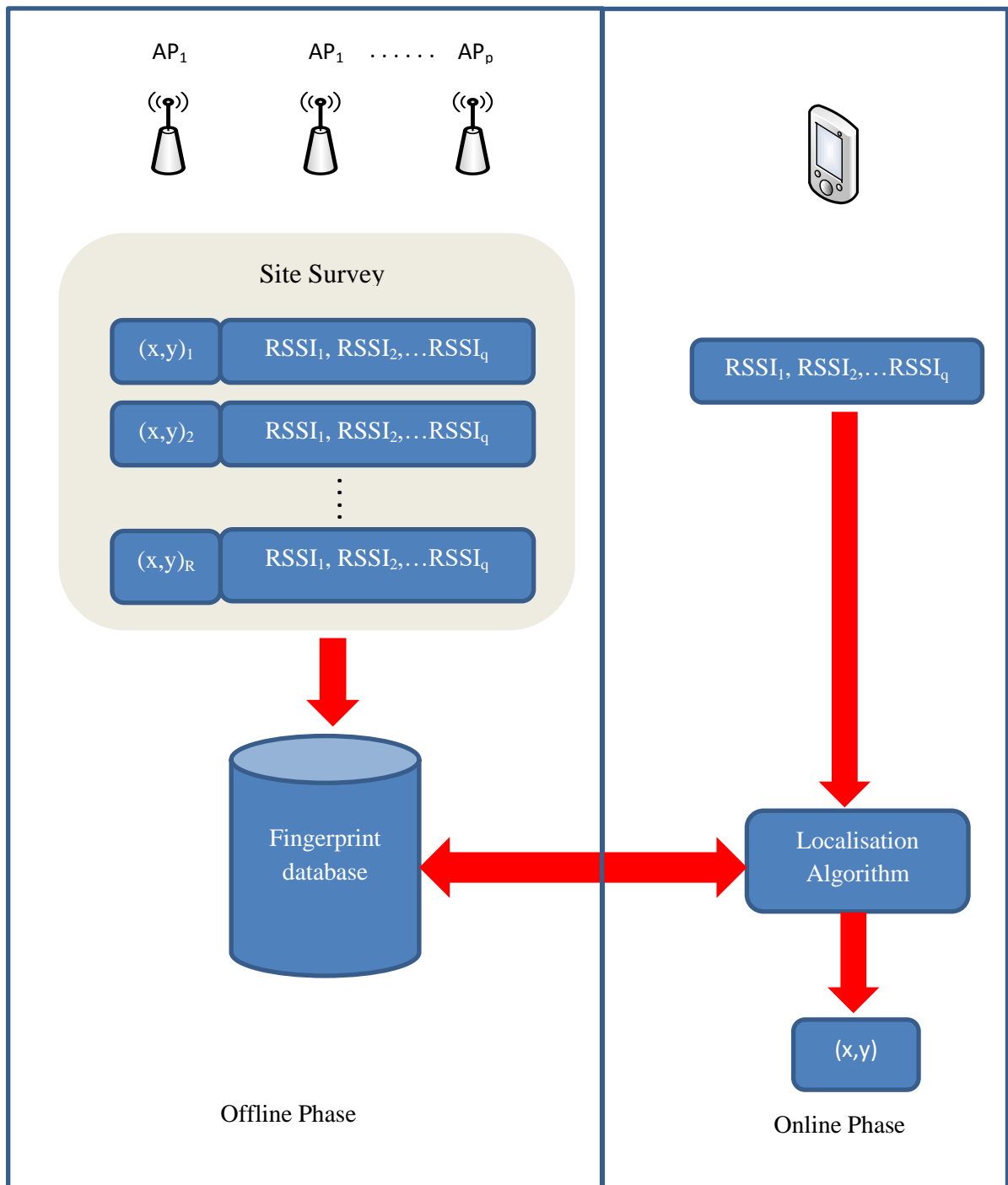


Figure 2.6: Two phases of fingerprinting: a) off-line phase b) on-line phase.

Wi-Fi indoor localisation algorithms can be divided into two main approaches. The first approach is called a deterministic technique while the second method is called a

probabilistic technique. The probabilistic approach consider the location estimation as a machine learning problem where the input models are the distributed signal strength in geographical area location [77]. However, Li et al. [12] have shown that fingerprint deterministic accuracy is quite close to the probabilistic technique with reduced complexity. The principles of Wi-Fi fingerprinting will be elaborated in the next sub-topics.

### 2.5.1 Deterministic Techniques

As aforementioned, the first Wi-Fi indoor localisation algorithms are called a deterministic technique. The deterministic algorithm uses a similar metric to differentiate between online signals and a radio map in the database. The space distance of each RSSI vector in the database is checked and compared to the sample RSSI during the online phase and the closest distance in signal space will return the user's location. Euclidean distance is a popular choice [78][79] to determine how far it is between RSSIs during localisation and RSSIs on radio map.

#### 2.5.1.1 K-Nearest Neighbours (KNN)

K-nearest neighbours (K-NN) is a deterministic algorithm [80] that returns the nearest neighbours (RP location) in term of signal space to the user. The basic distance space can be calculated as follows:

$$D_q = \left( \sum_{i=1}^n |s_i - S_i|^q \right)^{\frac{1}{q}} \quad (2.1)$$

where  $s_i$  is the RSSIs from the positioning phase, and  $S_i$  is the RSSIs from the database. The variable  $q$  depends on which distance the technique prefers and  $q=2$  is the Euclidean distance. Even though it is less accurate compared to the probabilistic algorithm, it is still preferred by many researchers for its low complexity in computation. Li et al. [12] have shown that the positioning accuracy of the deterministic algorithms is acceptable and not far from the probabilistic algorithm. K-NN depends heavily on the granularity of RP space. The more RPs there are in the coverage area, the more accurate the positioning accuracy. Nevertheless, this is labour-intensive during a site survey. So, there has to be a balance between these two factors. Some researches to solve this problem are highlighted in the next sub-chapter. Computation of the position of a user depends on average  $k$ -selection, as shown below:

$$\hat{x} = \frac{1}{k} \sum_{i=1}^k p_i \quad p_i \in D_{1:k} \quad (2.2)$$

### **2.5.1.2 Weighted K-Nearest Neighbours (WK-NN)**

WK-NN is an improvement over basic K-Nearest Neighbour (K-NN) [1]. The main idea of this improvement is to add a weighted sum to the fingerprint location as follows:

$$\hat{x} = \frac{1}{\sum_{j=1}^k w_j} \sum_{i=1}^k w_i p_i^k, \quad p_i^k \in D_k^n \quad (2.3)$$

where  $w_i$  is a weighting factor and can be calculated as the reciprocal of the distance between RSSI vectors in the online and offline phases.

## 2.5.2 Bayesian Estimation

Bayesian estimation is one of the methods that include the prior information of the situation and combine it with evidence from information contained in that sample. Deterministic methods give reasonable positioning accuracy, as described in the previous section. During the online phase, at each test point location, the Wi-Fi module collects RSSI information from the APs. The more RSSI data collected, the better the positioning accuracy. However fluctuations in RSSI readings translate into fluctuations in user position, and even though more data are collected, overall accuracy sometimes does not guarantee improvements in positioning accuracy. One reason is that each RSSI measurement is independent from the next measurement in a deterministic approach, and some valuable information is not exploited or used to improve positioning accuracy. Instead of applying simple average estimation, the Bayesian estimation approach considers other information, such as state and observation conditions which are useful to enhance positioning accuracy. The Bayes rule can be written as [81]:

$$p(s|x) = \frac{p(x|s) \cdot p(s)}{p(x)} \quad (2.4)$$

where  $s$  is state location,  $x$  is observation which in this case is RSSI data,  $p(s|x)$  is a posterior estimate of state, and  $p(x|s)$  is the likelihood of an observation's given state condition. The Bayes rule can be translated as the probability of being at location  $s$  given that observation  $x$  data are equal to the probability of observing  $x$  data at location state  $s$  and being at location state  $x$  in the first place, divided by the probability of getting observation data  $x$ .

Hence, the possible state location around the true state has to be determined and the state which is the most believable state gives us the true state. Here, the lookup table was checked to determine the possible surrounding state for each state location. The geometry of the building, which has various shapes, indicates that the surrounding possible state is different in numbers to the other true state location. The function of a normal distribution function is given by:

$$p(x) = \frac{1}{\sigma\sqrt{2\pi}} e^{-(x-\mu)^2/(2\sigma^2)} \quad (2.5)$$

Since the mean of  $p(x|s)$  is  $s$ ,  $\mu = s$  can be substituted which suggests that

$$p(x|s) = \frac{1}{\sigma\sqrt{2\pi}} e^{-(x-s)^2/(2\sigma^2)} \quad (2.6)$$

where  $x$  in this case is the observation or RSSI data and  $s$  is the state or location itself. For a higher dimensional condition, multivariate Gaussian distribution was used as the location in this situation is in two dimensions and consists of planes X and Y. Then, the density function of multivariate Gaussian distribution is given by:

$$p(x_1, \dots, x_k) = \frac{e^{\left(-\frac{1}{2}(x-\mu)^T \Sigma^{-1} (x-\mu)\right)}}{\sqrt{(2\pi)^k |\Sigma|}} \quad (2.7)$$

where  $x$  is a  $k$ -dimensional column vector,  $\Sigma$  is a covariance matrix, and  $|\Sigma|$  is the determinant of the covariance matrix. The equation can then state  $x$  and  $y$  locations for a two-dimensional position and  $k$  will be equal to 2.

### 2.5.3 Kalman Filter

The Kalman filter has been extensively used in estimating the state condition of a process. It has been widely applied in various fields like navigation, tracking object, control systems, robotic motion planning, computer vision and many more.

Outdoor positioning such as GPS gives high accuracy as long as a mobile terminal's line of sight is not blocked. On the other hand, there is no standard or proven solution yet for indoor positioning. Wireless Local Area Network (WLAN) has caught many researchers' attention as it is widely deployed in buildings. The main purpose of this technology is to design for wireless data communication and so it does not include anything specific for positioning or navigation. One of the main challenges when dealing with Wi-Fi signals is inaccuracy in measuring signals due to the presence of noise in sensors and systems. After applying a deterministic positioning estimation algorithm to Wi-Fi RSSIs signals, the next way to improve positioning accuracy is by applying a Kalman filter with certain assumptions being made.

Figure 2.7 depicts the general step of Kalman filter algorithm. It consist of several iterative processes including the prediction of state and error covariance, measurement updates with computation of Kalman gain and an estimation process, and lastly there is computation of error covariance which indicates how accurate estimates are. The Kalman filter structure has one measurement input  $Z_k$  and one estimation output  $\hat{X}_k$ . There are four system model A, H, Q, and R. A is the state transition matrix, H is the state to measurement matrix, Q is the covariance matrix of transition noise, and R is the covariance matrix of measurement noise. In step III,  $K_k$  is the Kalman gain which depend on  $P_k$  error covariance. Error covariance indicates the difference between Kalman filter estimation and the true value.

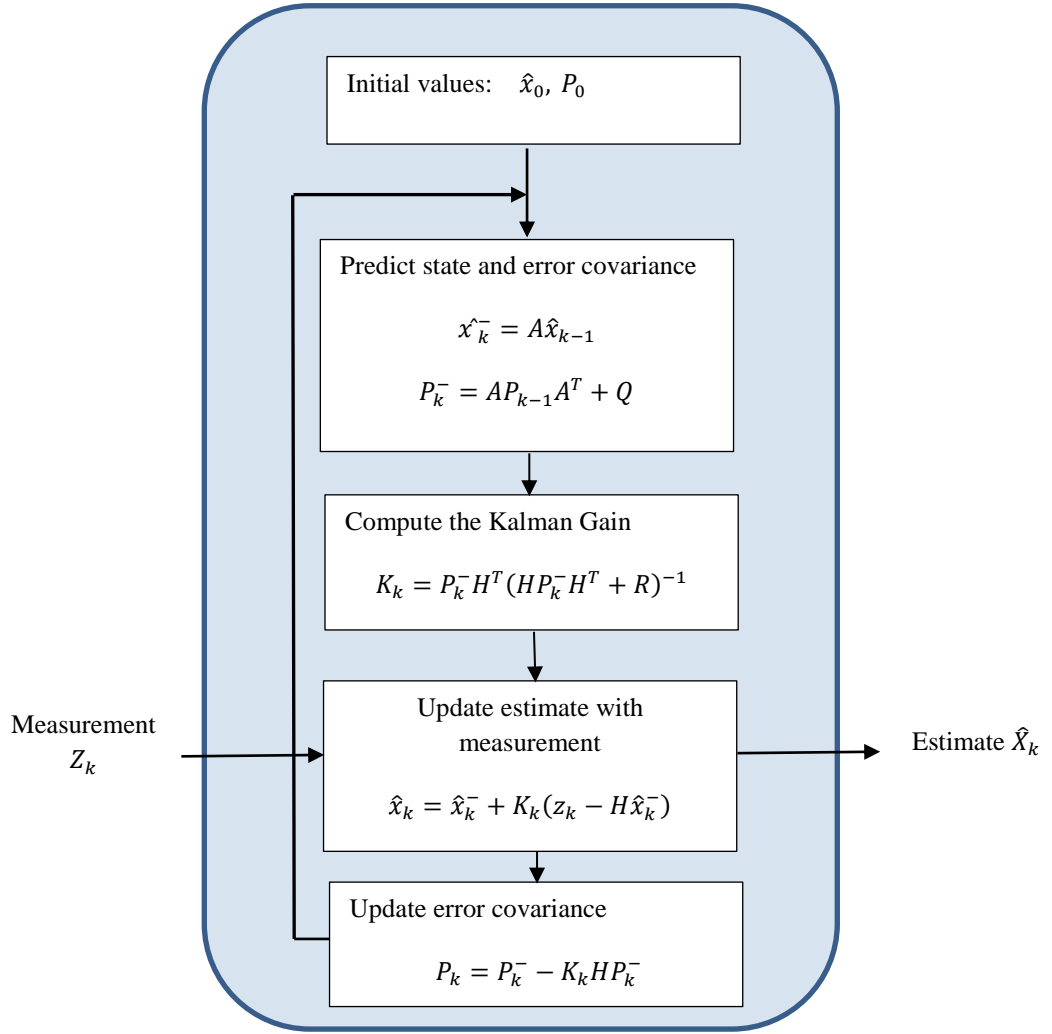


Figure 2.7: Kalman filter algorithm

## 2.6 Research on Wi-Fi Fingerprint Technique.

Recently, Wi-Fi fingerprint has attracted much attention where it does not require line-of-sight (LoS) measurement of APs. Traditional localisation which is based on trilateration and triangulation [16], [18] requires line-of-sight (LoS) measurement but it does not work well in buildings. The shadowing and multipath caused by obstacles such as wall and room partitions make it less accurate compared to fingerprint technique

[12], [82]. Ekahau and NavIndoors are among indoor positioning solutions which are based on Wi-Fi fingerprint technique. On average, location accuracy of this method can achieve up to 1-3m with high WLAN coverage. Different buildings have different shapes of geometry and number of access point's coverage where this can give different accuracy. Some researcher achieved from 8m to 10m mean error location [83] on field location while others get ~5m [84] mean error with both were based on same algorithm as comparison which is Nearest Neighbour method.

Y.Kim et al. [85] implemented peak-based Wi-Fi fingerprinting (PWF) which utilises temporal pattern of signal strength. Here the Wi-Fi sequence pattern along the route is used to determine the user locations. In PWF, the peak of signal sequence shows the location is closer to the Wi-Fi AP. A sequence of RSSIs data need to be collected in the first place when user is walking. Nevertheless, if the user is walking too fast the peak may be missed from being scanned by the Wi-Fi network interface module. This technique only works the best in narrow path such as hallway or corridor. HALLWAY [86] is one of the techniques based on analysis of spatial patterns of signal strength. Spatial pattern relates signals distribution on geographical area rather than recorded vector of RSSI. The patterns include RSSI order, signal landmark and coverage. HALLWAY technique identifies the difference of signal strength on each AP to classify the rooms. The RSSI strength order from each AP is noted to reduce the effect of signal fluctuation. This technique is only suitable for finding block region or rooms. Another problem with this technique is due to possibility of RSSI order in different room giving the same strength order.

To improve the location accuracy, collaborative localization technique can be implemented between Wi-Fi fingerprints with other localization technology. In most of the situation, Wi-Fi fingerprint acts as the main localization while the other localization technologies support through data fusion method. Personal Area Network (PAN)

including Bluetooth, Ultra-Wide Band (UWB) and ZigBee technologies are among technologies commonly used in collaborative localisation. These localisation technologies are usually used as distance constrain in location estimation. Bluetooth based positioning in the work by N. Patwari [87] have shown implementation for museum guidance. Bluetooth devices with different distance coverage were placed at specific given location to improve overall location accuracy. Even though this collaborative localisation does improve user location by knowing which cell identity based positioning, there are still costs for Bluetooth beacon/devices. Another collaborative method has been implemented by D. Rodionov [88] where combination of Wi-Fi fingerprint and RFID signal strength. The fingerprint technique on both systems gives several possible location estimations and error of each estimation is computed. Based on error variance on each sensor, data fusion algorithm calculates the user location. While these are several examples of collaborative technique with Wi-Fi fingerprint localisation, the extra cost to install the beacon or extra devices make it less popular choice for indoor positioning. People are still looking for promising indoor positioning without needing to spend any extra cost.

The availability of many sensors on smartphone nowadays makes it a huge potential for indoor positioning. To date, various hybrids positioning on different sensors and module have been utilised to get better accuracy. However, quite a few combine the Wi-Fi fingerprinting technique with vision sensor. MOVIPS (Mobile Visual Indoor Positioning System) in the work by Werner et al. [89] used combination of VBPS and WPS in which the Wi-Fi is to speed up the process of searching. Wi-Fi positioning will determine the coarse of positioning hence reducing the search for large images in database. Here, the image recognition was applied with distance calculation algorithm. The accuracy achieved was less than a metre; however in worse condition it can be unpredictable due to matching features of the images to database. Besides VBPS,

there is a research on positioning without need to construct database. Lee et al. [90] demonstrated the use of both front and rear vision sensors from the smartphone to determine the position in the hallway. The technique uses the ratio of perspective from the images. The technique can skip the challenge of using the database in VBPS [14], but it is less efficient and not effective in large environment.

One of the issues in Wi-Fi fingerprint technique is the change in the environment. The RSSI may vary in time due to this factor and others such as humidity changes and crowd of peoples. Recently, crowdsourcing solutions are one of the techniques that gain attention in the Wi-Fi fingerprint positioning. The approach is utilising the crowd in building or update the radio map through user collaboration. The key aspect is attracting volunteers to collect RSSI at certain locations which can contribute to the positioning system. The system will update RSSI with the latest data from user, hence increasing the location accuracy. Recent evidence shows that a giant company has already started the crowdsource project like Google's Indoor Maps. Despite its superiority which solves the labour intensive issue, it raises another new challenge such as incorrect data (polluted data), issues in managing the massive collecting data, and source from heterogeneous devices.

Prior studies have noted that the RSSI measurement from heterogeneous devices gives different accuracy of indoor localization. There are two factors that influence the RSSI reading, which are different Wi-Fi chipset embedded in devices and the antenna gain. Obviously, device used during creating radio map may differ from user devices during online phase. Different Wi-Fi chipsets have different levels of sensitivity on different Wi-Fi APs [64], [91]. The difference of antenna gain across the user devices gives different level of measurement. In addition, the antenna installation on user devices play a role on signal strength diversity due to signal received on different direction. F. Dong et al. [92], are among the first authors that highlighted about the

effect of heterogeneous devices on localisation. They proposed DIFF which utilises vector of signal strength difference. However this technique suffers from an increase in dimension as number of APs available increases. Another enhancement to the previous technique is implementation of signal strength difference (SSD) [64]. This technique uses a reference measurement from the AP and other RSSI measurements are deducted by the reference measurement. SSD only selects the subset of DIFF therefore it reduces computing overhead. However, there are certain drawbacks associated with the use of these methods where it suffers from signal noise fluctuation. At specific location, measurement of signal strength may return different level dBm reading from different Wi-Fi network interface controller (NIC), but at some other time it can return the same signal strength level due to heavy fluctuation of signals strength. As a consequence, the different levels of signal strength still return inconsistent location accuracy. Other author questioned the usefulness of this approach [93]. They proposed others solution which is based on homogenous signal strength pattern. In this method, each RSSI samples from various APs at RPs' location was recorded in order map. Index sequence order was given to each RSSI based on APs. The order matching during online phase acted like a filter which excludes the RPs that were far from the test point location. In overall, the signal noise fluctuation may disrupt the APs' RSSI sequence order on both offline and online phase especially measurement on corner space. Again the process could lead to localization errors.

Although some research has been carried out on localisation of heterogeneous Wi-Fi network interfaces card devices, no studies have been found focusing on mechanism of control or confining the location error itself. To the best of the researcher's knowledge, previous studies have only focused on signal strength difference which has been highlighted before as suffering from signal strength fluctuation. The availability of vision sensor is an opportunity to utilise it as calibration

with Wi-Fi fingerprinting technique. In the next chapter, how the indoor positioning algorithm focuses on confinement of location error and calibration point helps to improve overall indoor positioning experience will be highlighted.

## **2.7 Summary**

This chapter presents an overview of positioning techniques. Limitations of GPS in certain critical conditions, specifically in urban environments and inside building make most researchers in this field seek for alternative solutions. The most common methods and alternative solutions to enhance the location and positioning have been highlighted. There are three main groups in positioning that are wireless positioning system, movement based positioning system, and vision based positioning. The recent advances of smartphone make available different types of positioning system by utilising available sensors and wireless modules. Integrations between different types of positioning provide room for research of practical solutions that help to enhance the positioning accuracy.

## **CHAPTER 3: Setup and Measurement**

### **3.1 Introduction**

In the previous chapter, many potential positioning systems that are available have been elaborated. GPS has served well as the main positioning and navigation system outdoors. This is to be expected, as the whole system of GPS has been designed by the United States of America with navigation in mind from the beginning. The same applies to other global satellite navigation systems (GNSS), like GLONASS, BeiDou and Galileo. None of the systems mentioned can work flawlessly inside a building. For this reason, an alternative available potential system that is convenient to be implemented in a building is highly needed. The demand from Internet users and the spread of the Internet of things (IoT) make Wi-Fi systems always available in offices, homes, airports, restaurants, and shopping malls. This presents a tremendous opportunity to utilise them in the field of wireless positioning systems (WPS).

The importance of the fingerprinting technique has also been discussed in the previous chapter. So, in this chapter, elaboration on how the site survey for the collection of RSSIs at a chosen location was conducted will be detailed out. The factors that influence positioning accuracy will also be discussed.

### 3.1.1 Building Layout

The main challenge for a positioning system inside a building is the NLOS condition. As mentioned before, the layout and geometry of a building are factors that can put a signal into reflection mode whereby multipath fading could occur and decrease positioning accuracy. Many research techniques on Wi-Fi positioning consider a simple layout for a building with many available strategically located access points. In an actual condition, this can be the opposite. The layout of a building can take many shapes, ranging from just a big square open space to many rooms and narrow hallways. The same applies to the number of access points available. In reality, only one access point may cover a certain area and seldom does one find more than four APs overlapping with each other in a zone. In the first place, APs are located for the purpose of data communication coverage without thinking about supporting localisation. Another challenge in practice is the location to implement a Wi-Fi-based positioning system, where it is necessary to work with whatever conditions found without having to relocate the current AP's location.

Site survey in this work was on the B floor Infolab21, School of Computing and Communication, Lancaster University. Figure 3.1 shows the layout of the building and the site, which consists of a big space in the middle surrounded by lecturers' and researchers' room, and a narrow hallway towards the end of the site. These two different kinds of area zones were purposely selected to study the effectiveness of a single algorithm in various building shapes. Unlike outdoor localisation, 5 m accuracy will have a significant impact in indoor localisation as it can direct the user to an incorrect path or room. This is why improving accuracy is a huge challenge for indoor localisation. The red colour on the layout building shows the site survey coverage area.

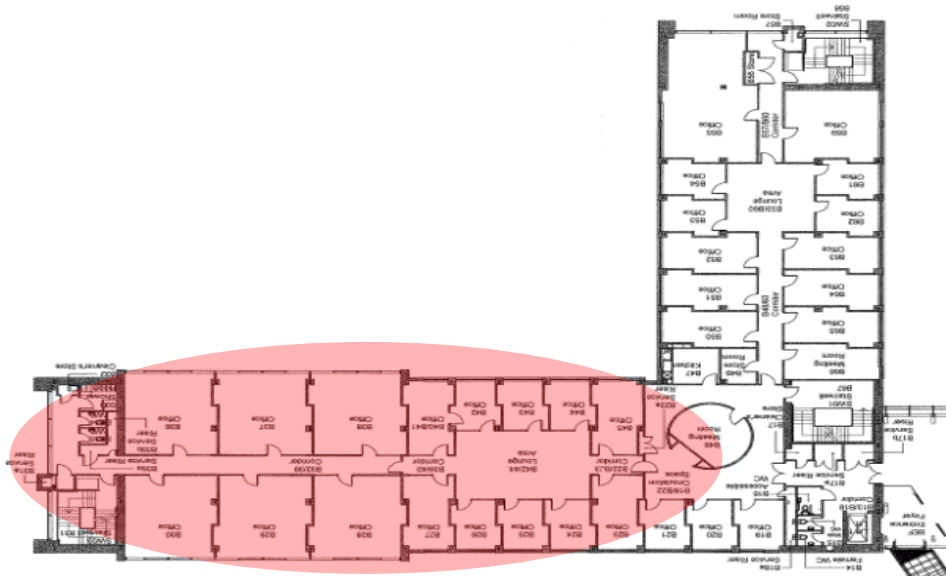


Figure 3.1: Layout of B floor, Infolab21, School of Computing and Communication, Lancaster University.

Before building the radio map, current AP locations were identified and the granularity of reference points (RPs) and paths during the online phase were determined. It was found that there was only one AP located in the middle of the coverage site, and another nearest AP near the coverage area, as shown in Figure 3.2 below. All APs were located inside the ceiling.

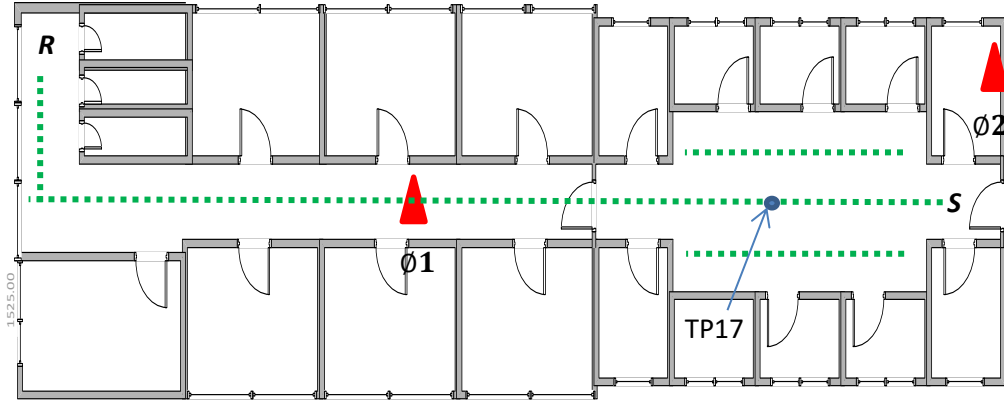


Figure 3.2: Detailed position of APs ( $\phi_i$ ), reference points (RPs/ green dot), and direction path movement points (S, R).

To make it easier, the size of the RPs is set to 1.5 metres in length and 1 metre wide. Point ‘S’ and ‘R’ are for the purpose of path movement in the next experiment.  $V$  access points (APs) located on the area are labelled as  $\phi_i$   $\{\phi_1, \dots, \phi_i, \dots, \phi_V\}$  with  $W$  RPs and locations as  $\{\theta_1, \theta_2, \dots, \theta_w, \dots, \theta_W\}$  in areas  $\phi_i = [x_i^{AP}, y_i^{AP}]^T$  and  $\theta_w = [x_i^{RP}, y_i^{RP}]^T$ . During the offline phase, there are  $N$  collected fingerprint measurements in different directions for all  $V$  APs stored in the database for all RP locations. The collected fingerprint signals are  $S_{RP}^w(m) = [S_1^w(m), S_2^w(m), \dots, S_i^w(m), \dots, S_p^w(m)]$ , where  $S_i^w(m)$  is the  $m$ th measurement of RSSI (in dBm) at  $RP_w$  from  $AP_i$ . In this case, in order to get a stable pattern for RSSI, the  $m$ th measurement should be within 1 minute of observation for each AP. During the online phase, unknown Test Points' (TPs) positions,  $\theta = [x, y]$ , will be along the path from route point S to point R. Here a random signal is collected from each AP at TPs  $s(m') = [s_1(m'), s_2(m'), \dots, s_i(m'), \dots, s_p(m')]$ , where  $s_i(m')$  is the  $m'$ th random RSSI measured at TPs from  $AP_i$ .

Figure 3.3 depicts the sample of RSSI data from AP available at one of the TP locations. From that TP position, five different RSSI data can be sensed which were from different APs' MAC address: A8:9D:21:B2:DC:30, A8:9D:21:CC:55:30,

A8:9D:21:B2:DC:31, A8:9D:21:CC:55:31, and A8:9D:21:B2:DC:32. The RSSI measurement showed that the signals always fluctuate and have different level of signal strength ranging from -50dBm to -70 dBm. The diverse pattern of RSSI value at certain location allowed us to utilize it as one of the key factor to determine user location. However, the fluctuations of the RSSIs measurement led it to be inconsistent on location accuracy. One of the possibilities of RSSI fluctuation is due to the fading effect of either fast or slow fading where the signals propagate in different directions caused by the building geometry.

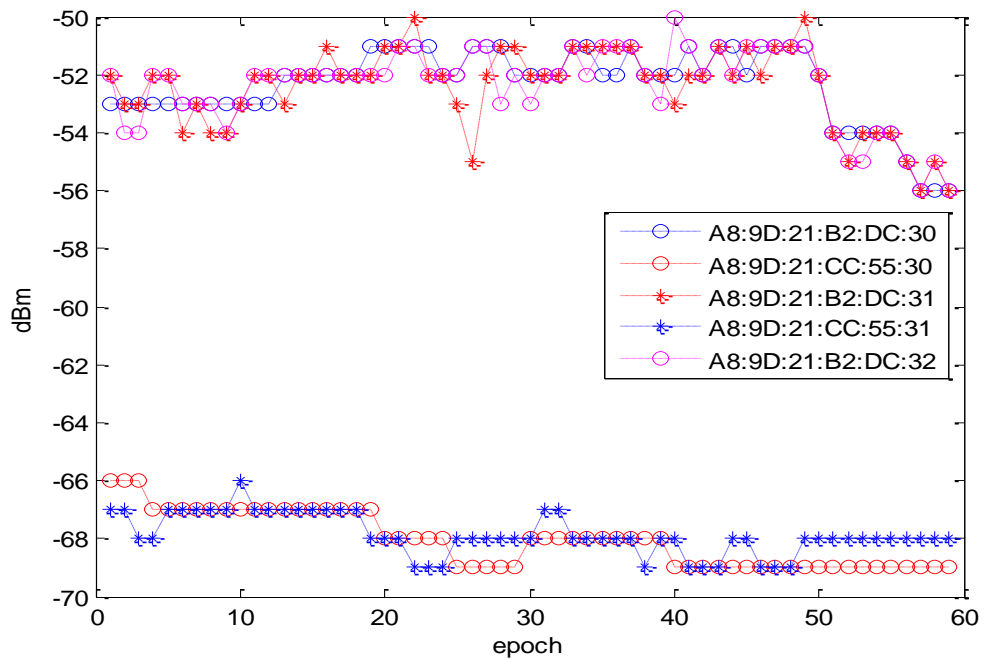
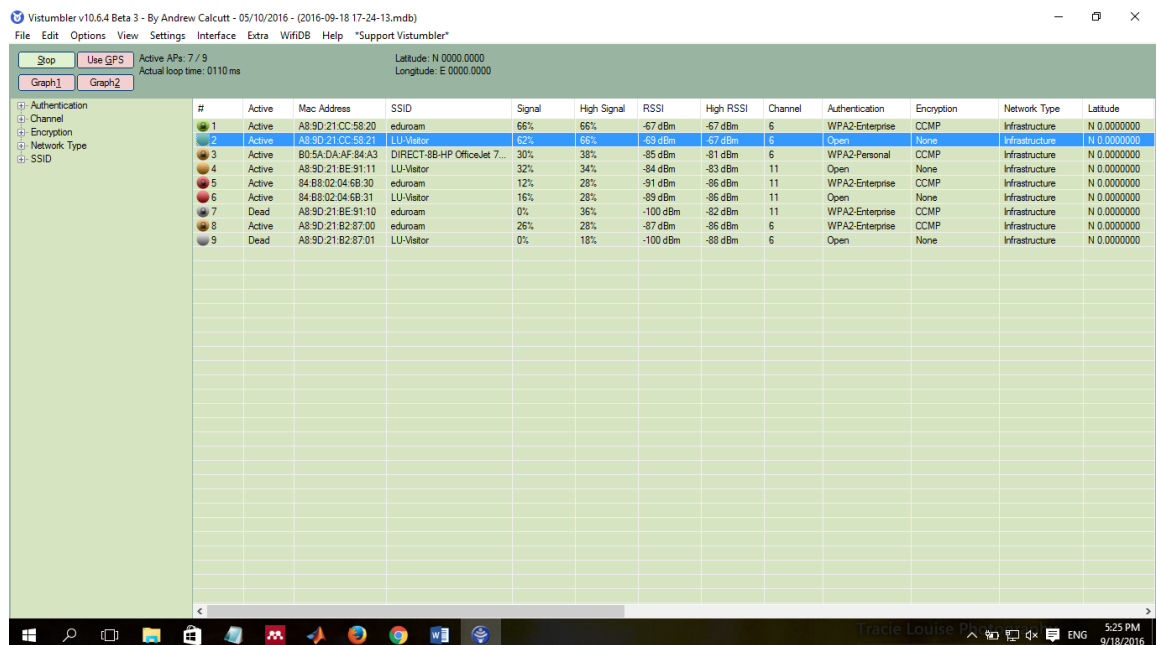


Figure 3.3: RSSIs from different MAC address at one of TP location.

## 3.2 Simulation Tools

### 3.2.1 Vistumbler

To collect the RSSIs available at each RP, Vistumbler is the preferred software as this is open-source and free. It was developed based on donation [94]. Vistumbler is the software used for scanning Wi-Fi access points, which are within range of the Wi-Fi adapter. It supports Wi-Fi 802.11a/b/g/n WLAN standards. After finding a Wi-Fi access point, Vistumbler satisfies enough requirements to capture critical data, such as network SSID, RSSIs from all APs available at the location, APs' MAC addresses, the encryption being used, network channel, time and much more. This software has been used by other researchers in the field of indoor positioning to gather all necessary data [95] and also as war driving software in cyber security [96][97]. Figure 3.4 depicts the graphic user interface (GUI) of Vistumbler software.



Vistumbler v10.6.4 Beta 3 - By Andrew Calcutt - 05/10/2016 - (2016-09-18 17:24-13.mdb)

File Edit Options View Settings Interface Extra WiFiDB Help \*Support Vistumbler\*

Stop Use GPS Active APs: 7 / 9 Actual loop time: 0110 ms Latitude: N 0000.0000 Longitude: E 0000.0000

Graph1 Graph2

#	Active	Mac Address	SSID	Signal	High Signal	RSSI	High RSSI	Channel	Authentication	Encryption	Network Type	Latitude
1	Active	A8 9D 21 CC 58 20	eduroam	66%	66%	-67 dBm	-67 dBm	6	WPA2-Enterprise	CCMP	Infrastructure	N 0.0000000
2	Active	A8 9D 21 CC 58 21	LU-Vistor	62%	66%	-69 dBm	-67 dBm	6	Open	None	Infrastructure	N 0.0000000
3	Active	B0 5A DA A5 84 A3	DIRECT-8B-HP OfficeJet 7...	30%	38%	-85 dBm	-81 dBm	6	WPA2-Personal	CCMP	Infrastructure	N 0.0000000
4	Active	A8 9D 21 BE 91 11	LU-Vistor	32%	34%	-84 dBm	-83 dBm	11	Open	None	Infrastructure	N 0.0000000
5	Active	84 B8 02 04 68 30	eduroam	12%	28%	-91 dBm	-86 dBm	11	WPA2-Enterprise	CCMP	Infrastructure	N 0.0000000
6	Active	84 B8 02 04 68 31	LU-Vistor	16%	28%	-89 dBm	-86 dBm	11	Open	None	Infrastructure	N 0.0000000
7	Dead	A8 9D 21 BE 91 10	eduroam	0%	36%	-100 dBm	-82 dBm	11	WPA2-Enterprise	CCMP	Infrastructure	N 0.0000000
8	Active	A8 9D 21 B2 87 00	eduroam	26%	28%	-87 dBm	-86 dBm	6	WPA2-Enterprise	CCMP	Infrastructure	N 0.0000000
9	Dead	A8 9D 21 B2 87 01	LU-Vistor	0%	18%	-100 dBm	-88 dBm	6	Open	None	Infrastructure	N 0.0000000

Windows taskbar: 5:25 PM 9/18/2016

Figure 3.4: GUI of Vistumbler.

For each  $\theta$  location, a sequence of  $S$  RSSIs fingerprints was collected in each direction from each  $\emptyset$  AP location available. All recorded data were stored in \*.CSV file format before being transferred to MATLAB for post-processing. Detailed information data from the \*.CSV file that can be extracted in this research are shown in Figure 3.5 below.

```
SSID,BSSID,MANUFACTURER,SIGNAL,High Signal,RSSI,High  
RSSI,AUTHENTICATION,ENCRYPTION,RADIO TYPE,CHANNEL,BTX,OTX,NETWORK  
TYPE,LABEL,LATITUDE, LONGITUDE,SATELLITES,HDOP,ALTITUDE,HEIGHT OF  
GEOID,SPEED(km/h),SPEED(MPH),TRACK ANGLE,DATE(UTC),TIME(UTC)
```

Figure 3.5: Detailed information from the \*.CSV file.

Vistumbler supports a GPS adaptor, but in this research it was not used, as the GPS receiver is not fully functional for indoor purposes. Another useful function provided by Vistumbler is the level of RSSI from each AP to the laptop, which can be monitored continuously. From there, the first idea of the location that has the best signal strength was obtained. Figure 3.5 depicts the GUI from Vistumbler, where RSSI level can be monitored. The sampling time of RSSIs can be set by the user and each RSSI pattern level can be monitored depending on sampling interval, as shown in Figure 3.6. All collected data from Vistumbler then arranged in order to suit the MATLAB. MATLAB is used in this research to develop algorithms and analyse the results.

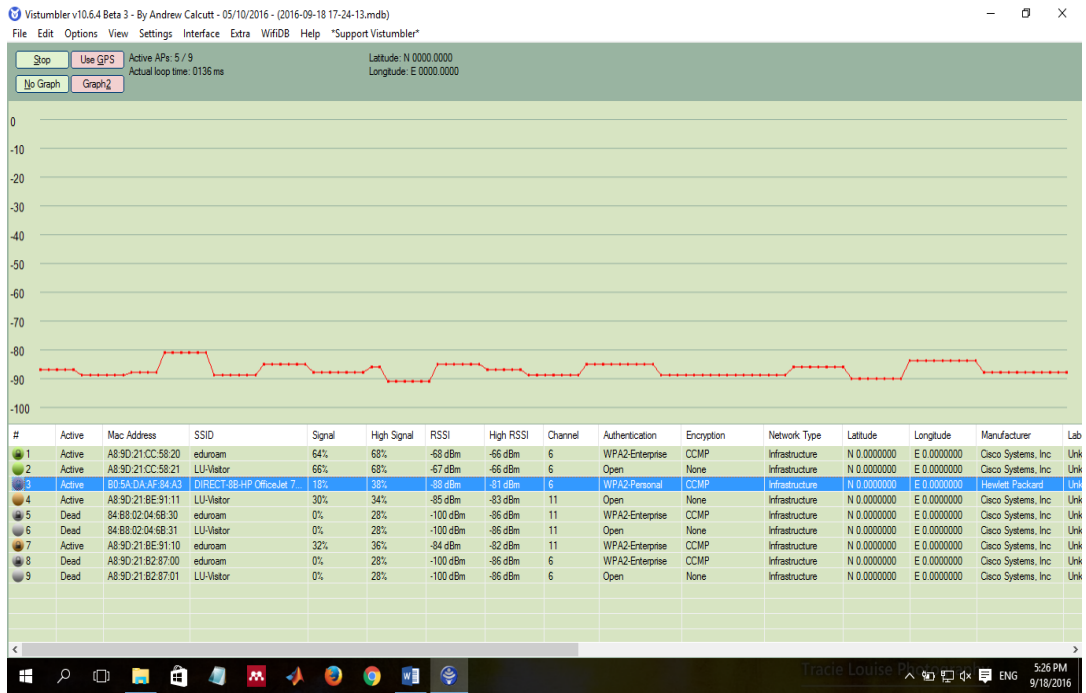


Figure 3.6: Monitoring RSSI level from one of AP available.

### 3.3 Wi-Fi Deterministic Algorithm

There are two types of fingerprint algorithms which are based on deterministic and probabilistic approaches. Deterministic is less complex, making it more practical in terms of processing efficiency. On the other hand, a probabilistic approach yields more accurate results and processing times. Some researchers [98][99] have proven that with modifications the existing deterministic approach can rival the results of a probabilistic technique with less processing time. Therefore, to exploit a fast algorithm it was decided to implement a deterministic location-based estimation algorithm technique in this work.

The early part of this research uses deterministic approach based on K-Nearest Neighbour (K-NN) algorithm as a comparison for lower complexity [12],[100]. As

mentioned in Chapter 2, the conventional deterministic technique consists of two main phases, an off-line phase and an on-line phase. Usually, during the off-line phase, many samples of Wi-Fi signal strength RSSIs are collected, for at least a minute, at certain dedicated reference points (RPs). These RSSI data are stored in a reference database. During the on-line phase, a few samples of RSSI from each access point are collected at particular Test Points (TPs) and matched to the database. The nearest match will return the location and position which are recorded early during the off-line phase. How far signal strength match is represented by distance is given as follows:

$$D_q = (\sum_{i=1}^n |s_i - S_i|^q)^{\frac{1}{q}} \quad (3.1)$$

B. Li et al. [101] stated that the number of  $q$  does not necessarily improve the positioning accuracy. However, the simulation results show the opposite, as presented in Figure 3.7; Euclidean distance in which  $q$  equals to 2 provides better accuracy, hence in this work Euclidean distance was used. The results confirm that at particular and specific locations for the number of  $K$ , from one to five,  $q$  equals to two returns the smallest error compared to whenever  $q$  is equal to one.

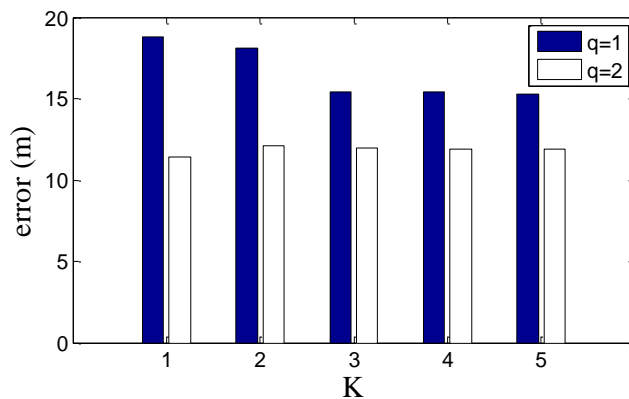


Figure 3.7: Comparison of errors for different distances  $q$ .

As starting point, the K-NN (Nearest Neighbour) was implemented as a pioneer by RADAR [80]. The parameter K corresponds to the selected number of smallest distances in a matrix generated by equation (3.1). For example, if the return distance matrix from equation (3.1) consisted of 42 points for RPs and only three smallest distances were utilized from a set of 42, here the number of K will be equal to 3. It is anticipated that for the selection of K, this should be done as a compromise between accuracy and complexity (higher values of K leads to better accuracy but higher complexity). Figure 3.8 shows a block diagram of the K-NN fingerprint W-Fi algorithm.

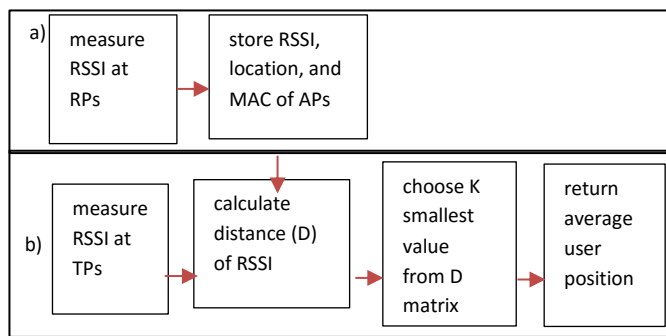


Figure 3.8: Phases of Wi-Fi fingerprint deterministic technique: a) off-line phase b) on-line phase.

### 3.4 Unplanned Environment and Influence Factors

Many researchers [102], [103],[104] have shown that under ideal conditions where there are enough access points (APs), a simple layout of building geometry and strategic AP locations, K-NN will return less location error which average could be less than 5 metres. For indoor positioning, a location error radius higher than 5 metres will

have a significant impact location on other rooms. This is a huge challenge for indoor positioning compared to outdoor positioning.

The test area was set up on Level B, Infolab21 building at Lancaster University, as shown in Figure 3.9. A detailed elaboration of the experimental set-up has been explained previously.

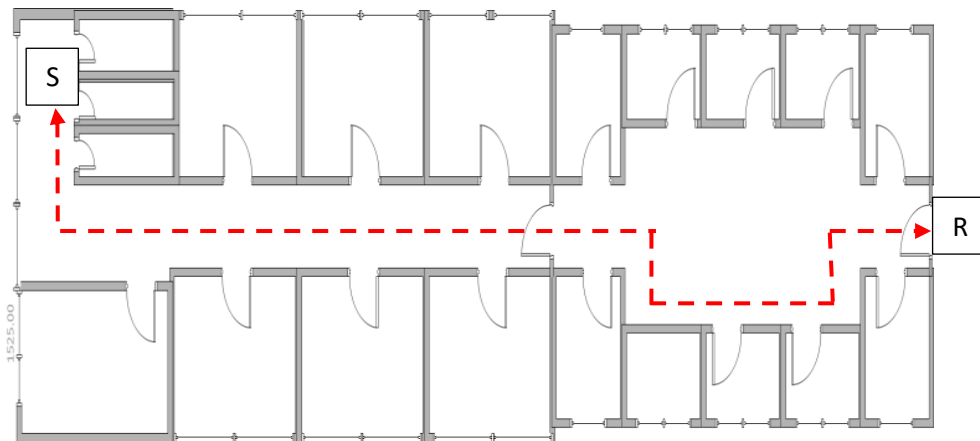


Figure 3.9: Direction of movement from point S to point R, and vice versa.

In practical situation, there are certain factors that are beyond control such as:

- the number of access points (APs) available;
- the location of access points (APs);
- variety in the geometry of the layout building.

In many cases, a higher number of access points is available, which is good for localization as many signal strength RSSIs can be collected from all APs. This will slightly reduce the number of positioning errors. Most studies or development using a positioning algorithm approach worked under well conditions where the locations of APs were in strategic locations. For example, in a single room, up to four APs can be found which helps to differentiate different strength levels of Wi-Fi signals, hence

improving localization. It was found that on Level B, Infolab21, there were only a few access points available near the coverage area, so it was a huge challenge to perform localization. At some part of coverage area, RSSI can only be detected from a single access point while at certain part it was very hard to differentiate the different level of RSSI reading. These will contribute to huge localisation error. The test area consists of a narrow hallway and an area rectangular in shape.

This research started with a basic conventional technique, the K-NN (Nearest Neighbour) algorithm. The K-NN algorithm is heavily dependent on the scale granularity of Reference Points (RPs), hence a maximum spacing of 1.5m was specified for the experiment. The work began by collecting RSSI readings from available APs' MAC address for the path shown in Figure 3.8, from R to S. The K-NN algorithm was implemented for the whole-path movement. Figure 3.10 shows the results for errors between actual locations and estimations based on the K-NN algorithm and different numbers for K from 1 to 5. The values for K refer to the number of nearest RPs considered in the calculation, so increasing this value will yield more accurate results at the expense of computational processing. These errors show a single K-NN algorithm struggling to maintain errors at less than 5 metres for the whole path.

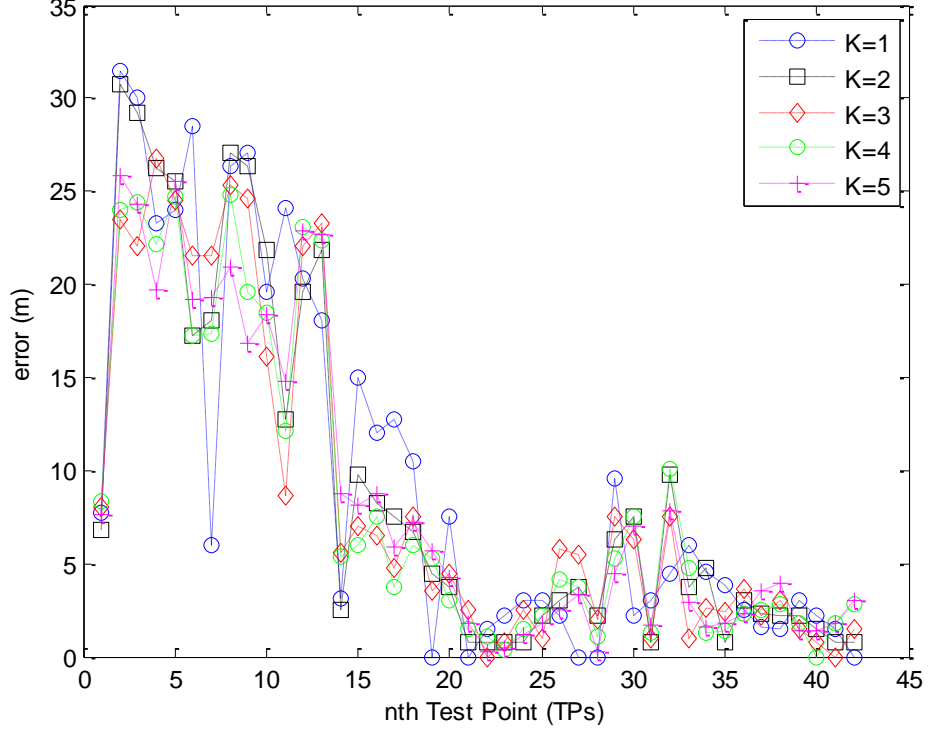


Figure 3.10: Error distribution for nth TPs location for different numbers of K.

In general, the results show quite similar patterns for all the different values of K and based on the graph, it is clearly shown that the same signal strength properties can be found up to 30 m from the actual position, as indicated in Figure 3.9. L. Koski et al. [83] introduced coverage area technique and compared their algorithm with conventional Nearest Neighbour method. Their work on real RSSI data resulted in K-NN with mean error of 9.9 metres and maximum up to 31.3 metres. Basically, the early result shows the same range of error in location where at certain location it can be up to 30 metres. A new parameter called accumulated accuracy of simulation along the dedicated path route is introduced. The accumulated accuracy is given by:

$$A = \int_0^n (f(n) - f_o(n)) dn \quad (3.2)$$

where  $f_o(n)$  is the base line of zero error.

Based on the graph in Figure 3.9, the accumulated accuracy along the path from S to R was calculated with different values of K as shown in Table 3.1.

Table 3.1: Accumulated accuracy for different values of K.

<b>Value of K</b>	<b>Accumulated Accuracy</b>
1	405.5004
2	386.9982
3	367.9317
4	356.8099
5	362.8102

The increments of  $K$  from 1 to 5 show some improvement indicating that increasing the number calculated of the nearest point will give better accuracy. After looking at value of  $K$ , it has been decided that  $K$  equals to 3 is enough for this algorithm. As suggested by Binghao Li et al. [12] even though the higher number of  $K$  gives better accuracy, the accuracy of selected  $K$  of bigger than three is not significant enough. Along hallway, RPs are distributed in one row, side by side, which would supposedly return the best accuracy for selected  $K=1$ . This shows that different values for  $K$  in different regions will have a significant impact on accuracy. A future solution for this case is a design dynamic algorithm selection number with  $K$  depending on the region of the map [78]. As an algorithm comparison in this research, the designed algorithm will be compared to several conventional algorithms such as this  $K$ -NN with

K equals to three. This has been highlighted before that K bigger than three gives insignificant huge improvement on accuracy than the number of selection point to process.

G. Lui et al. [91] mentioned several challenges in dealing with different kinds of Wi-Fi chipsets in different devices, such as data dropout data “signal strength catching”. This study looked into these problems and investigated how far they affect positioning accuracy based on the same algorithm. Figure 3.11 depicts positioning errors for a laptop, tablet and mobile phone. The results indicate that positioning error patterns are quite close between a tablet and the mobile phone but more accurate for a laptop. There are several factors that could contribute to these results, such as differences in antenna gain and chipsets in each device. Table 3.2 describes the accumulated accuracy value for different devices.

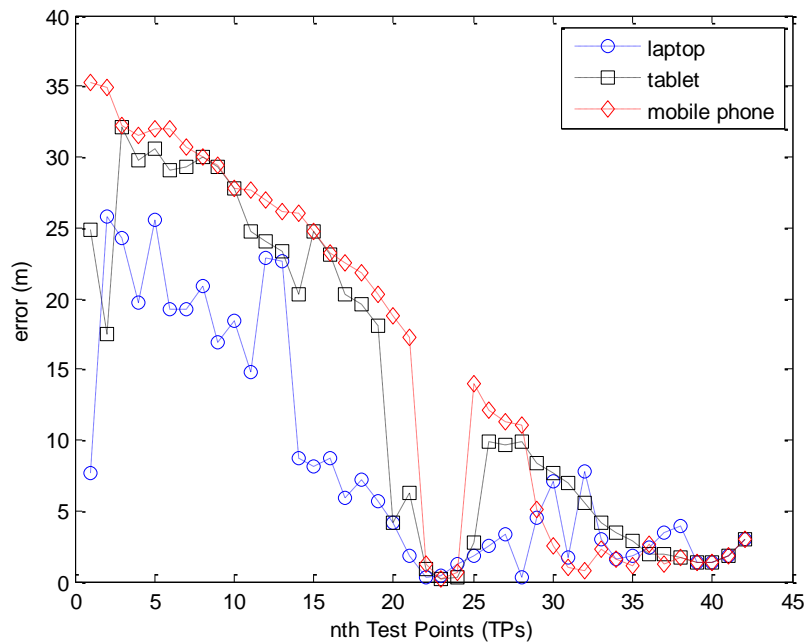


Figure 3.11: Error distribution for different devices based on K-NN algorithm (K=3).

Table 3.2: Accumulated accuracy for different devices.

Type of Device	Accumulated Accuracy
Laptop	362.8102
Tablet	574.2124
Mobile Phone	649.2623

Subjects' movement factors were tested in different directions (S to R and R to S). In this case, the RPs in the database were matched to the TPs in both directions. As depicted in Figure 3.12, different reference directions gave slight variances in accuracy, even in this case, where the database of collected RSSI had already taken into account user direction at every particular RP. This is because different directions have different patterns of signals being blocked by the subject along the signal path, which also affects the readings for each access point's RSSI. Table 3.3 shows the accumulated accuracy for different path directions from point S to R, and vice versa. Even though the errors obtained with the K-NN algorithm are slightly different for the two directions, the overall accumulated accuracy can have a significant impact on user navigation, especially indoors, which demands stricter tolerance for accuracy as compared to outdoors.

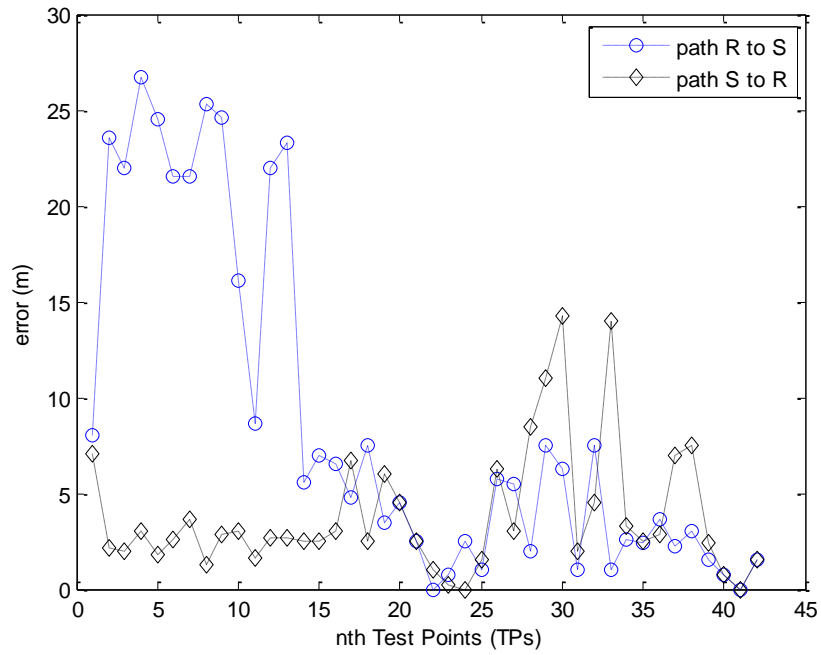


Figure 3.12: Location error estimated for different path directions based on K-NN algorithm (K=3).

Table 3.3: Accumulated accuracy for different path directions.

Path	Accumulated Accuracy
R to S	367.9317
S to R	160.6483

The combined effects of these three factors, different types of devices, number of selection point K and directions of movement, lead to uncertainties in positioning accuracy. To the best of the researcher’s knowledge this challenge has not been addressed before as a whole and it is intended to address this in this research. An intuitive solution to this problem will be to incorporate several integrated algorithms

with calibration point to minimize the influence factors leading to higher accumulated accuracy.

### **3.5 Summary**

This chapter has described on measurement process, simulation tools used in this research, and factors that influence the conventional Wi-Fi fingerprint algorithms. The place of site survey has been described and how the survey has been done during off-line phase and on-line phase were also explained. Vistumbler site survey was chosen to measure the RSSI from all APs at particular location. All important data were then arranged in order to suit the MATLAB. MATLAB has been chosen to develop the algorithm and analyse the results. Based on the collected data, basic Wi-Fi fingerprint algorithms have been developed. Simulation were performed on this conventional algorithms with different Wi-Fi chipset/devices, number of point selection in the deterministic algorithm, and different path movements. Based on these early results, number of point selection equals to three was chosen for deterministic technique (K-NN and WKNN). Results from this investigation also show that position accuracy of conventional Wi-Fi deterministic fingerprint algorithm may vary depending on different devices (Wi-Fi chipset) and directions of path movement. In the next chapter, the newly designed algorithm to reduce the uncertainties effect of these factors will be elaborated and comparison will be made between new algorithm and conventional Wi-Fi fingerprint techniques.

## **CHAPTER 4: Indoor Positioning**

### **4.1 Introduction**

Most of the indoor positioning algorithm has single layer estimation. In this chapter, combination of several layer algorithms which is based on deterministic technique is proposed. The chapter begins with brief estimation and theory related to this integrated algorithm. Simulations were conducted to evaluate its performance by comparison to other Wi-Fi location estimation algorithms.

### **4.2 Bayesian Technique**

Deterministic methods give reasonable positioning accuracy, as described in the previous section. During the online phase, at each test point location, the Wi-Fi module collects RSSI information from the APs. The number of RSSI used in data collection depends on the Vistumbler setting. In this case, an assumption was made that up to 60 samples of RSSI could be collected when the scan started. In the first stage, each RSSI reading was applied to the deterministic positioning algorithm to get the location of the user. To begin with, the entire output from the deterministic positioning algorithm was just averaged. Instead of applying simple average estimation, the comparisons are made to the Bayesian approach. The Bayesian estimation approach considers other information, such as state and observation conditions which are useful to enhance positioning accuracy.

Figure 4.1 shows the static position output of more than 50 samples of RSSI data during the on-line phase via the K-NN algorithm where two types of estimation are

presented. The blue horizontal line is the actual location from X and Y meter measurements at TP 17 (middle of the space in Figure 3.2). The black dots are the output of every RSSI sample based on average estimation, while the red dots show the output from a Bayesian iterative estimation.

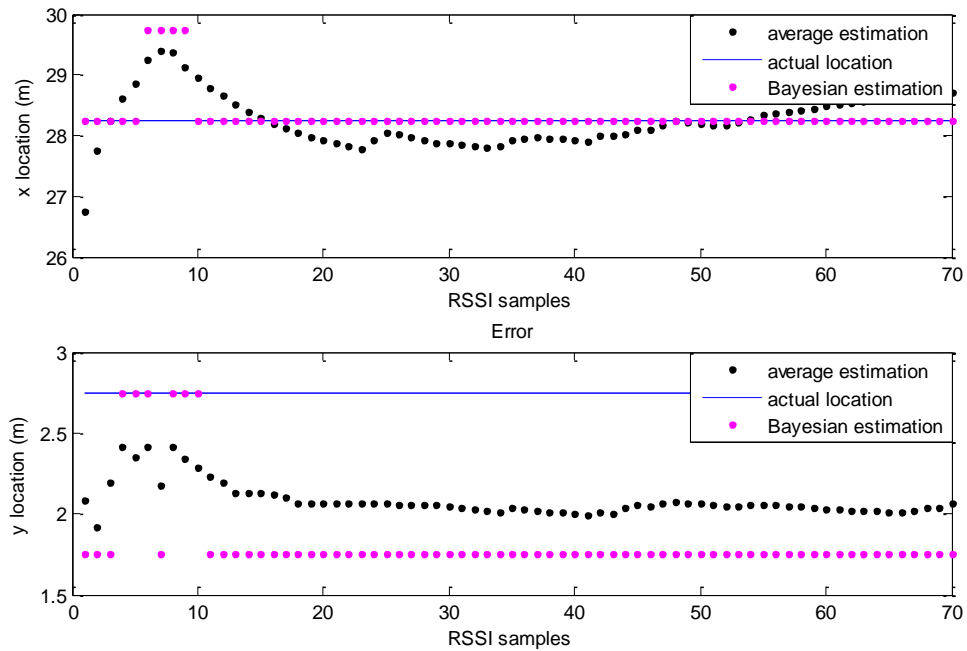


Figure 4.1: Average estimation (black dotted) vs. Bayesian estimation (red dotted) for each RSSI sample at TP 17.

Based on the graph in Figure 4.1, it is clearly shown that average base estimations fluctuate along with the number of RSSI samples. An iterative Bayesian estimation gives more stable results after just 10 RSSI samples. It is clearly shown that a Bayesian iterative technique is more immune to RSSI fluctuation, which is clearly the main problem with average estimation.

Figure 4.2 depicts an example of error distribution at selected TP path. In this scenario, 70 RSSI samples were collected for each TP location. The red dotted line shows an average estimation of 70 RSSI samples at TP locations, while the blue dotted

line is based on iterative Bayesian estimation. The average estimation has random fluctuation in location error along the selected TP selection, where some are acceptable errors of less than 5 metres but some have unacceptable errors of up to 25 metres. The Bayesian estimation with knowledge of the prior state helps to decrease overall location error for each TP location to less than 5 metres.

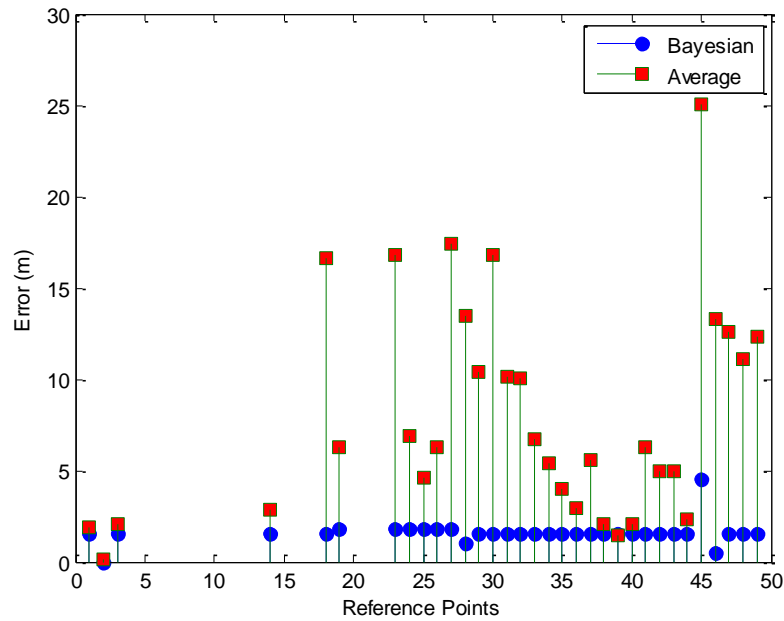


Figure 4.2: Bayesian estimation vs average estimation.

Table 4.1 shows the accumulated accuracy of average estimation and Bayesian estimation from K-NN deterministic algorithm. It is clearly show that Bayesian estimation give better location accuracy compare to average estimation.

Table 4.1: Accumulated accuracy of average estimation vs Bayesian estimation.

Estimation	Accumulated Accuracy
Average Est	265.3971
Bayesian Estimation	51.3167

Figure 4.3 shows a comparison on processing time of average-based estimation versus the Bayesian estimation. For most of the conditions, Bayesian estimation processing times are five times compare to average-based estimation, while at certain positions this can rise to up to eight times longer. In spite of more processing time, Bayesian estimation give better accumulated accuracy for whole path movement.

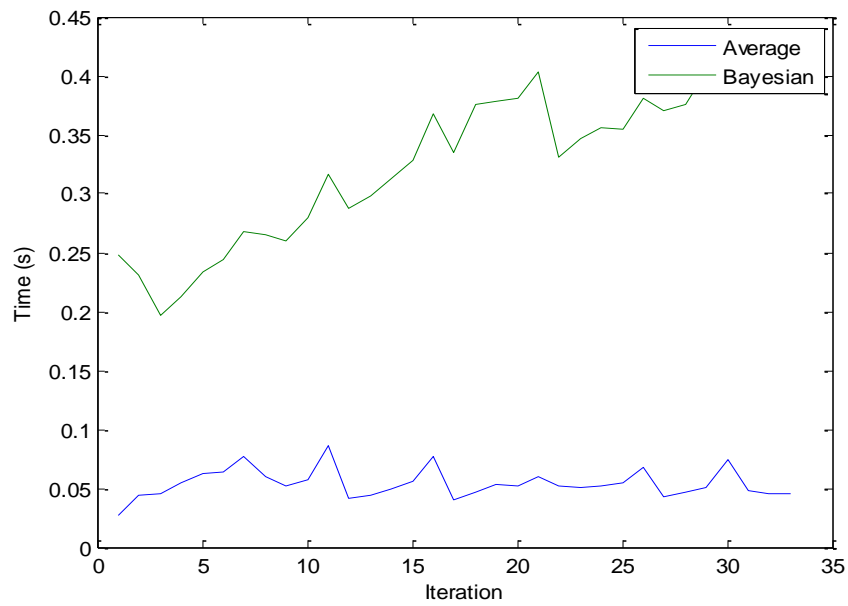


Figure 4.3: Ratio of processing time for average and Bayesian estimation.

### **4.3 Enhanced Weighted K-Nearest Neighbour (EWKNN)**

K-NN is based on a fixed number chosen from the nearest distance matrix. If  $K$  is set to three, this means that the three best nearest distances in the distance matrix will be selected in further calculations. In some cases, a similar pattern of signal strength distribution will appear in other positions which are far from actual positions. As a result, false estimation points will be included in an average calculation to determine a positioning point. This will lead to a decrease in positioning accuracy whereby points that should be ignored are included in the K-NN algorithm. So, the best way to proceed is to have a dynamic selection for  $K$  whereby neighbours' position points which are far from the actual positions are neglected [105].

The geometry of the building plays some role in affecting positioning accuracy. In a corridor or hallway, the space is narrow and long. Usually, RPs are positioned in a row and there will definitely be less near neighbour points than in an open space like a hallway. This is the reason why it is necessary to vary the selected number for K-NN based on the space type. The flow chart of dynamic value of  $K$  in EWKNN is shown in Figure 4.4.

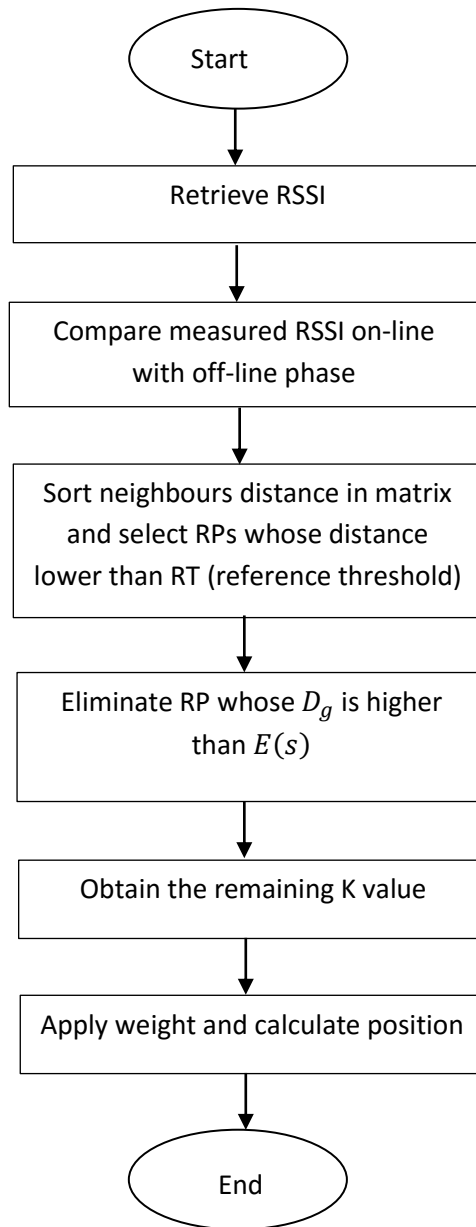


Figure 4.4: Flow chart of EWKNN.

A comparison of on-line and off-line RSSIs will produce a set of neighbour distances in a matrix and then this is sorted from low to high. Only distances ( $D_i$ ) lower than a threshold value are selected.  $G$  denotes the remaining RPs and  $S_g$  denotes the difference between  $D_1$  and  $D_g$  where  $g = 2, 3 \dots G$ . The average of differences is obtained as follows:

$$E(s) = \frac{(S_2 + S_3 + \dots + S_G)}{G-1} \quad (4.1)$$

RPs that have a larger  $S_g$  than  $E(s)$  were again neglected and the remaining numbers for RPs determine the number of K. To further improve accuracy, each RP's location was weighted according to its  $D_i$  [105]. Figure 4.5 depicts a simulation result comparison on deterministic positioning algorithm based on K-NN, WKNN, and EWKNN. The locations of test points are from point S to R with K equals to 3, while it is dynamic for EWKNN. The reason why K equals to 3 was chosen is because whenever K is greater than 3, the result does not have significant impact on improving the accuracy. The results show slight improvement for WKNN compared to conventional K-NN while EWKNN shows another minor accuracy improvement in overall for test points on path movement from point S to point R.

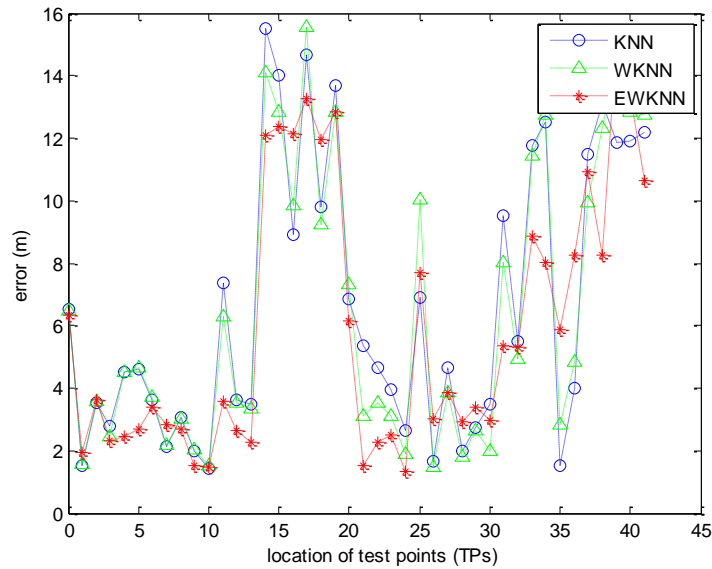


Figure 4.5: KNN (K=3) vs WKNN (K=3) vs EWKNN.

## 4.4 Design the Kalman Filter

The Kalman filter is a statistical algorithm which can estimate the state of the process given noisy data. The flow of Kalman filter iteratively predicts and estimate the prediction with input measurement until some criteria is met. For indoor positioning, the Kalman filter process consists of vector of moving object  $X$  in  $(x,y)$  coordinates and velocity with the coordinates as the only measurement. The state and measurement model are given below:

$$\text{State model: } X_k = AX_{k-1} + W \quad (4.2)$$

$$\text{Measurement model: } Z_k = HX_k + V \quad (4.3)$$

Matrix  $A$  is the state transition matrix that describes motion of the system which in this cases the equation relationship of position and velocity. Matrix  $H$  shows relationship between state variable and measurement.

$$\hat{X}_k = \begin{bmatrix} x_k \\ y_k \\ v_{xk} \\ v_{yk} \end{bmatrix}, A = \begin{bmatrix} 1 & 0 & \Delta_t & 0 \\ 0 & 1 & 0 & \Delta_t \\ 0 & 0 & 1 & 0 \\ 0 & 0 & 0 & 1 \end{bmatrix}, H = \begin{bmatrix} 1 & 0 & 0 & 0 \\ 0 & 1 & 0 & 0 \end{bmatrix}$$

$$Z_k = \begin{bmatrix} x_k \\ y_k \end{bmatrix}$$

$Q$  and  $R$  are the process noise covariance matrix and measurement noise covariance matrix, respectively. These two parameters will affect measurement and prediction of the Kalman filter process. Between these parameters, process noise covariance is hard to determine, which is determined by experience or experiment. J. Yim et al. [106],[107] have highlighted based on their experiment the ratio between  $Q$  and  $R$  that

really effects the performance of the Kalman filter. By following the step, it was found that Q equals to 0.00001 gives optimum results. The initial condition as follows was setup:

$$Q = \begin{bmatrix} 0.00001 & 0 & 0 & 0 \\ 0 & 0.00001 & 0 & 0 \\ 0 & 0 & 0.00001 & 0 \\ 0 & 0 & 0 & 0.00001 \end{bmatrix}$$

$$R = \begin{bmatrix} 1 & 0 \\ 0 & 1 \end{bmatrix}$$

$$P_0 = \begin{bmatrix} 5 & 0 & 0 & 0 \\ 0 & 5 & 0 & 0 \\ 0 & 0 & 5 & 0 \\ 0 & 0 & 0 & 5 \end{bmatrix}$$

$$\hat{x}_k = \begin{bmatrix} 32.75 \\ 2.75 \\ 0 \\ 0 \end{bmatrix}$$

## 4.5 Algorithm Description

The main idea of the algorithm is to combine several layers of process before the final location can be determined. Figure 4.6 shows the concept of the proposed indoor localization algorithm. The widespread of WLAN in the building makes it the favourite choice for indoor positioning. The main input parameter will be receiving signal strength indicator (RSSI) from Wi-Fi module. Wi-Fi fingerprint involves collection of signals to create the radio map. Later the closest pattern match between sample vector signal and the radio map will determine the early location of that particular signal. In the early location estimation stage, Bayesian estimation was implemented and the accuracy

depends on the number of RSSI vector sample. Finally, Kalman filter was implemented to improve the location accuracy.

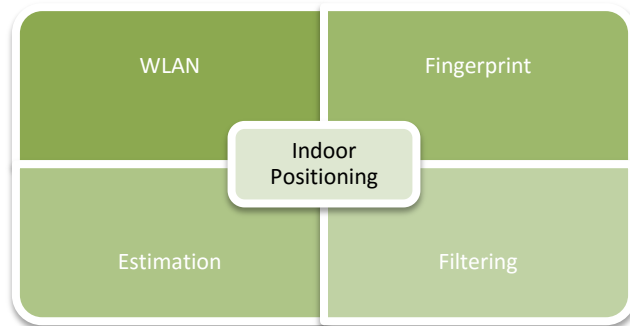


Figure 4.6: Indoor positioning concept

There are numerous techniques for position estimation based on collected observations. One common method is K-Nearest Neighbour (K-NN). K-NN works by comparing observation values during an on-line phase and observation of mean values during an off-line phase. To facilitate simple and fast algorithm calculation, a deterministic method was chosen in this work. However, the instability of RSSIs during the on-line phase compared to each mean RSSI's value in the database will return a scatter pattern of estimated positions. If a simple average of estimated positions is taken, the final estimated location will also fluctuate according to the number of RSSI samples as shown in Section 4.2. To overcome this problem, iterative Bayesian estimation was implemented in the algorithm. This technique needs less sampling of RSSI numbers and return stable position estimations. Each new RSSI value in the on-line phase is compared to the database through the EWK-NN algorithm and an early estimated position will be retained. In this algorithm, 10 RSSIs or more is sufficient to get stable results.

Unlike in other researches, a *dynamic localisation region* was implemented in this work instead of clustering techniques. Several clustering techniques that have been implemented are affinity clustering techniques [108], mainly to reduce computational cost. Clustering techniques are methods for grouping a set of objects with the same group characteristics. In this field, some clustering techniques include signal strength distribution and clustering of offline database locations. This is done to reduce the computational cost by reducing RP searching and this helps to increase the accuracy of localisation.

A different technique aside from a clustering algorithm was used. The technique is based on user history profiling, which utilises iterative Bayesian technique. In the implementation of Bayes rules, information about prior position is as important as object movement history. From a prior position, the next possible user location is estimated within certain area coverage. This coverage area comprises several adjacent RPs' locations surrounding the prior location, which might be a possible actual location during localisation. This coverage area is called a *localisation region*, where the next possible actual location will be in this area. Based on prior location, all adjacent RP locations which have been listed in a lookup table can be determined. Different prior locations will give different lists and total numbers of adjacent RP locations due to the different geometries of buildings. Figure 4.7 depicts the *localisation region* where a localisation process will determine an estimated location in this region. This figure shows a user walking from left to right in sight of the building through a hallway and an open square space. The *localisation region* is dynamic in shape based on prior location and building geometry. Also, the *localisation region* will be updated in each cycle of the localisation process.

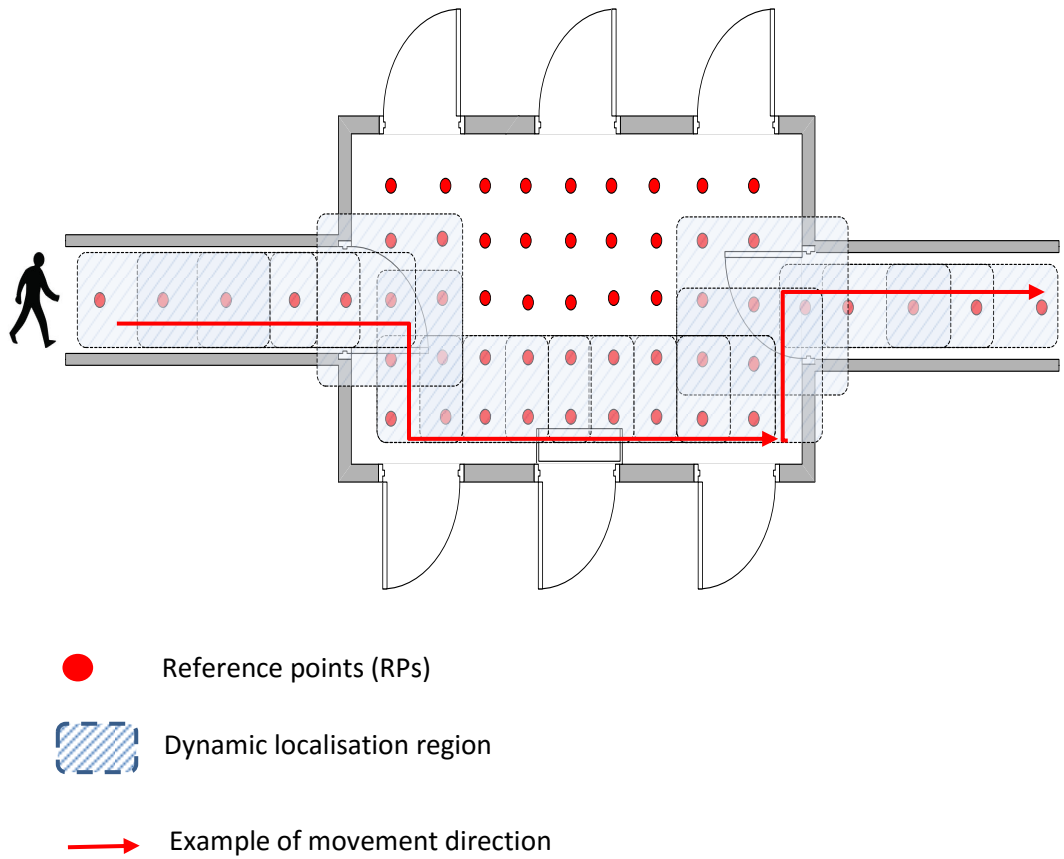


Figure 4.7: Dynamic shape changes in the localisation region depending on prior location.

As elaborated in Section 4.2, the likelihood function needs to be calculated for each earlier position from EWK-NN to give each possible RP location in the *localisation region*. The return value of the likelihood function is retained and used in the next iterative cycle process until there are enough RSSI values for each location. After completing the iterative process, the position is estimated from the highest return probability value based on possible RP location points. After the new position has been estimated, this will become the new prior position for the next iterative process and the lookup table for RPs adjacent to the current position will be updated. This cycle will be repeated in the next localisation process. Figure 4.8 shows the flowchart of the proposed algorithm.

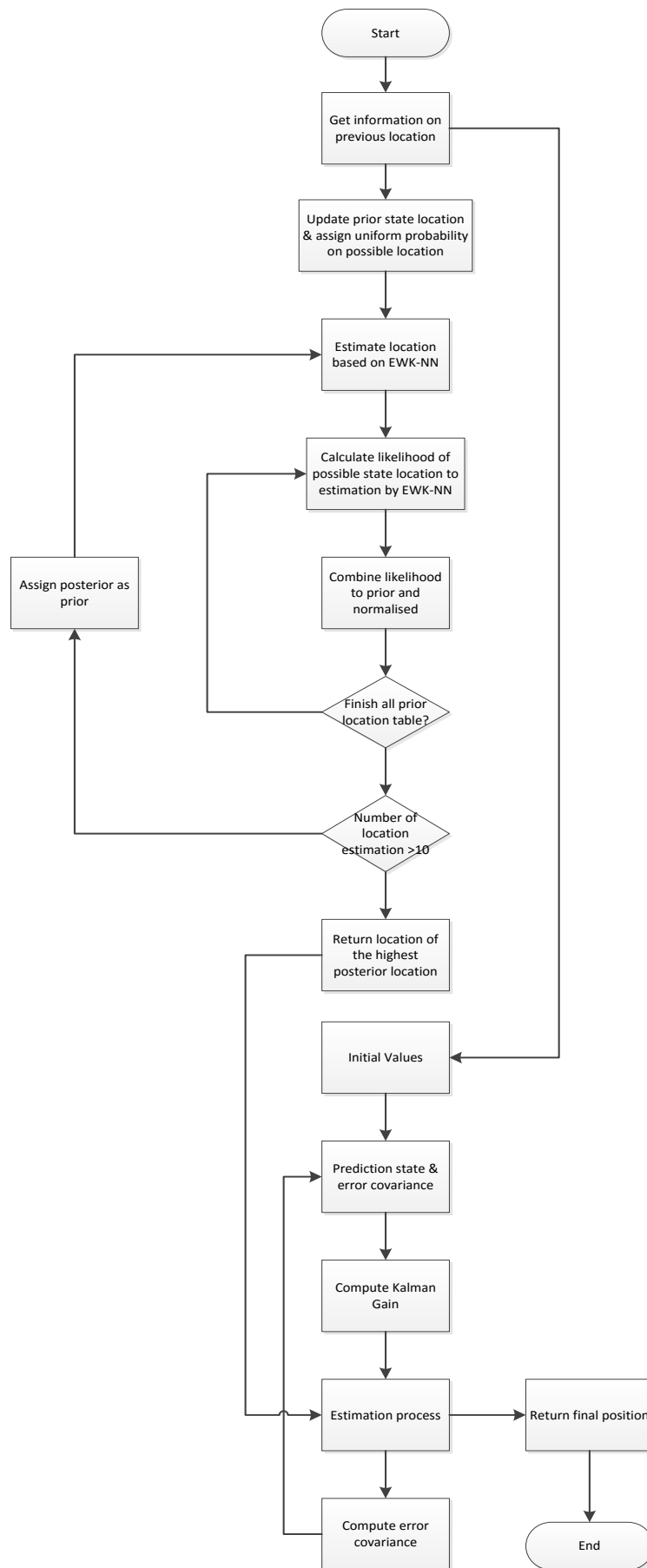


Figure 4.8: Flow chart of the proposed algorithm.

The pseudo code of the algorithm can be summarised as below.

#### Algorithm 1

1. Get previous location
2. Update prior state location and assign localisation region.
3. Update table of possible location based on localisation region.
4. Assign uniform probability on each possible location in localisation region.
5. For each RSSI>10

Estimate location based on EWK-NN

End

Return early location

6. Calculate likelihood of possible state location

For each location based on EWK-NN location

For each entry of location in prior table

Combine likelihood and prior

End

Get posterior location

End

Return location of highest probability from posterior location.

7. Previous location from 1 will be the initial location value.
8. Define noise covariance R as diagonal matrix with values:

$$R = \begin{bmatrix} 1 & 0 \\ 0 & 1 \end{bmatrix}$$

9. Define process noise covariance Q with values:

$$Q = \begin{bmatrix} 0.00001 & 0 & 0 & 0 \\ 0 & 0.00001 & 0 & 0 \\ 0 & 0 & 0.00001 & 0 \\ 0 & 0 & 0 & 0.00001 \end{bmatrix}$$

10. Initialize matrix A:

$$A = \begin{bmatrix} 1 & 0 & \Delta_t & 0 \\ 0 & 1 & 0 & \Delta_t \\ 0 & 0 & 1 & 0 \\ 0 & 0 & 0 & 1 \end{bmatrix}$$

11. Initialize matrix H:

$$H = \begin{bmatrix} 1 & 0 & 0 & 0 \\ 0 & 1 & 0 & 0 \end{bmatrix}$$

12. Initialize the position  $X=(x,y)^T$

13. Initial the error covariance.

14. Compute the Kalman gain

15. Correct the position estimate with input measurement from 5.

Update error covariance.

16. Repeat again step 1 for next localisation process.

## 4.6 Direction Movement and Number of Samples

Based on Section 3.3, the hypotheses can be analysed based on several factors that influence positioning accuracy. These factors are:

- Movement direction: The direction of path movement chosen is from point S to point R and vice versa. Previous results show different path movements give different shapes of error distribution along the path, even at the same TP locations.
- Number of RSSIs samples before estimation: In Section 4.2 it has been stated that the estimation level has a significant impact on improvements in accuracy.

In this work, different numbers of RSSI samples were included in this newly designed algorithm. First there were 50 RSSI samples from available APs and then this was reduced by half to 25 RSSI samples.

- Different Wi-Fi chipset: Two different devices were used during the online phase. The first mobile device uses a Qualcomm Atheros chipset which is the same Wi-Fi chipset used during the site survey, while the second device used is a Broadcom Wi-Fi chipset. The results from the two different chipsets used were then compared.
- Mixture of different levels in the positioning stage: In the early stage, basic deterministic algorithms were implemented, from basic K-NN to WKNN and EWKNN. There are two types of estimation, the first is just average based while in the second iterative Bayesian estimation is applied. In the last layer, improvements were made by implementing a Kalman filter with certain assumptions made as mentioned in Section 4.4.

#### **4.6.1 Movement Direction from Point R to Point S**

In this scenario, the performance of several algorithms on different movement directions, with different number of RSSI samples included in the algorithm calculation, and different Wi-Fi chipsets were investigated. The layout site was B floor, Infolab21, School of Computing and Communication, as shown in Chapter 3. Based on the layout, there are two ways with different directions. In the first condition, the user moves from point R to point S, and in the second condition the user moves from point S to point R. The numbers of RSSIs from APs chosen in this scenario were 25 and 50 samples. Both sample numbers were chosen based on previous simulation presented in Section 4.2,

where the number of samples must be greater than 10. The last factor mentioned is different Wi-Fi chipsets. In this scenario, two types of well-known chipsets were used, i.e. the Quantum Atheros and Broadcom chipsets.

The simulation started with movement direction from point R to point S. During the on-line phase, RSSIs were sampled at each dedicated TP location for each direction. The error distribution for each TP location is presented with different types of algorithms included in the proposed algorithm. Figure 4.9 below shows the distribution of errors for the proposed algorithm (EWKNN+Bayes+Kalman filter) compared to other positioning algorithms for movement direction R to point S, for a Qualcomm Atheros Wi-Fi chipset with 25 sample RSSIs. Based on the graph, it is clear that only two algorithms give constant error distribution of below 5 metres, which are KNN with Bayesian estimation and EWKNN with Bayesian estimation and a Kalman filter. With the deterministic algorithm K-NN and WKNN, location error rises suddenly at more than 20 metres from TP points 6 to 10. It is clear that a combination of uncertain RSSI values from APs causes the location error distribution to fluctuate. The newly designed algorithm, which works based on a localisation region, performed well to contain errors in this kind of situation but with a short period of huge localisation errors from point 6 to point 10.

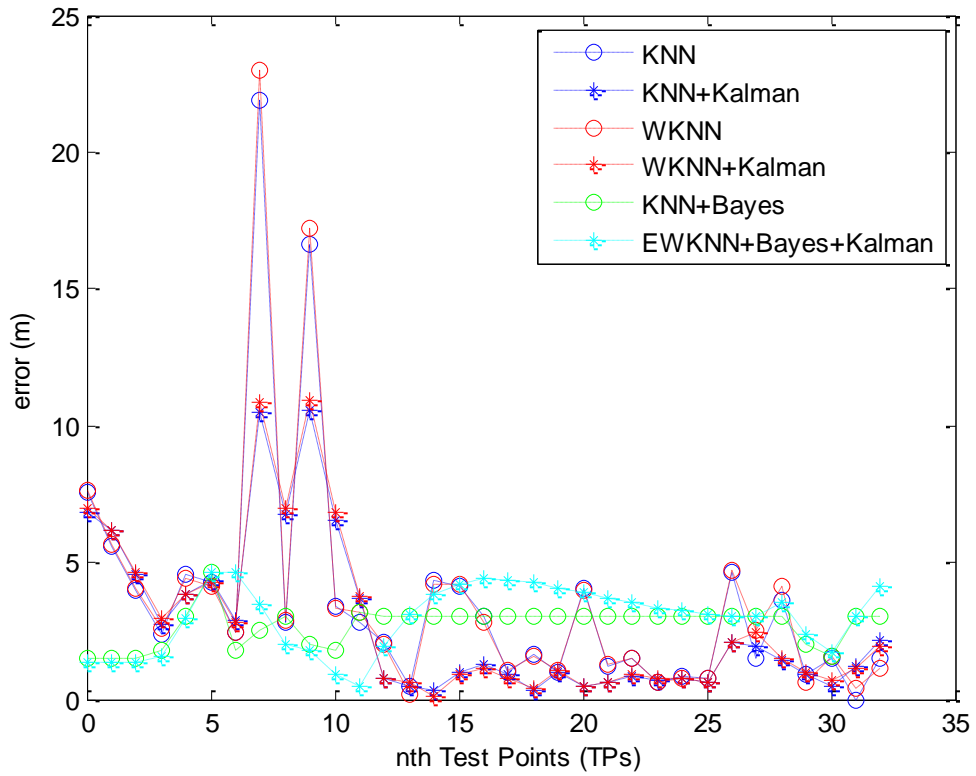


Figure 4 9: Error distribution for a Qualcomm Atheros Wi-Fi chipset with 25 RSSI samples.

Figure 4.10 depicts the distribution of errors from an algorithm comparison as shown in Figure 4.9 but with doubled number of RSSIs, up to 50 samples. Based on both graphs in Figures 4.9 and 4.10, it can be seen that they are almost identical. The errors in positioning reach above 5 metres at the same TP point locations, which are from point 6 to point 10 for a normal deterministic algorithm, even though RSSI samples are doubled what they were before.

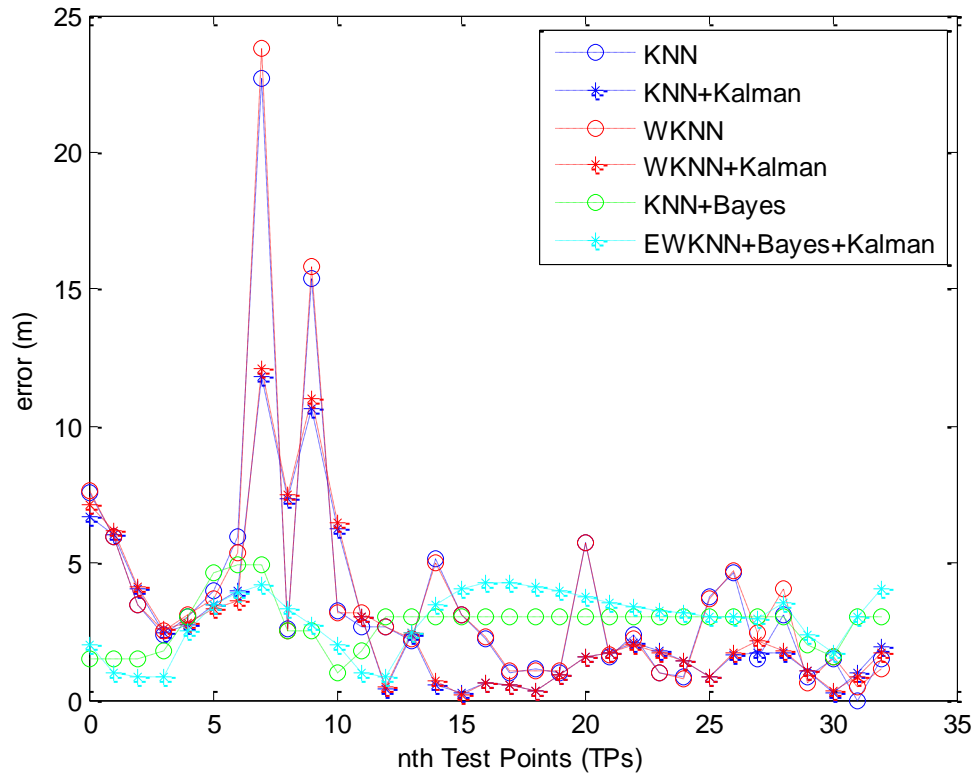


Figure 4.10: Error distribution for a Qualcomm Atheros Wi-Fi chipset with 50 RSSI samples.

Figure 4.11 depicts the distribution of average RSSI measurements from four different MAC address available on RPs location during offline phase (blue colour) and online phase (red colour). The vertical red dotted line show the RP location that return highest location error on deterministic algorithms. The average RSSI from available APs on online phase is approximately -74dBm and -62dBm, while the average RSSI during site survey is -68dBm and -58dBm (highlighted in blue region). The horizontal red dotted line show that the RSSI measurement of -74dBm and -62dBm in term of distance is closer to other RSSI measurement at RP number 44, 45 and 46. As a result, single layer positioning algorithm like conventional deterministic methods return higher location error up to 24m caused by selection of wrong RPs location. In contrast, the proposed algorithm with dynamic localisation region implementation only selects the

adjacent RPs' location from the update lookup table during localisation. The highest return probability in this dynamic localisation region will determine the approximate user location. This will keep the margin of error in control for each localisation process.

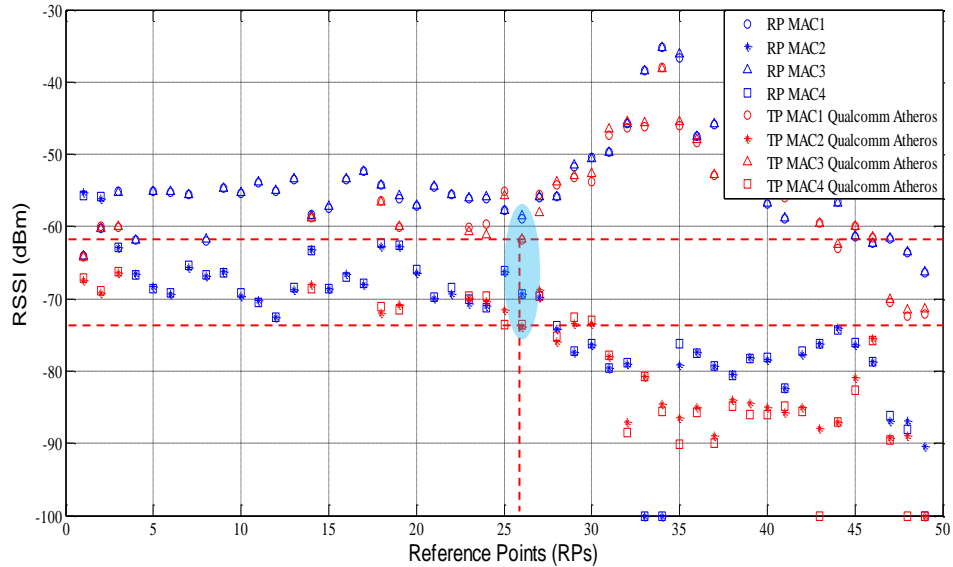


Figure 4.11: Average RSSI distribution during offline phase and online phase.

Based on distribution of location errors of conventional deterministic algorithms in Figure 4.9 and Figure 4.10, the areas that contribute to higher error in location estimation were traced on the layout. Figure 4.12 below shows the layout area where the online phase has been conducted. The green boxes show the area location of TPs with return of location estimation below 5 metres, while the red boxes show the area with conventional deterministic algorithm estimates of more than 5 metres of error. One of the reason that the areas were returning high error due to the fact that the signal from the APs to that particular region was not in line-of-sight (LOS). The geometry of the building in these cases in which the wall blocks the signal propagation at multiple times degraded the signal strength of the RSSI. The destructive and constructive due to

multipath fading also contributes to the fluctuation of the signals strength reading in RSSI from the APs.

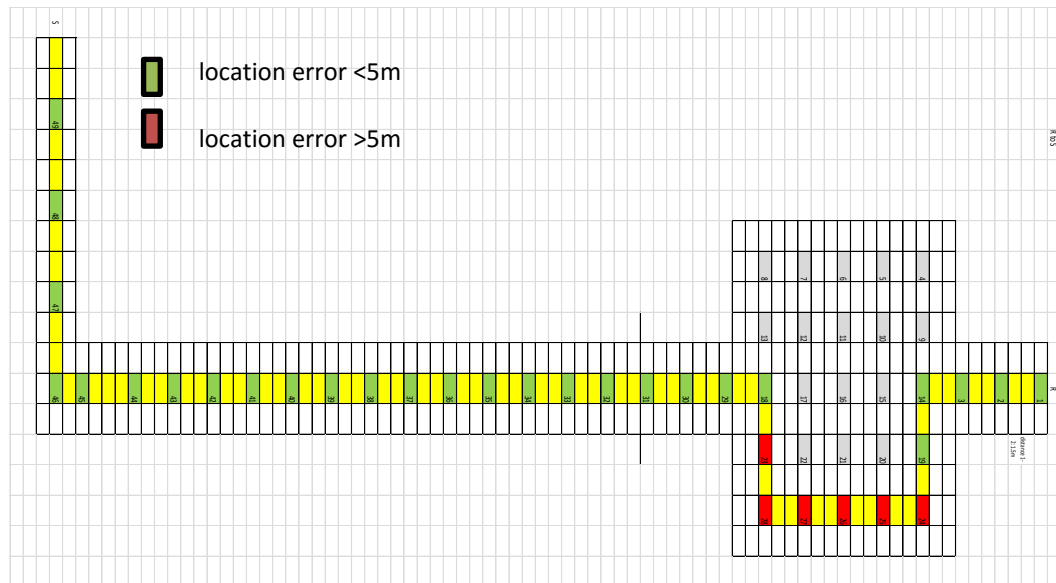


Figure 4.12: Accuracy map on layout building for Qualcomm Atheros chipset.

Next, error distribution using the same algorithm based on 25 RSSI samples was plotted using a Broadcom Wi-Fi chipset. The results in Figure 4.13 show different error distribution patterns compared to Figure 4.9 which is based on a Qualcomm Atheros chipset. Based on the graph, a conventional K-NN and WKNN algorithm shows that positioning errors start to hit 5 metres from TP points 21 to 29. In this scenario, gradually increasing errors are the main reason that both K-NN with Bayesian estimation and EWKNN+Bayes+Kalman filter algorithms follow the same pattern. This is because in a conventional deterministic algorithm, there is increasing location error from TP point 21 onwards, where the localisation region calculated keeps the process in the wrong region. Therefore, with the proposed algorithm (EWKNN+Bayes+Kalman Filter), positioning error also increases gradually like the conventional deterministic algorithm.

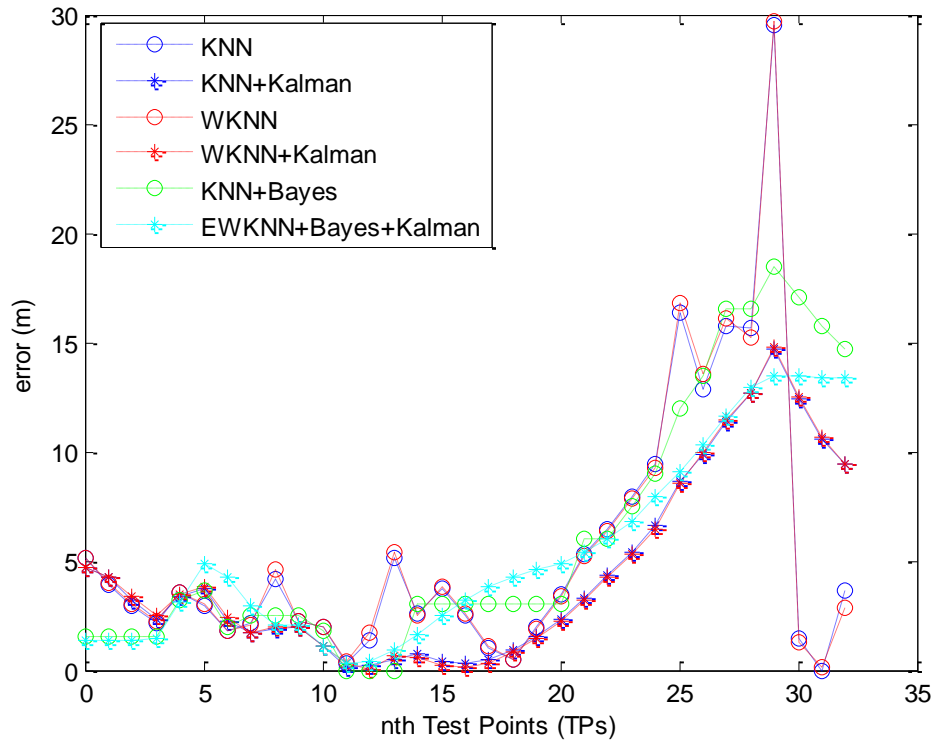


Figure 4.13: Error distribution for a Broadcom Wi-Fi chipset with 25 RSSI samples.

Figure 4.14 depicts a graph of error distribution for various positioning algorithms using the same Broadcom Wi-Fi chipset, but with doubled number of RSSI samples. Roughly, the graph patterns are very similar to the graph in Figure 4.13.

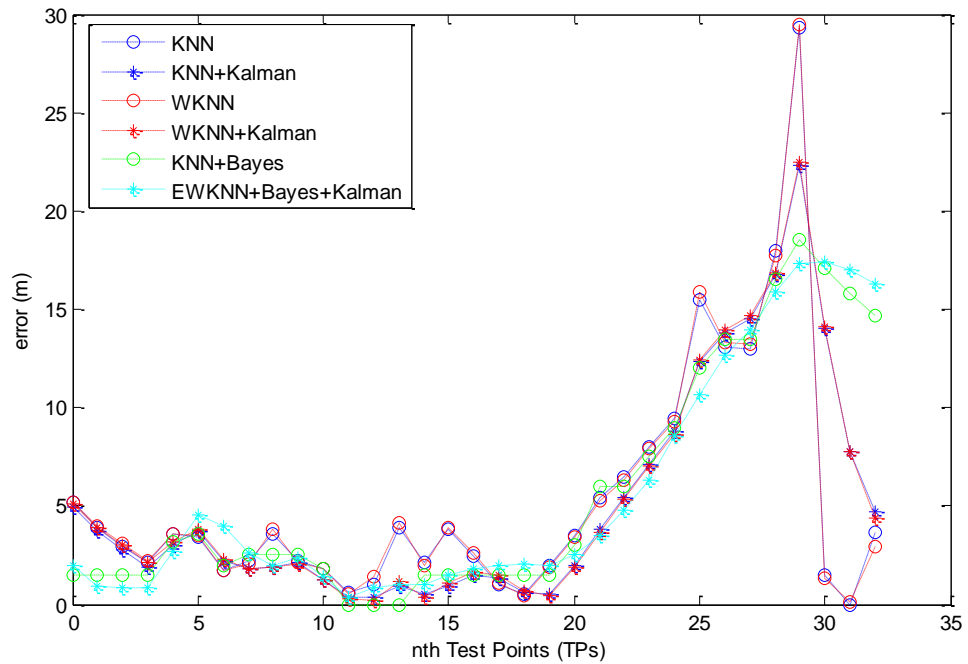


Figure 4.14: Error distribution for a Broadcom Wi-Fi chipset with 50 RSSI samples.

Based on error distribution in Figure 4.13, the different distribution of RSSI between offline phase and online phase was looked into details. Figure 4.15 depicts the distribution of average RSSI measurement from four different MAC address available on RPs location during offline phase (blue colour) on Qualcomm chipset and online phase (green colour) on Broadcom Wi-Fi chipset. The vertical red dotted line show the RP location that return highest location error on deterministic algorithms. Based on RSSI distribution at all RPs location, it can be seen that there are obviously different RSSI measurements using Qualcomm Wi-Fi chipset during offline phase and measurement on Broadcom chipset during online phase. This shows that different Wi-Fi chipset manufacturers have different sensitivity levels. The different patterns are hard to judge as some locations give almost similar reading while some places give a difference of up to  $\sim 20$ dBm. The horizontal red dotted line show that the RSSI measurement of  $-55$ dBm,  $-55$ dBm,  $-66$ dBm and  $-68$ dBm in term of distance is closer to other offline

RSSI measurement. Due to this factor, whenever the deterministic algorithm is applied, it tends to pick up the nearest distance RSSI measurement at the other RPs location which leads to error in location of up to 30 metres as shown in Figure 4.13 and Figure 4.14.

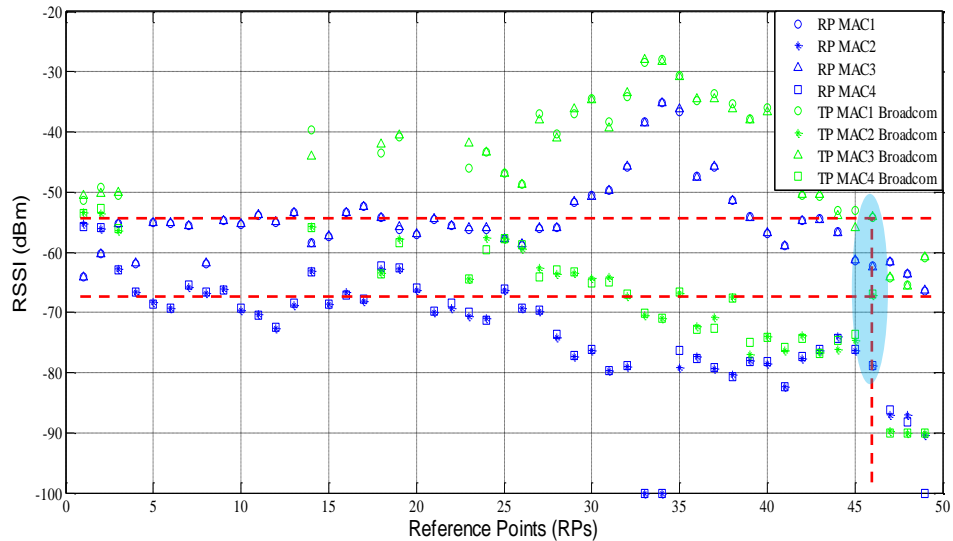


Figure 4.15: Average RSSI distribution during offline phase and online phase.

Based on the results in Figure 4.13 and Figure 4.14, the conventional deterministic algorithm that contributes to higher error in location estimation was traced on the layout area. Figure 4.16 below shows the layout area where the online phase has been conducted. The green boxes show the area location of TPs that give return of location estimation below 5 metres, while the red boxes show the area with conventional deterministic algorithm estimates of more than 5 metres location error. As explained on RSSI distribution in the previous graph, the different sensitivity levels of both Qualcomm and Broadcom Wi-Fi chipset leads to different area of position during the location estimation process.

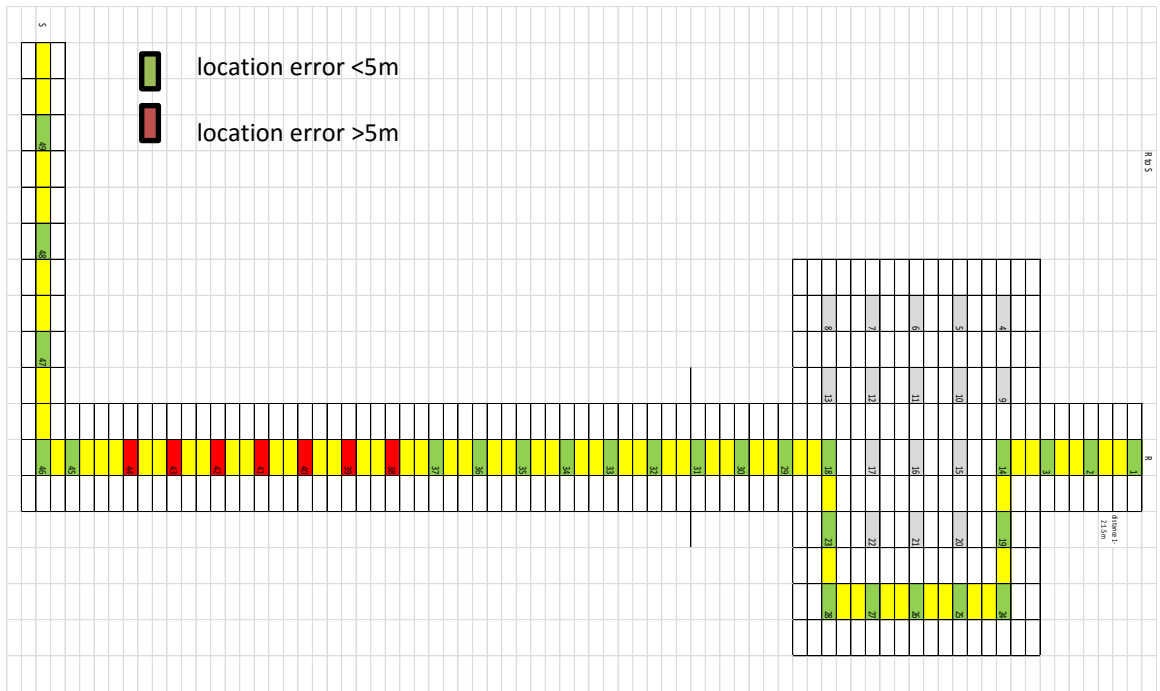


Figure 4.16: Accuracy map on layout building for Broadcom chipset.

#### 4.6.2 Movement Direction from Point S to Point R

The error distribution patterns at the same TP locations were then compared to the previous results in Section 4.6.1, but with movement in the opposite direction. From Figure 4.17 below, it can be seen that the patterns of error distribution are a little bit different, even when using the same Wi-Fi chipset and number of RSSI samples. This is because when movement direction is in the opposite direction, the blockage and reflected signals do not follow the same path as before. The user's body and antenna radiation pattern could give readings of signal strength at different levels, thus giving different positioning accuracy, even at the same location. In this scenario, the proposed algorithm performs well below 5 metres, until it reaches TP point 18. However, from this point onwards, the overall distribution is still slightly better than with basic deterministic techniques.

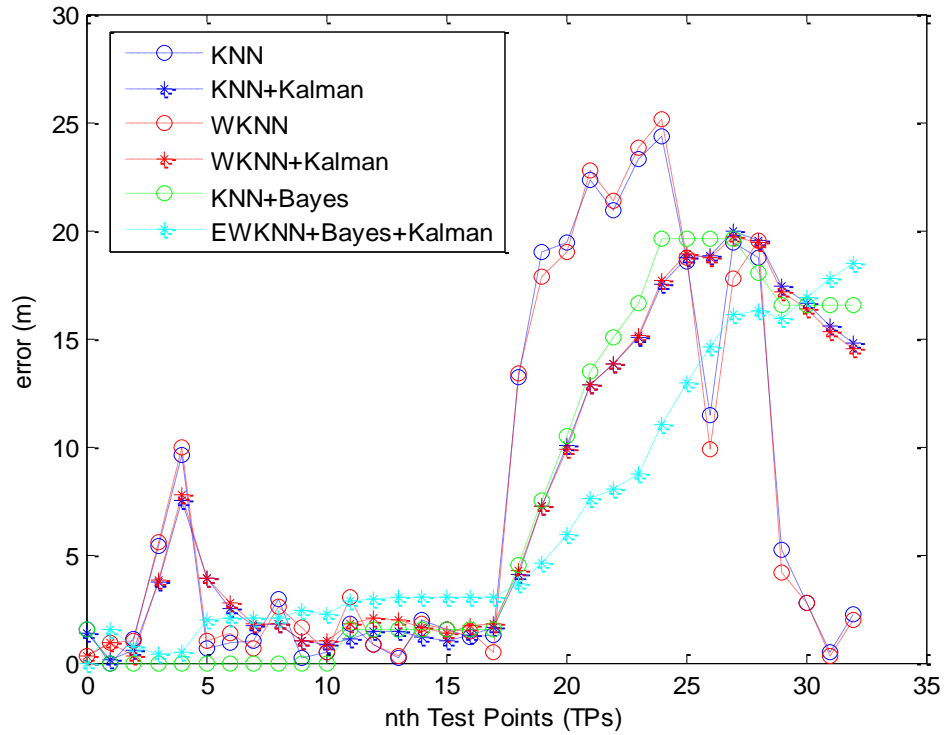


Figure 4.17: Error distribution for Qualcomm Atheros Wi-Fi chipset with 25 RSSI samples.

The number of RSSI samples processed was then doubled to 50 samples at each location and the error distribution for each algorithm is as depicted in Figure 4.18. The error distributions for each algorithm, in Figures 4.16 and 4.17, show very similar patterns.

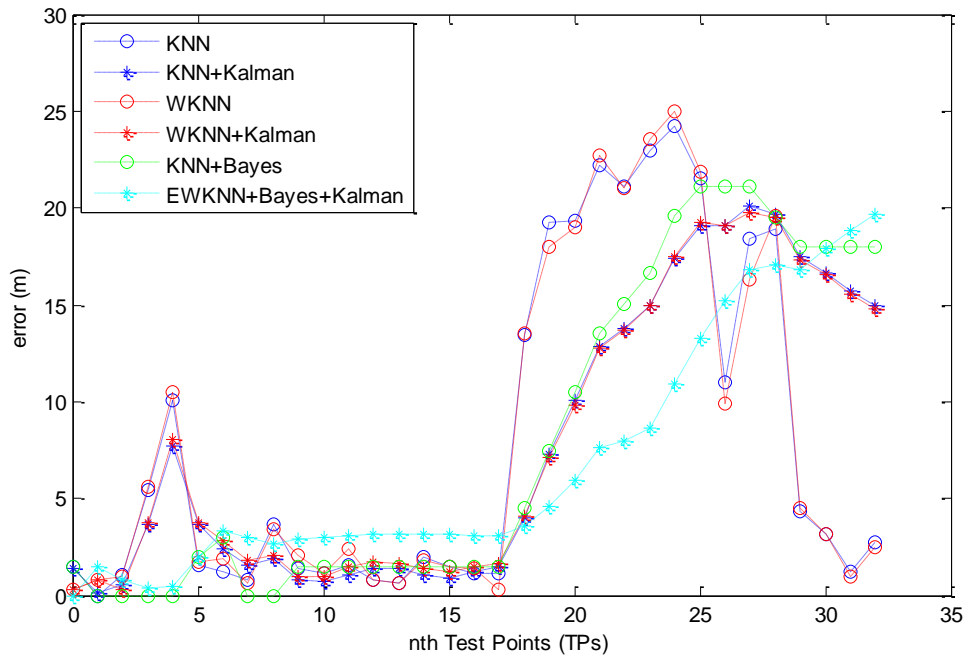


Figure 4.18: Error distribution for Qualcomm Atheros Wi-Fi chipset with 50 RSSI samples.

The scenario of how the location error is high after TP 17 was analysed in term of RSSI distribution. Figure 4.19 depicts the distribution of average RSSI measurement from four different MAC addresses available on RPs location during offline phase (blue colour) and online phase (red colour). Both measurement phases are based on the same Wi-Fi chipset which is Qualcomm Atheros. Based on Figure 4.17, it was found that the highest location error on TP 17 is related to RP number 27 (vertical red dotted line) on Figure 4.19. This is because the closest distance of RSSI at RP location 27 to RSSI referring to offline phase (blue colour) are at RP location number 42, 44 and 45. As a result, the location estimation of K-NN and WKNN algorithms selected this 3 RPs point as the nearest distance and returned high error compared to the actual user position.

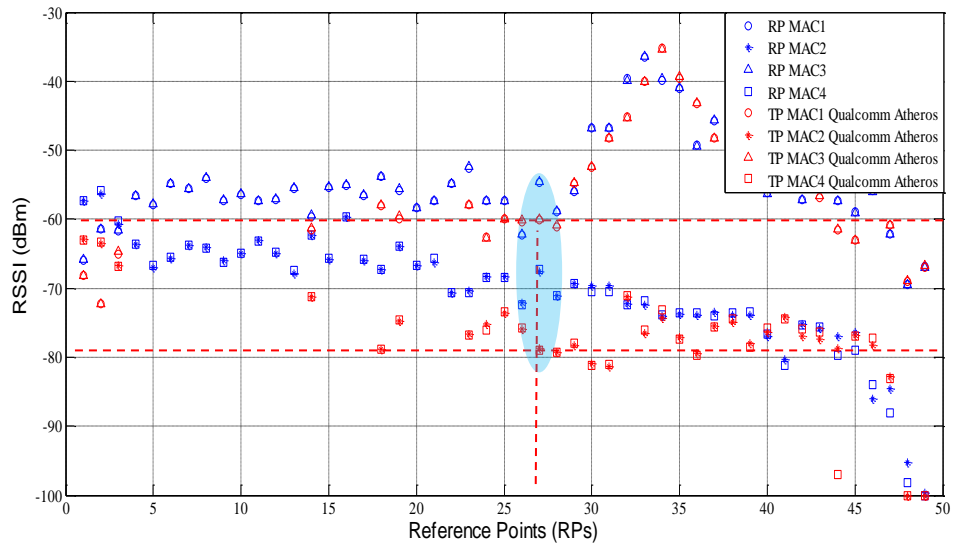


Figure 4.19: Average RSSI distribution during offline phase and online phase.

Based on the error distribution in Figure 4.17, the deterministic algorithm that contributes to higher error in location estimation was traced on the layout area. Figure 4.20 below shows the layout area where the online phase has been conducted. The green boxes show the area location of TPs that return the location estimation below 5 metres, while the red boxes show the area where conventional deterministic algorithm estimates more than 5 metres location error. The locations that contribute to higher error in location are almost in the same region as shown in Figure 4.16 but with slightly broader region. This shows that the opposite movement direction have a slight difference in error location area.

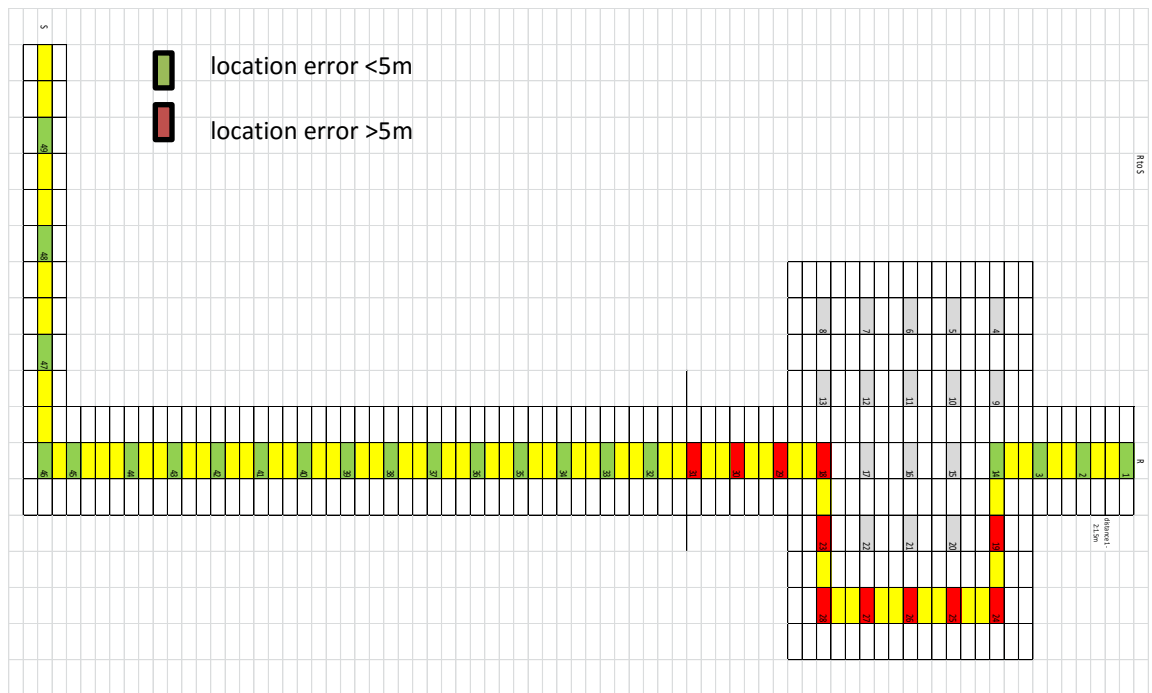


Figure 4.20: Accuracy map on layout building for Qualcomm Atheros chipset

The proposed algorithm performs very well along the path from point S to point R, as depicted in Figure 4.21. The location error is always below 5 metres for all TP locations. From TP point 3 to point 13, it can be seen that the output results from the KNN+Bayes algorithm suddenly rise from almost zero positioning error to 5 metres of errors. However, the output from EWKNN+Bayes+Kalman filter gradually increases for error location. This is the effect of the design Kalman filter which balances the output between prediction and measurement values.

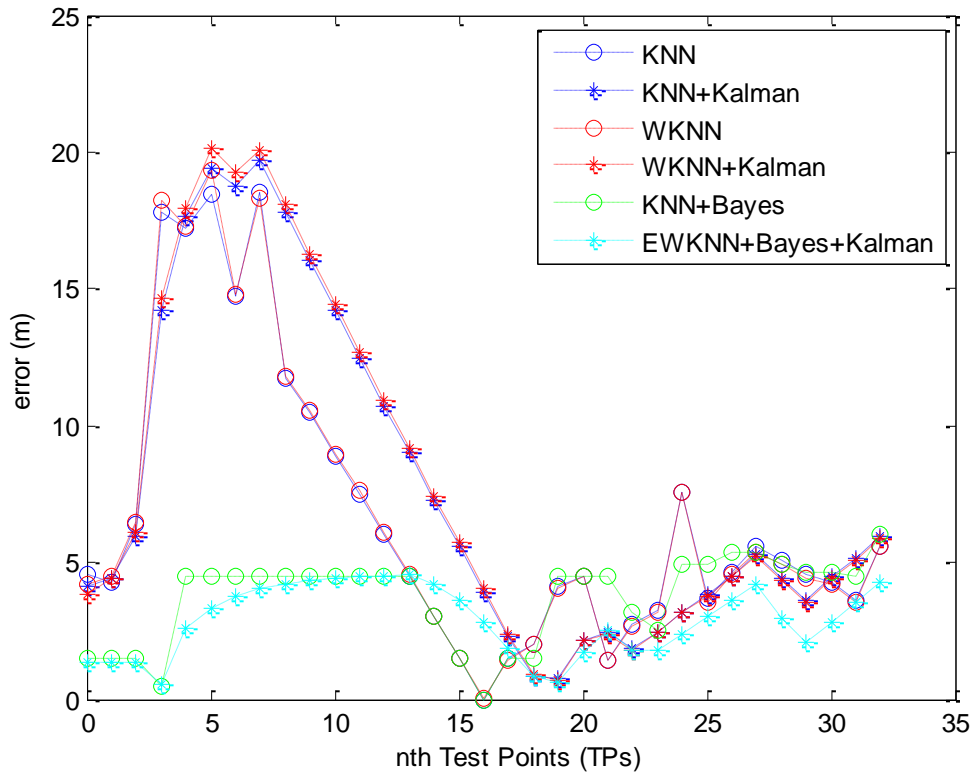


Figure 4.21: Error distribution for Broadcom Wi-Fi chipset with 25 RSSI samples.

Figure 4.22 shows the results for positioning error from 50 RSSI samples using measurements from a Broadcom chipset. Mostly, the error distribution shows similar patterns as in Figure 4.21.

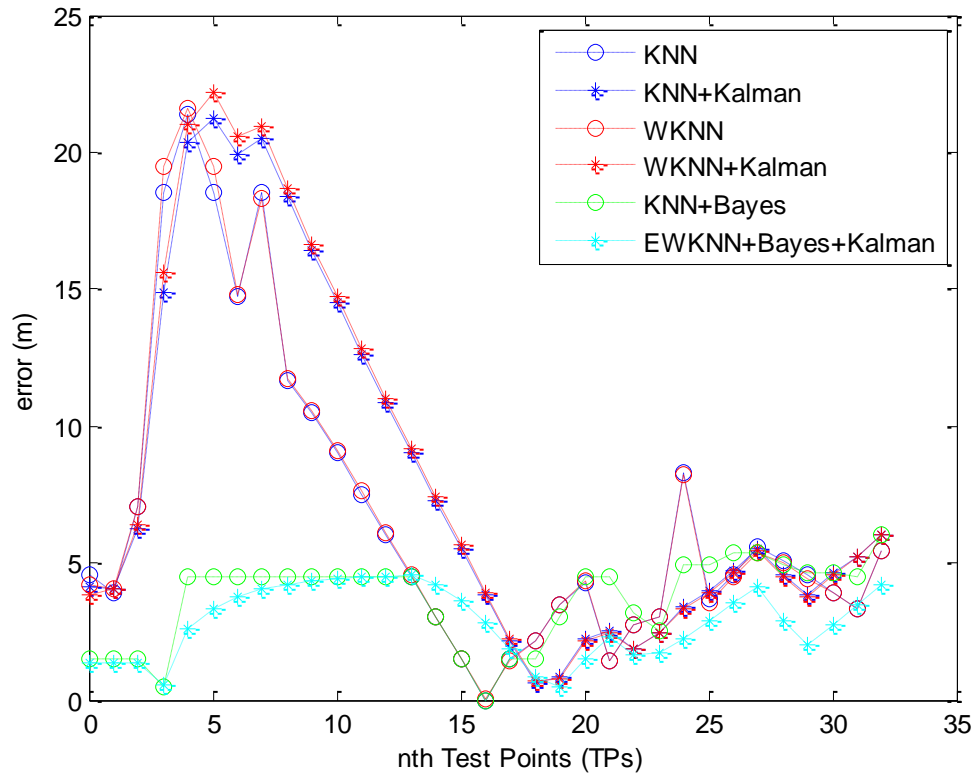


Figure 4.22: Error distribution for Broadcom Wi-Fi chipset with 50 RSSI samples.

Figure 4.23 depicts the average RSSI distribution during offline phase and online phase on different Wi-Fi chipset for direction movement from S to R point. The vertical red dotted line show the RP location that return highest location error on deterministic algorithms. Based on Figure 4.21, the largest location error is on TP number 5 which corresponds to RP number 44. It can be seen clearly that at the same RP location, both Wi-Fi chipset give different level of signal strength. As a result, the difference between offline and online measurement is almost 15dBm at the same location and from the same AP. This larger difference leads the K-NN algorithm to choose the closest distance of RSSI on different RP at number 18, 23, 30 and 31 which is far from the actual location. Consequently, the wrongly chosen RP location leads to estimation of the wrong location.

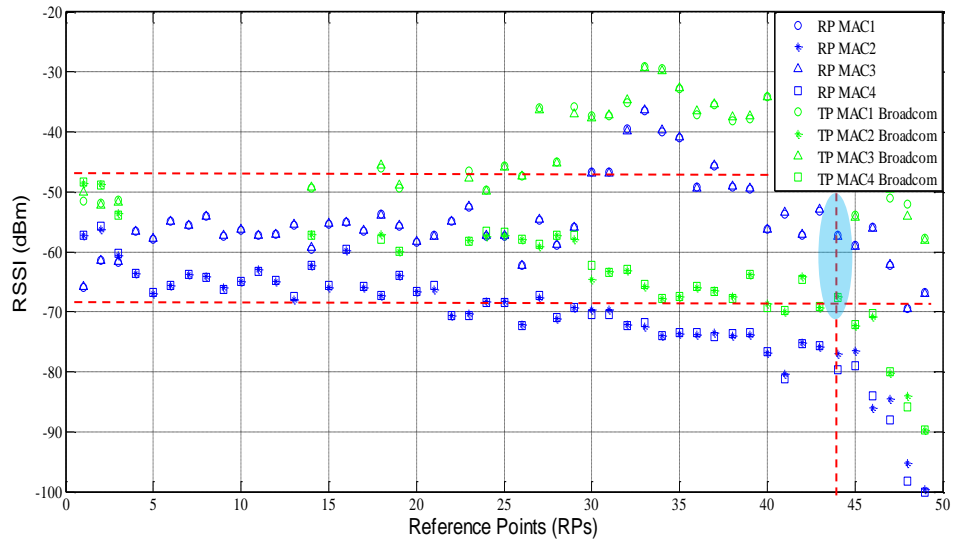


Figure 4.23: Average RSSI distribution during offline phase and online phase.

Figure 4.24 shows the areas that contribute to high estimation error based on Wi-Fi deterministic algorithm. The red boxes show the points that have error in estimated location higher than 5 metres. As explained before on RSSI distribution on previous graph, the different sensitivity level of both Qualcomm and Broadcom Wi-Fi chipset leads to different area of position during location estimation process.

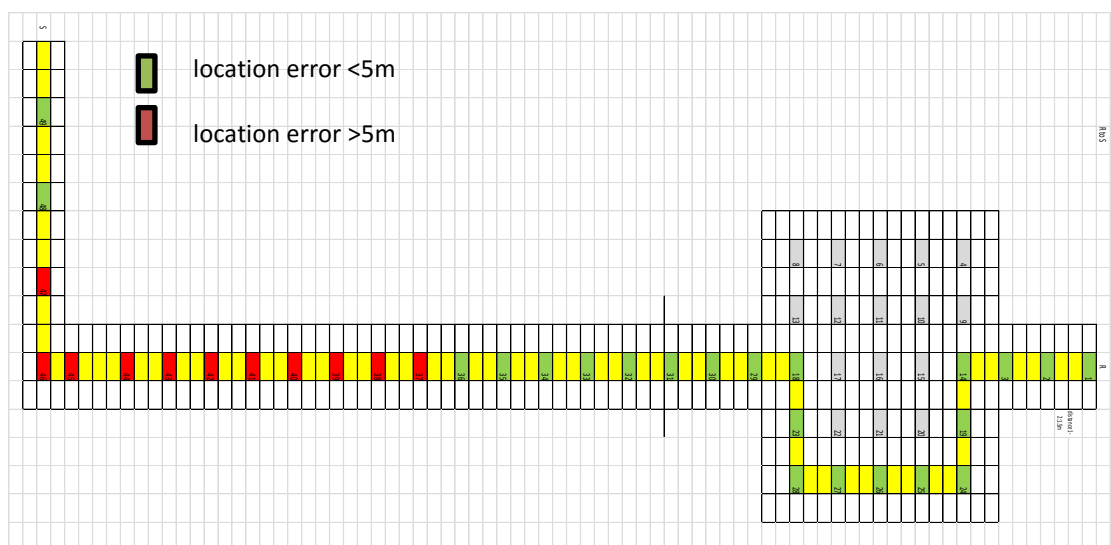


Figure 4.24: Accuracy map on building layout for Broadcom chipset.

## 4.7 Overall Results

The accumulated accuracy of eight combinations with different kinds of parameters, such as the number of RSSI samples, Wi-Fi chipsets and movement direction are presented in Table 4.2. Eight different scenarios give different patterns of error distribution, as shown in Sections 4.6.1 and 4.6.2. As can be seen, the effects of double the number of RSSI samples for all the scenarios are almost insignificant. Figures 4.16 to 4.22 show that the patterns of error distribution are very similar. The accumulated accuracy in Table 4.2 shows that across all algorithms for both 25 and 50 RSSI samples, the numbers are very close. This shows that even increasing the number of RSSI samples does not significantly improve positioning accuracy. And in some cases, positioning accuracy results are better with fewer RSSI samples. In four out of eight scenarios, the accumulated accuracy shows that other algorithms are better than the proposed algorithm. However, in total, the proposed algorithm gives better overall positioning accuracy.

Table 4.2: Accumulated accuracy of different algorithms.

Direction	Wi-Fi Chipset	Number of RSSIs samples	Algorithms					
			K-NN	WKNN	K-NN + Kalman Filter	WKNN + Kalman Filter	K-NN + Bayesian estimation	EWKNN + Bayesian + Kalman Filter
Point R to Point S	Qualcomm Atheros	25	118.528	121.7752	101.7806	103.4829	90.4909	92.7658
		50	125.6128	128.8719	106.3673	107.8658	92.1453	94.2072
	Broadcom	25	179.7866	181.2023	147.4695	147.2358	198.1297	176.1536
		50	176.8632	177.4372	149.6832	148.2570	186.1297	161.4242
Point S to Point R	Qualcomm Atheros	25	254.0451	253.2184	255.9532	258.6883	242.091	215.4907
		50	260.3334	259.4693	256.0950	258.0509	262.0671	226.8049
	Broadcom	25	219.5944	220.535	254.8172	257.7336	121.9718	95.8129
		50	223.9111	225.4635	264.5392	268.6933	120.4718	94.1010

Based on all the simulation results in Table 4.2, the CDFs of positioning error for the various algorithms were generated as illustrated in Figure 4.25. It can be observed that the proposed algorithm which is combination of EWKKN, Bayesian estimation and Kalman filter with dynamic localisation region performed the best with location error of less than 5m for 65% of the time, whereas conventional deterministic (K\_NN and WKNN) with Kalman filter gave 48%. The basic K-NN and WKNN gave location error of less than 5m for 45% of the time. This shows that implementation of Kalman filter gave improvement to the deterministic technique with 3%, while the proposed algorithm did improve the CDF by 20% more.

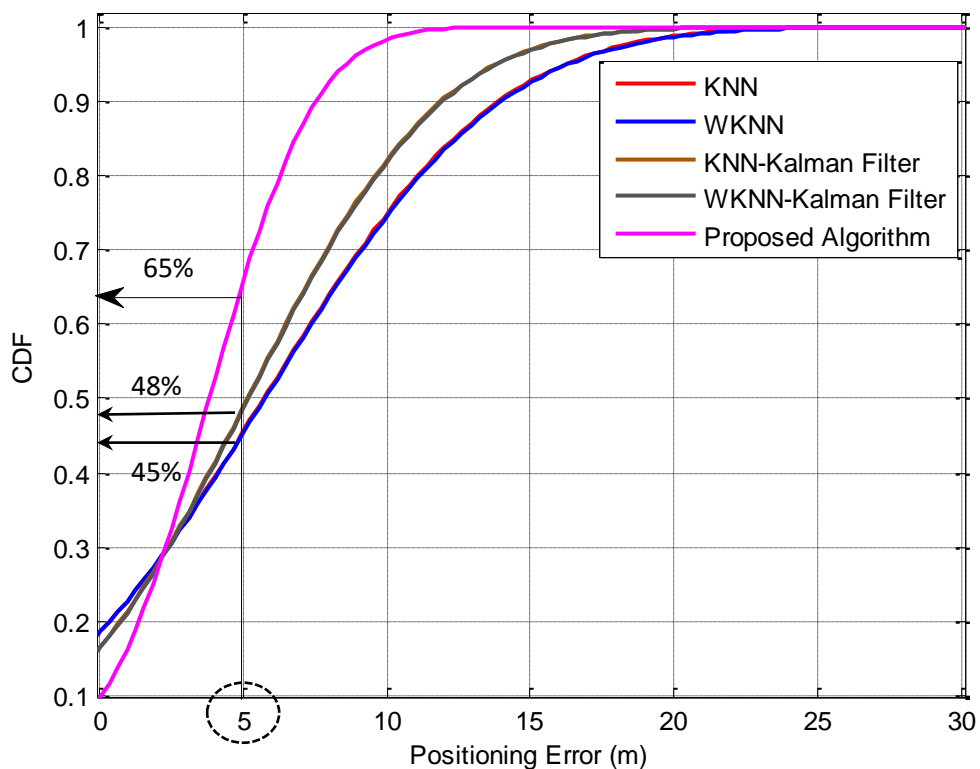


Figure 4.25: Performance positioning error comparison between proposed algorithm and several location estimation algorithms.

## 4.8 Summary

In this chapter, an integrated location-estimation algorithm simulated with real RSSIs measured at each TP location has been elaborated. As mentioned in Chapter 3, the site survey was of a real situation where the number of APs was limited and there was uncertain coverage, the positions of APs have been determined earlier and with various shapes of building geometry. Several simulation Wi-Fi deterministic fingerprint techniques (with  $k=3$ ) have been compared with the proposed algorithm. A few factors have been investigated, such as the number of RSSI samples included in the simulation, different Wi-Fi chipsets and different path routes. The output results of the proposed algorithm were compared against conventional approaches: K-NN, WKNN, K-NN + Kalman filter, WKNN + Kalman filter. The results of the entire algorithm have been analysed based on location error distribution pattern graphs and accumulated accuracy. Based on all the various scenarios, it was found that the proposed algorithm worked the best in terms of average positioning error. Increasing the number of RSSI samples did not significantly improve the location accuracy. The early hypothesis is proved where movement direction and heterogeneous Wi-Fi devices have influence on location accuracy. Furthermore, the distribution location error on certain area for deterministic method have been analysed in term of RSSI distribution for both offline and online phase. It can be seen that at some point, the distance selection from deterministic algorithm picked up wrong location. Here, the proposed algorithm which is an integrated EWKNN, Bayesian estimation and Kalman filter together with implementation of *dynamic localisation region* did improve the CDF of location error by 20% of the time for error of less than 5m. At this stage, the use of dynamic coefficient as possible correction on location error is not used in this research which is

out of scope. A few ideas to utilise the statistical information from RSSI distribution will be discussed in section 6.2.

# **CHAPTER 5: Enhanced Indoor Positioning Utilising QR Calibration**

## **5.1 Introduction**

In the previous chapter, a new integrated Wi-Fi indoor positioning based on fingerprint have been proposed. Unlike other forms of single layer Wi-Fi positioning, the combination of these three techniques gives an overall performance that is more immune to fluctuation in RSSI which causes errors to increase along with path movement. This algorithm has been designed to match with calibration point to prevent error from being accumulated. QR code calibration will be introduced in this chapter, and the area of QR code location will be identified to get effective indoor positioning.

## **5.2 Location Based Calibration (LBC)**

The proposed Wi-Fi fingerprint algorithms in the previous chapter not only take into account how to minimise the effect of error fluctuation, it is also designed to suit the purpose of calibration. As mentioned before, the use of QR code in Wi-Fi positioning has been proposed by other researchers [109][55]. However, the functions of a location estimation algorithm and calibration are quite separated from the beginning. A calibration point only tells the system the correct or actual position of a user at a particular calibration position; after that, the positioning algorithm starts to resume the function of Wi-Fi fingerprint positioning without remembering the last calibration point.

To enhance the accuracy of the Wi-Fi fingerprint algorithm along with path movement, the proposed algorithm combines the two most influential groups in positioning, which are signal-based positioning and vision-based positioning [14]. Most of the current devices integrate various kinds of sensors [60], therefore utilising these sensors might improve location accuracy. The main types of positioning are signal-based positioning, Wi-Fi fingerprint positioning as explained in Chapter 4, and vision-based positioning which utilises a vision sensor. In this work, a calibration point utilising QR code is proposed. Figure 5.1 depicts a block diagram showing integration between signal-based positioning and vision-based positioning.

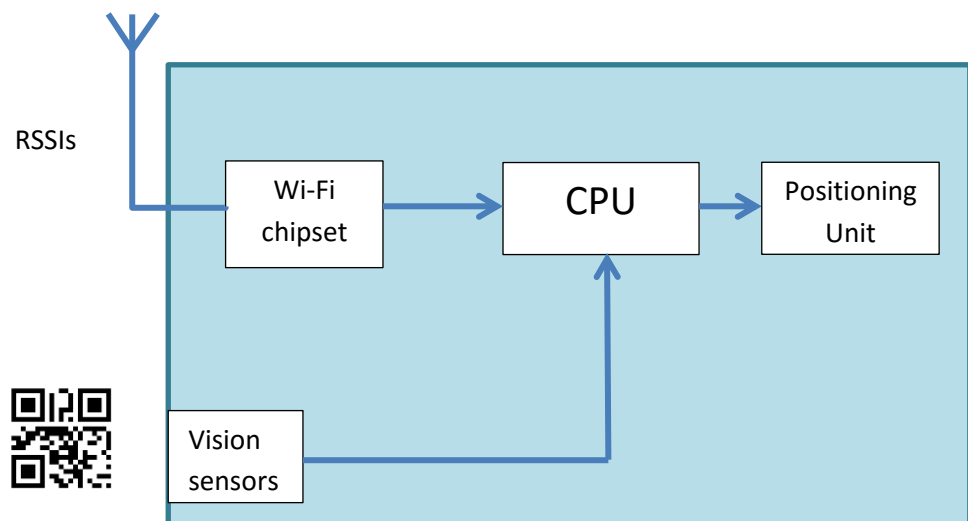
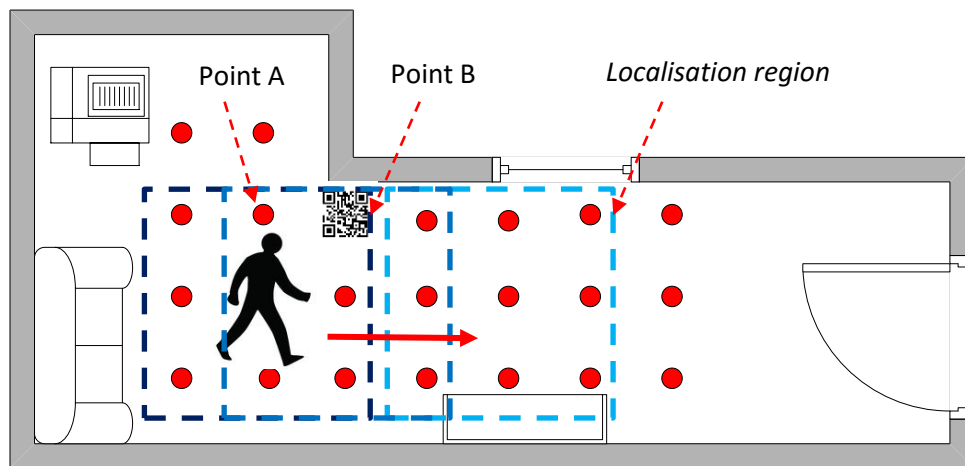


Figure 5.1: Block diagram of a combination of W-Fi fingerprint technique and QR vision-sensor-based calibration.

In addition, our previous developed algorithm was designed to suit the purpose of calibration from the beginning. This is done by utilising the *localisation region* from a previously known location. Imagine that a user walk into a large building and move from one point to another point. User devices will scan for any RSSIs from all access

points available and try to find the closest match with RSSI distribution stored earlier in user devices. The closest match will return the position of particular RSSI from a previous offline phase. Then, this estimation position will be kept in memory and later used in the next time cycle. Before the next position is calculated, based on iterative Bayesian estimation, all adjacent reference points' positions near the current positions which are stored in memory will be evaluated for the highest probability point. These adjacent reference points' positions are called the confinement area, where it is believed that the user may still be in. The maximum probability at a particular point in the *localisation region* will return the estimated user location. The process will be repeated in the next cycle to determine the user's position. After several localisation processes, location errors estimated from the beginning can accumulate, as the exact user location is not known. Figure 5.2 depicts an example of a building layout with a user walking to the right through reference points assigned during the off-line phase.



● Reference points (RPs)

Figure 5.2: Building layout and *localisation region* with QR calibration.

### 5.2.1 Algorithm Description

Let say the user is at point A as depicted in Figure 5.2, estimated by the previous algorithm as mentioned in Chapter 4. At this estimated location, the position could be the exact location or perhaps contains some error. If there is a mistake in location estimation before, that means the area of confinement is not exactly as accurate as desired.

When the user moves to the next position, say B position, there is a QR calibration point. The user then scans the QR code and information about the exact current location can be retrieved. This valuable information will be used by the algorithm to update the exact current location and set a new *localisation region* by referring to an adjacent reference points table. This current area of localisation is seen to be highly accurate, which consists of several reference points.

Next, the user will move to another nearest reference point which is still in the right *localisation region*. Enhanced weighted-KNN (EWKNN) is then executed to estimate the initial user location. Then, iterative Bayesian estimation will “compare” the initial position estimated by EWKNN with every single reference point in the localisation region. The output will be a probability value for each reference point’s location in this area. The highest probability point may be the nearest location of the user’s position. If there is an error in position estimation, it is still very low as the initial calculation of points is only in the right confinement area. This is how the algorithm works seamlessly with QR code for calibration.

As the user scans the QR code, location error is reset to zero. Now the exact location is known, and a new localisation region of adjacent reference points can be referred in the lookup table. When the user moves to other nearest reference points, the estimation of user location will be calculated, and the *localisation region* of reference

points will be updated. The possibility of position error based on the estimation of new locations will be reduced at this time, because the exact location before is already known, thus the exact user location should be in the region of the confinement area. Furthermore, the error location is definitely about the size of the *localisation region*. If the estimated position appears to be the exactly the true location, this means in the next localisation there could be a high possibility of low location error because the right *localisation region* is still in place.

The process will be repeated in the next cycle and will as a whole improve accumulated accuracy for indoor positioning. Therefore, several integrated layers of a positioning algorithm consist of deterministic EWKNN for initial positioning calculation, finding the best match between online RSSI values and offline RSSIs, and iterative Bayesian estimation to further improve position estimation with an updated *localisation region*, which works well with QR calibration code. Figure 5.3 depicts an algorithm flowchart for enhancing a Wi-Fi fingerprint with QR calibration.

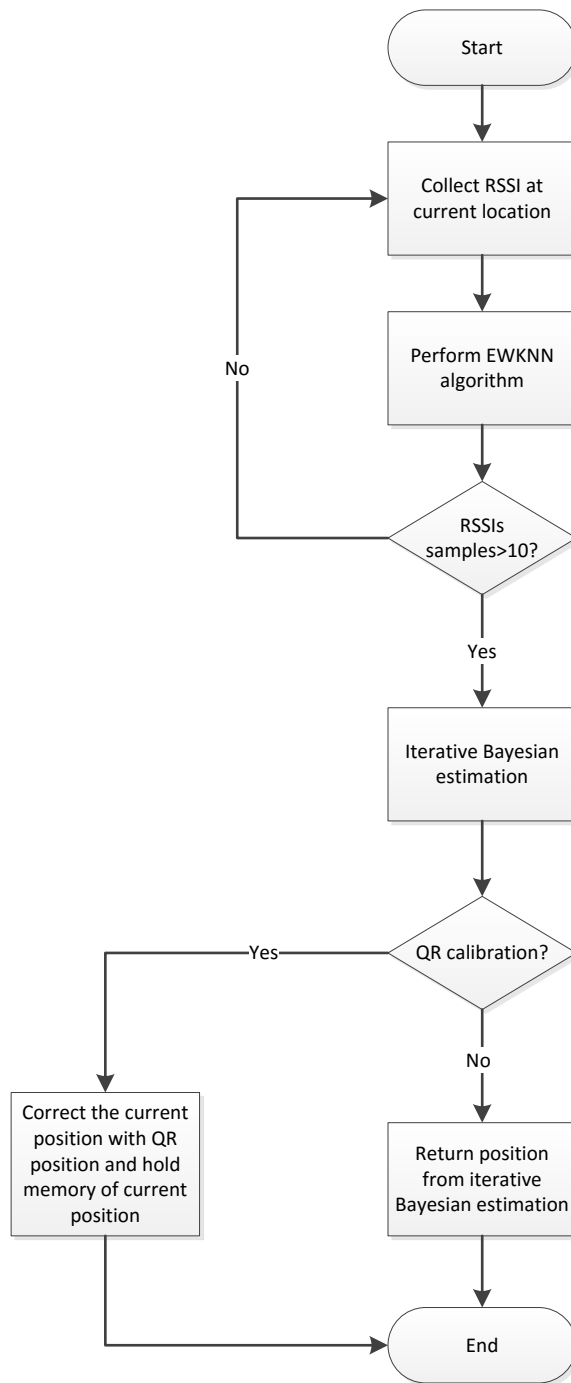


Figure 5.3: Flowchart of algorithm to enhance Wi-Fi fingerprint with QR calibration.

## Algorithm

1. Get previous location
2. Sample RSSI
3. For each RSSI > 10
  - Estimate location based on EWK-NN
  - End
  - Return early location
4. Update prior state location and assign localisation region.
5. Update table of possible location based on localisation region.
6. Assign uniform probability on each possible location in localisation region.
7. Calculate likelihood of possible state location.
  - For each location based on EWK-NN
    - For each entry of location in prior table
      - Combine likelihood and prior
      - End
      - Get posterior location
    - End
    - Return location of highest probability from posterior location
8. If there is input from QR code, decode the QR code information
  - Get the position of QR code location
  - Update the location region from QR information
  - Update the table of possible location based on QR information
  - Else
  - Return position from iterative Bayesian estimation
9. Repeat step 1 on next cycle

10. End

### **5.2.2 Results of Location Based Calibration (LBC)**

This section presents the results achieved in the simulation. The simulation was conducted in the Infolab21 building, and the layout details can be seen in Chapter 3. The RSSIs were collected at TP locations on Level B, Infolab21, and a few scenarios have been created to evaluate the performance of the proposed algorithm.

As shown in Chapter 4, applying iterative Bayesian estimation needs a sample of at least 10 RSSIs in order to get consistent and accurate results. Therefore, at each TP point, we sampled up to 25 RSSI values before estimating the user's position. On top of that, RSSIs measurements were taken in different movement directions as it is known that this will give different error distributions and so this is good to test the algorithm. Here, the user moved in a certain direction, from point R to S, and back again. And again, a different type of Wi-Fi chipset was used in each direction to evaluate the algorithm's performance. This is because different Wi-Fi chipsets have different sensitivities and reactions to RSSIs readings and thus will give different patterns of accuracy.

The results showing the error distribution along the path movement for the algorithm are described in section 5.2.1. A comparison has been made with a deterministic K-NN algorithm as this is basic and popularly used in Wi-Fi fingerprinting [80], [12], [110]. Another comparison was made with K-NN implemented with a Kalman filter, as explained in Chapter 4.

### 5.2.2.1 Point R to Point S – Qualcomm Atheros

In this section, part of the simulation results for the same algorithms are presented in two different graphs. The first graph is an algorithm comparison without any calibration point, while the second graph is an algorithm comparison with QR calibration. Figure 5.4 depicts a comparison of algorithms between K-NN, K-NN with a Kalman filter and EWKNN with Bayesian estimation without any calibration point. As discussed in Chapter 4, the deterministic technique which was used, EWKNN, is integrated with iterative Bayesian estimation and is more reliable than the other two algorithms. It gives fewer error spikes and keeps the error distribution below 5 metres.

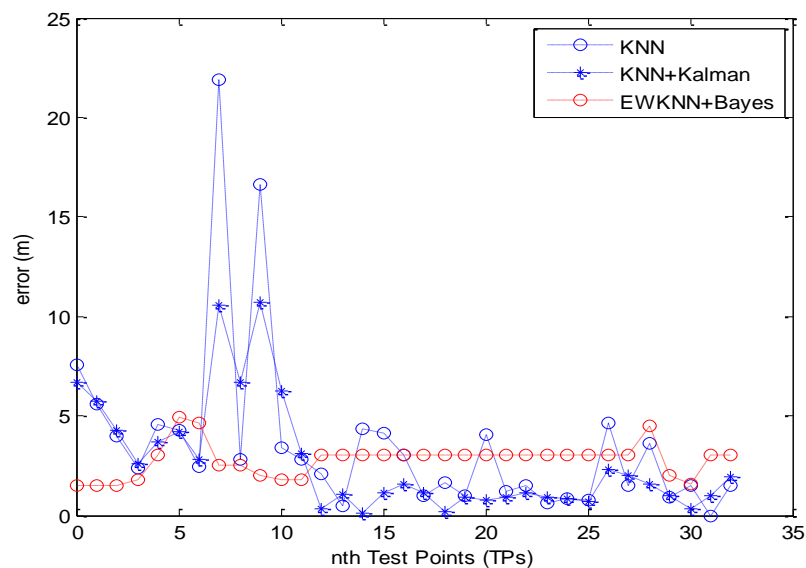


Figure 5.4: Comparison of EWKNN with Bayesian estimation, basic K-NN and K-NN with Kalman Filter, without QR calibration.

In Figure 5.4, it can be seen that errors start to increase dramatically from points 5 to 10 onwards. Therefore, it has been decided to do QR calibration at point 5, just before the errors surpass the 5-metre value. Figure 5.5 depicts the results for the same algorithms

with a QR calibration point. Positioning information on QR code immediately reduces the errors to zero and improves the accuracy from point 5 to point 8. Compared to a conventional K-NN algorithm, QR calibration only improves the point where the QR code is located, while at other TPs it only gives the same results.

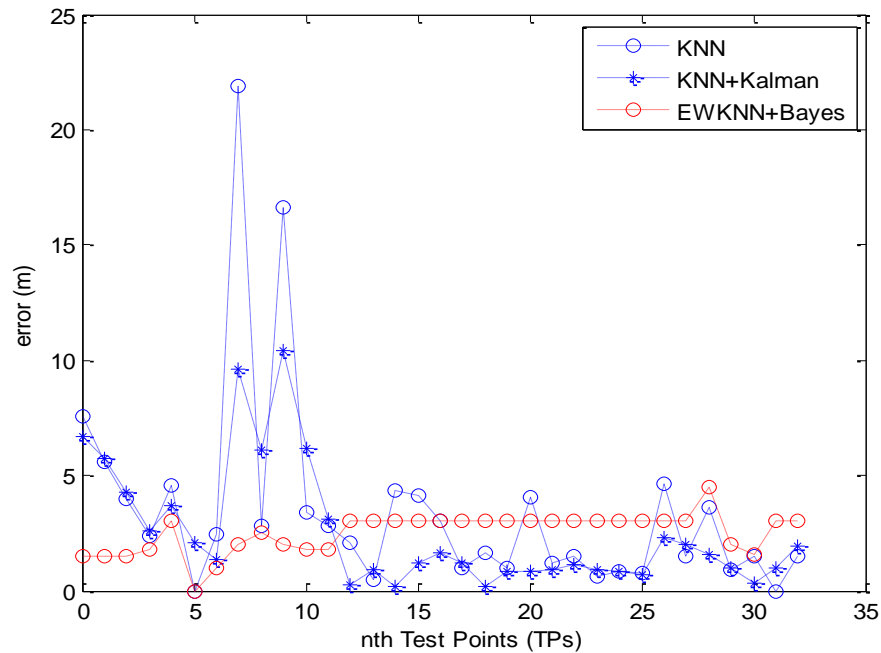


Figure 5.5: The effect of QR calibration (at point 5) on three different algorithms.

### 5.2.2.2 Point R to Point S – Broadcom

Figure 5.6 depicts the error distribution from point R to point S with a different Wi-Fi chipset. As can be seen, from TPs 1 to 20, there is good accuracy for all three algorithms. However, after point 20, location errors become apparent and shoot up at 30 metres for K-NN. A similar pattern applies for the other two algorithms, as errors rise dramatically after TP 20. Now it is known that the main region of error distribution

is beyond 5 metres. To prevent errors rising steeply, it was decided to do QR calibration in the region with high possible errors, as shown in Figure 5.7.

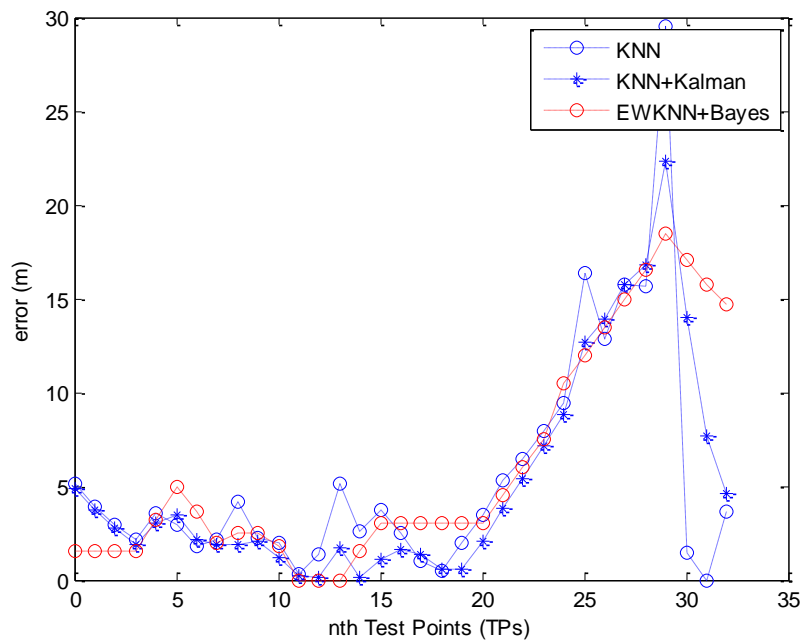


Figure 5.6: Comparison of EWKNN with Bayesian estimation, basic K-NN and K-NN with a Kalman filter, without QR calibration.

QR calibration at point 25 helps to bring all errors down to zero. Beyond that point, the K-NN and K-NN with a Kalman filter remain the same as before, but they go up drastically at 30 metres. However, a different effect on EWKNN+Bayes is observed when the error results go up drastically, where the increase in errors can be controlled and reaches a peak at 10 metres. Then, the errors fall gradually whenever the results for K-NN show a downward trend.

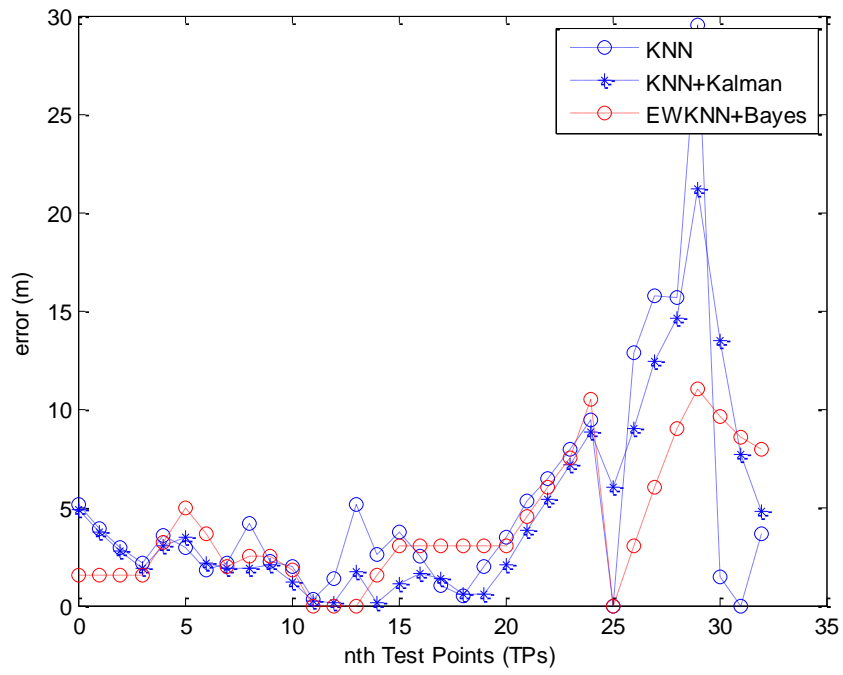


Figure 5.7: The effect of QR calibration (at point 25) on three different algorithms.

### 5.2.2.3 Point S to point R – Qualcomm Atheros

Figures 5.8 and 5.9 show the same trend in error distribution. The errors rise significantly from point 18 to point 25 and then plummet noticeably towards the last TPs. QR calibration at point 25 gives better results for EWKNN with Bayesian estimation compared to the other two algorithms.

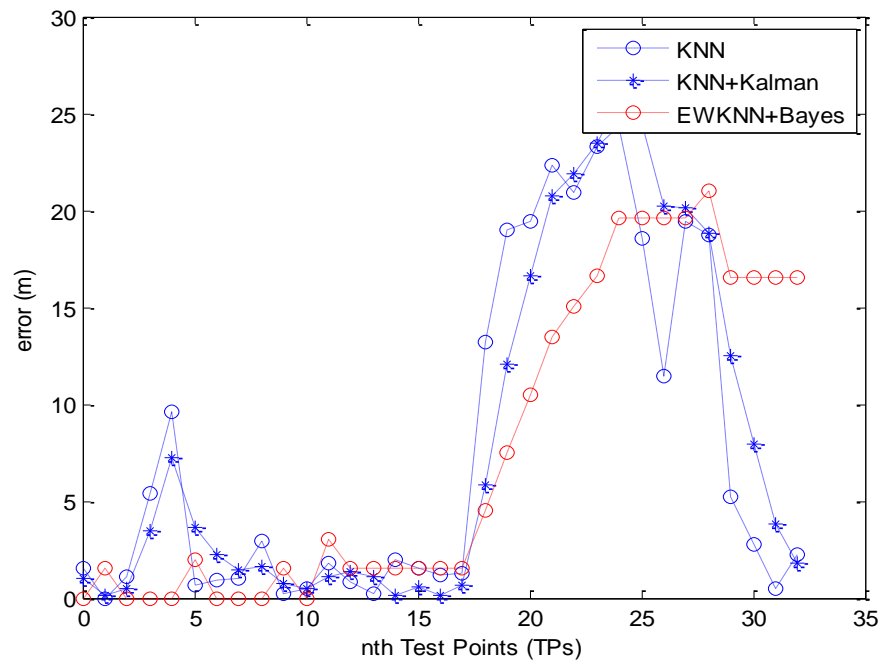


Figure 5.8: Comparison of EWKNN with Bayesian estimation, basic K-NN and K-NN with Kalman Filter, without QR calibration.

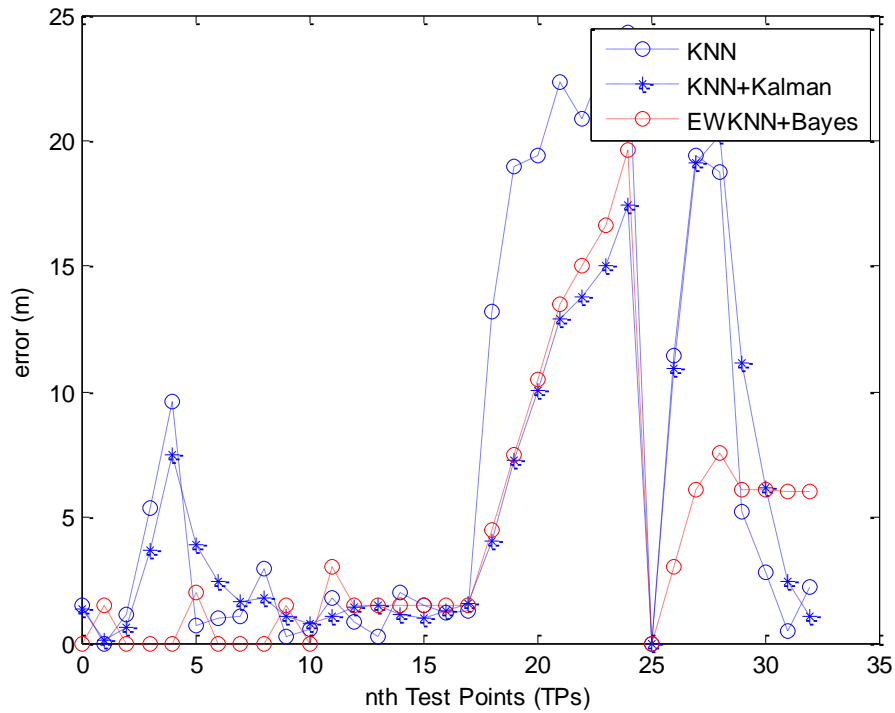


Figure 5.9: The effects of QR calibration (point 25) on three different algorithms.

#### 5.2.2.4 Point S to point R – Broadcom

Figure 5.10 and 5.11 show different patterns that have not been seen before. There is a region of significant error from point 3 to point 12 for K-NN. However, the output from the proposed algorithm shows consistent error results at 4 metres error in this region. When calibration point at TP 5 was scan as shown in Figure 5.10, the position was corrected at the actual position that has accuracy 100% till TP 16. This happens whenever just after calibration of the location error of basic deterministic shows the downward trend. The effect of the downward trend means the estimation of user position becomes near to the actual user position. Combined with EWKNN-Bayesian estimation, which utilises the region of the confinement area each time in

localisation, this gives high accuracy for user's position. The results show zero errors from TP 5 to TP 16, as shown in Figure 5.10.

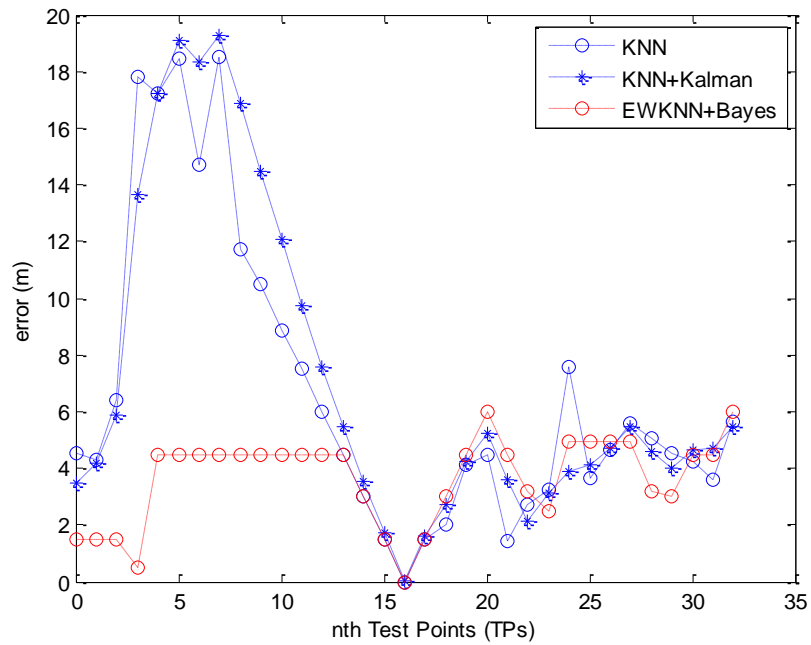


Figure 5.10: Comparison of EWKNN with Bayesian estimation, basic K-NN and K-NN with Kalman filter, without QR calibration.

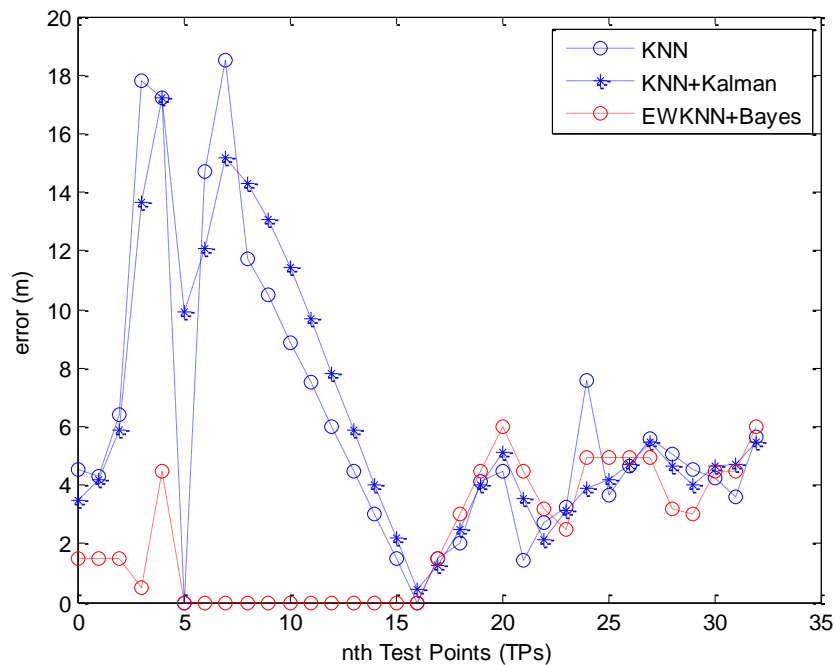


Figure 5.11: The effects of QR calibration (at point 5) on three different algorithms.

The results on previous graphs show that the location of QR calibration point is suggested to be in the region of the high location error. Based on TPs location, the point was traced on the layout map as show in Figure 5.12. By implementing this algorithm that was designed with calibration point, the calibration area has been identified instead of putting the QR code everywhere.

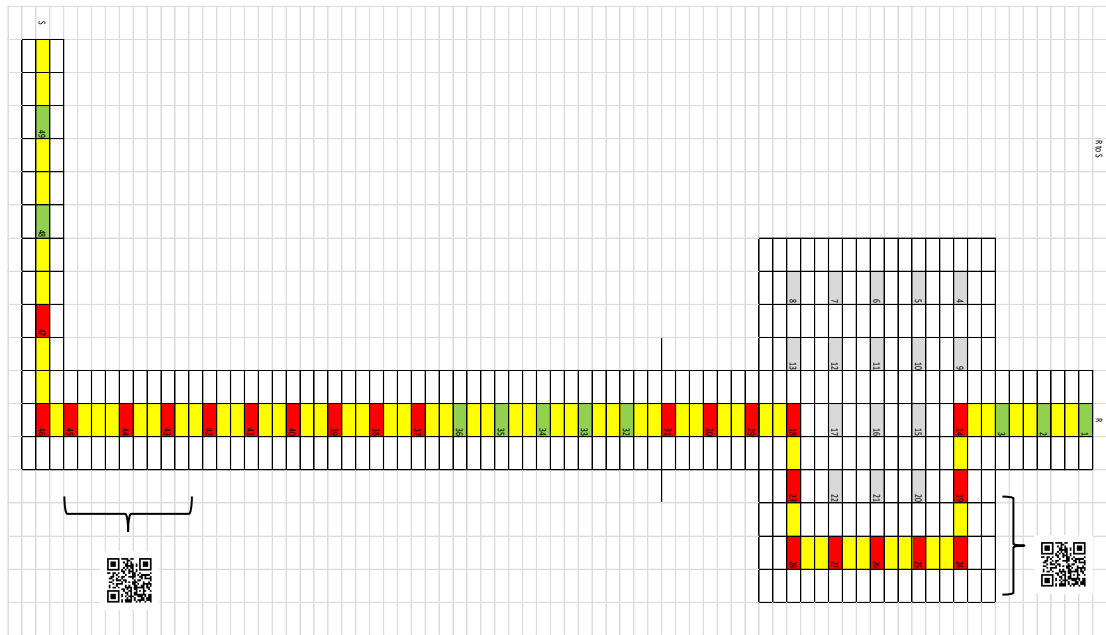


Figure 5.12: Area location of QR code calibration

### 5.3 Kalman Filter Modification on QR Calibration

The results for the previous algorithm in Section 5.2 do not take into account the presence of noise. As explained in the previous section, even though the new algorithm shows resistance to positioning uncertainty, location estimation could still change significantly between TPs due to RSSI uncertainty. To smooth out the results, a Kalman filter was applied to the previous algorithm.

#### 5.3.1 Algorithm Description

The Kalman filter algorithm has been explained in detail in Section 2.5. It consists of several steps including a prediction layer, an adaptive Kalman gain calculation and lastly an estimation layer. Figure 5.12 shows the process of implementing Kalman filter with QR calibration. In state  $k$ , the output from EWKNN and Bayesian estimation goes through the process of standard Kalman filter. At the beginning in state  $k$ , the early results are treated through the prediction layer, estimation layer, and Kalman gain between the layers is computed. The outputs of the estimation state and error covariance are passed to the next cycle state, which is  $k+1$ . Then, the standard process of using Kalman filter continues.

When a user scans QR code at a dedicated calibration point, information about that particular position is known. In this scenario, the results of  $x_k$  and  $P_k$  are not passed to the next cycle,  $k+2$  state. Here, measurement in this state which is the position information from QR calibration will be an estimation state and used in the next cycle state. So, the layer process of prediction, Kalman gain calculation and

estimation can be skipped. To make it simple, the error covariance value at this state is reset to the initial value just like the first state calculation of the Kalman filter.

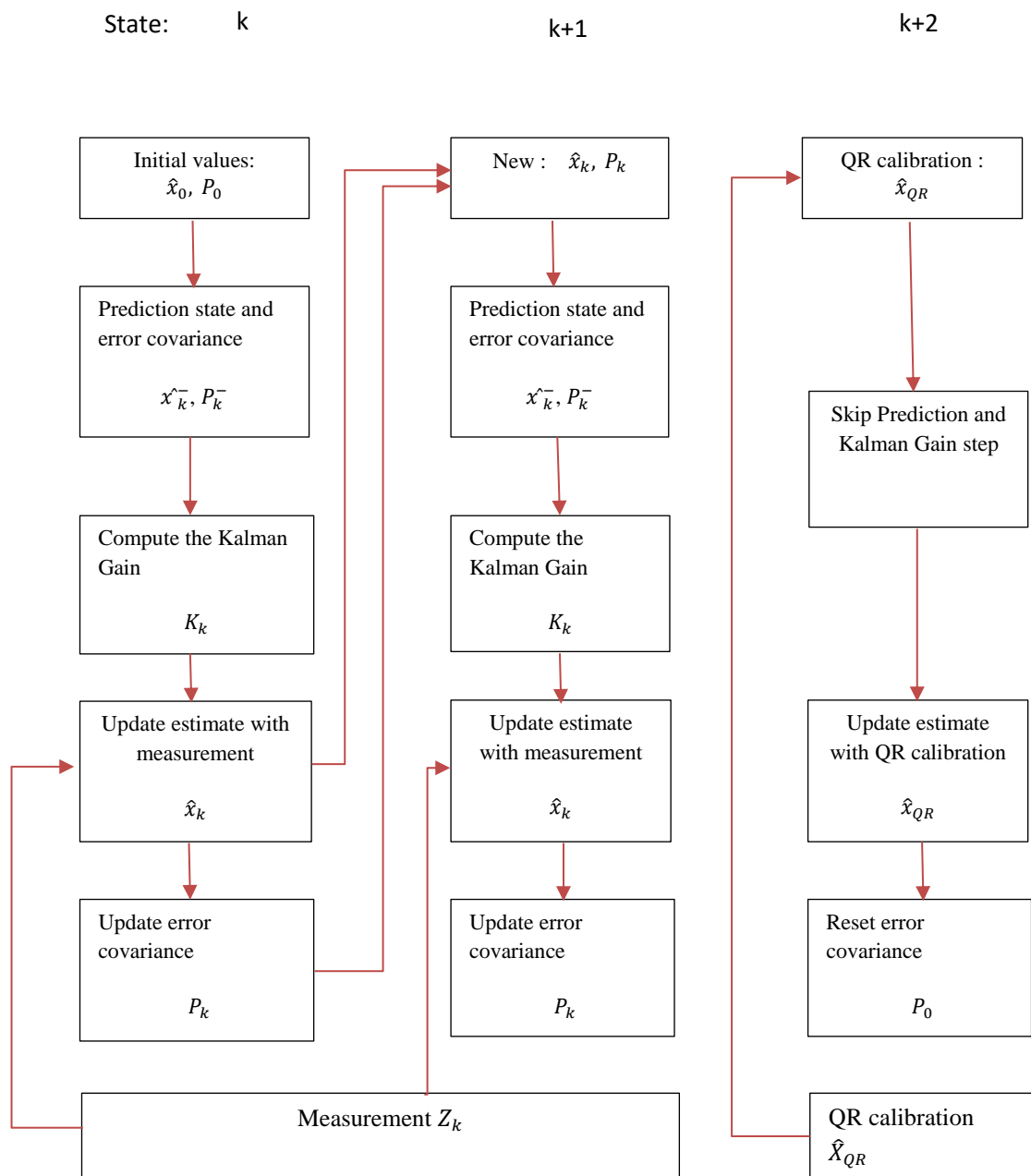


Figure 5.13: Kalman filter process with QR calibration.

If there is no QR calibration point in the next state, the steps will follow as in a normal Kalman filter process. The flow chart for the algorithm is shown in Figure 5.13 below.

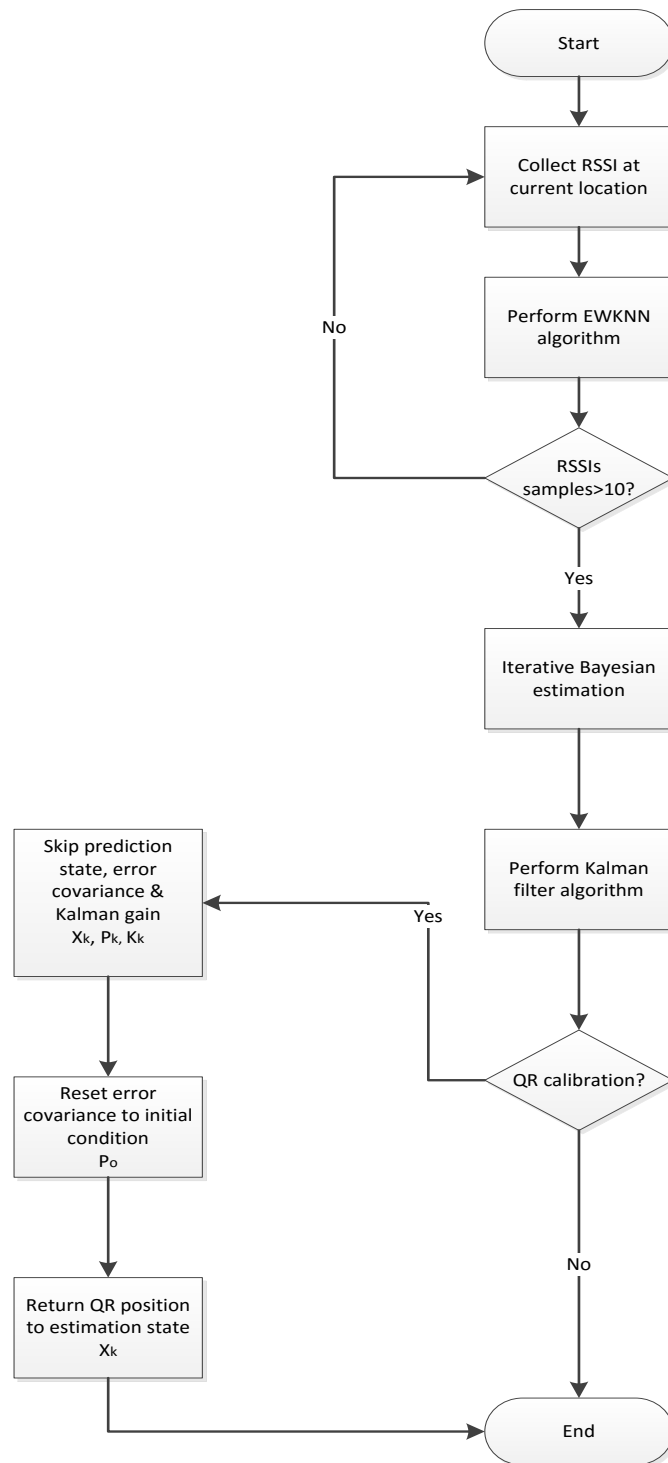


Figure 5.14: Flowchart for algorithm enhancement with QR calibration and Kalman filter.

## Algorithm

1. Get previous location
2. Sample RSSI
3. For each RSSI > 10
  - Estimate location based on EWK-NN
  - End
  - Return early location
4. Update prior state location and assign localisation region.
5. Update table of possible location based on localisation region.
6. Assign uniform probability on each possible location in localisation region.
7. Calculate likelihood of possible state location.
  - For each location based on EWK-NN
    - For each entry of location in prior table
      - Combine likelihood and prior
      - End
      - Get posterior location
    - End
  - Return location of highest probability from posterior location
8. If there is input from QR code, decode the QR code information
  - Get the position of QR code location
  - Skip prediction state
  - Skip Kalman gain
  - Set error covariance matrix to initial condition  $P_0$
  - Update the location from QR information
  - Update the table of possible location based on QR information

Else

Return position from normal stage of Kalman filter output

9. Repeat step 1 on next cycle

10. End

### **5.3.2 Results of Location Based Calibration (LBC) with Kalman Filter**

This section discusses the simulation results from integrating EWKNN with iterative Bayesian estimation and combined with Kalman filter utilising QR calibration algorithm. Simulation was done based on the previous algorithm with 25 RSSI samples for each TP. The results for this algorithm with a Kalman filter was compared to other algorithms such as basic K-NN or K-NN with a Kalman filter, and the EWKNN+Bayesian estimation algorithm itself. The results presented here are for two different directions, point S to point R and vice versa, and different Wi-Fi chipsets to evaluate the algorithm in various conditions.

#### ***5.3.2.1 Point R to point S – Qualcomm Atheros***

Figure 5.14 depicts the simulation results for four different type of algorithms, which are KNN, K-NN with Kalman filter implementation, EWKNN+Bayesian estimation, EWKNN+Bayesian estimation with Kalman filter algorithm implementation. All these results assume that calibration was done at TP 5. Both EWKNN + Bayesian estimation and EWKNN+Bayesian with Kalman filter show consistent errors of below 5 metres for all TPs when compared to K-NN and K-NN with a Kalman filter. From the graphs, the effect of the Kalman filter is to smoothen out

uncertainty in the results of location error. Most of the time, EWKNN+Bayesian with Kalman algorithm produced only slightly fewer errors compared to EWKNN + Bayesian estimation with QR calibration, except from point 14 to point 23. Between these points, the output of EWKNN + Bayesian estimation with QR calibration shows constant errors at 3 metres, so the Kalman filter process tried to slowly reach that point and make it a little bit above 3 meters in location error.

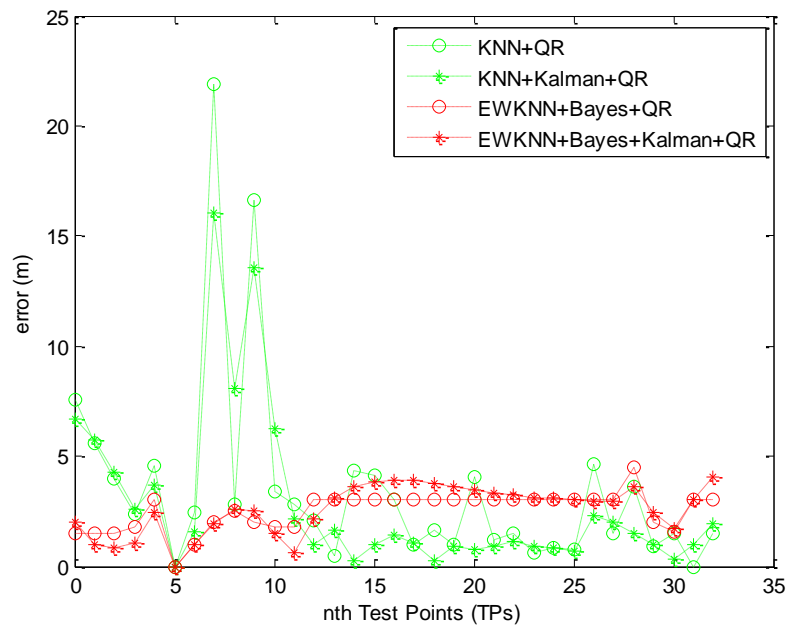


Figure 5.15: The effects of QR calibration (at point 5) on four different algorithms.

### 5.3.2.2 Point R to point S – Broadcom

Figure 5.16 shows the simulation results for the same algorithms as before but with a different Wi-Fi chipset. The error pattern is different from the previous algorithm as errors are concentrated at the end of the path when moving from point 22 to point 32. The results for EWKNN+Bayesian estimation and EWKNN+Bayesian estimation with a Kalman filter do not show significant differences in accuracy. After

calibration point TP 25, the output of EWKNN+Bayesian estimation with a Kalman filter is almost the same for location errors as the EWKNN+Bayesian estimation algorithm until point 29. This is because the effect of error covariance was reset to the initial value and so new Kalman gain just needed to be calculated again. The incremental errors form a constant rising gradient, the output of a Kalman filter, and the results are almost the same until a change in gradient at point 30, where the output of the EWKNN+Bayesian estimation algorithm shows a sharp drop. The Kalman filter tried to compensate for this drastic change and this makes the output remain slightly higher for error distribution after point 30.

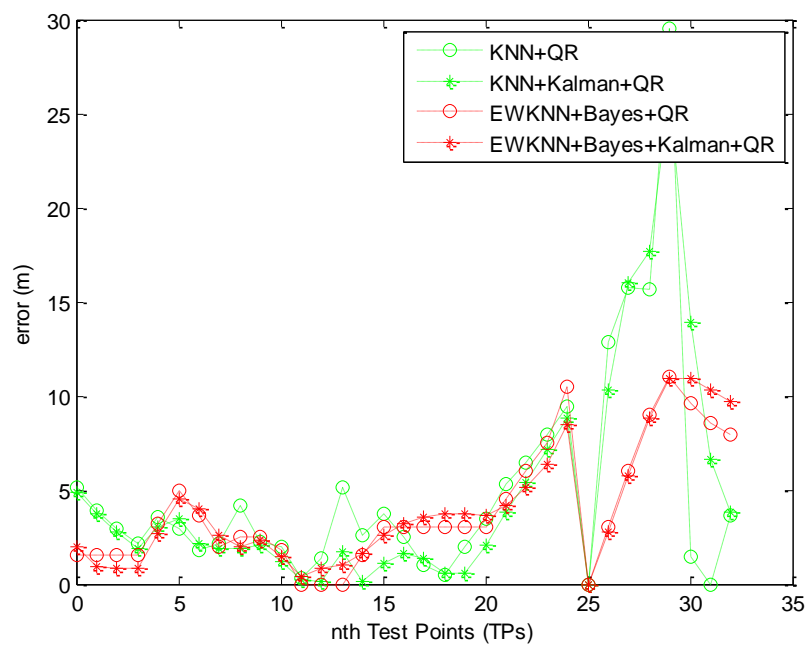


Figure 5.16: The effects of QR calibration (at point 25) on four different algorithms.

### 5.3.2.3 Point S to point R – Qualcomm Atheros

Figure 5.17 shows the results for a different type of algorithm on the Qualcomm chipset but with various directions. The errors start to exceed 5 metres from point 18 to point 29, which is basically the same location region as the results in Figure 5.16. The calibration point was at TP 25, and both EWKNN+Bayesian estimation and EWKNN+Bayesian estimation with Kalman filter implementation show better location accuracy compared to K-NN and K-NN with Kalman filter improvement. After the calibration point, the proposed algorithm shows gradual increment in location error due to the fact that the region is still high in location error where the basic K-NN error reaches above 20 metres. When the error of K-NN shows a decrement in location error, the result of the proposed algorithm shows some increment in positioning accuracy.

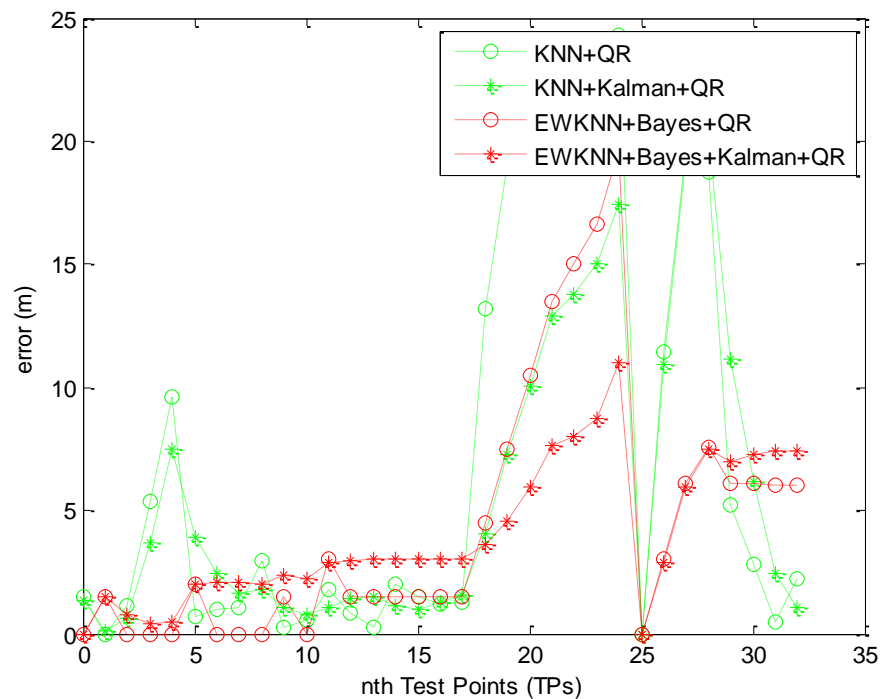


Figure 5.17: The effect of QR calibration (at point 25) on four different algorithms.

### 5.3.2.4 Point S to point R – Broadcom

Figure 5.18 shows a comparison of four different kinds of algorithms with the QR calibration point at TP 5. As discussed in Section 5.2.2.3, the output of EWKNN with Bayesian estimation utilising QR calibration gives accurate results after calibration point, up to twelve points ahead. The output of the algorithm with a Kalman filter is almost the same. However, at TP point 5 and from point 17 to point 20 the output through a Kalman filter shows slightly better accuracy. This is because the Kalman filter process tried to smooth up the output of the EWKNN+Bayesian estimation algorithm that has suddenly increased significantly.

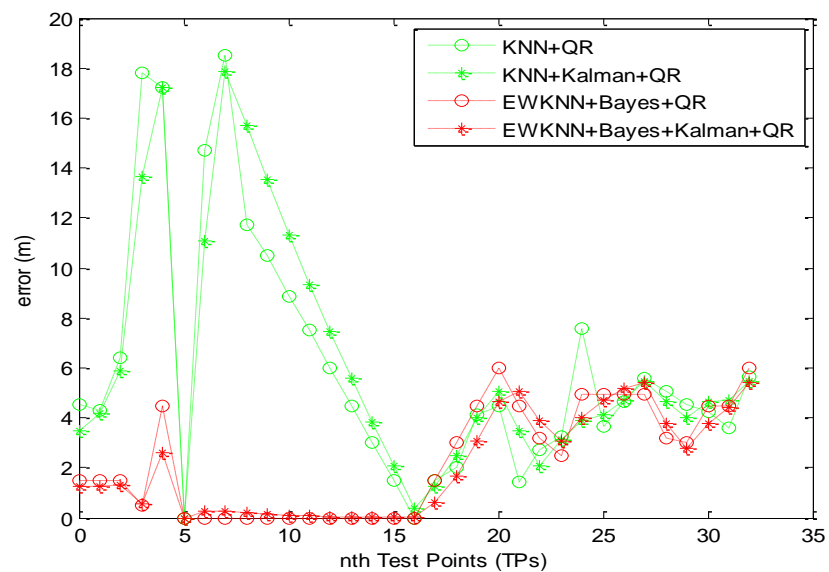


Figure 5.18: The effect of QR calibration (at point 5) on four different algorithms.

### 5.3.3 Overall Results

All results presented above for different directions of path movement and different Wi-Fi chipsets have been analysed. Comparisons have been made among the four different kinds of algorithms. The accumulated accuracy of all results presented in Chapter 4 has been calculated and is shown in Table 5.1 below.

Table 5.1: Accumulated accuracy comparison of algorithms with QR calibration.

	Calibration Point	Algorithms (Accumulated Accuracy)			
		1. K-NN + QR	2. K-NN + Kalman filter + QR Calibration	3. EWKNN + Bayesian estimation + QR	4. EWKNN + Bayesian estimation + Kalman Filter + QR
R to S Qualcomm	5	114.2202	93.5535	82.4895	85.4833
R to S Broadcom	25	163.4246	157.9958	129.5624	131.6238
S to R Qualcomm	25	235.5311	185.5368	145.0710	131.8887
S to R Broadcom	5	201.1544	205.8520	75.5223	69.5113

From this table, it can be seen that accumulated accuracy has been calculated for four different kinds of scenarios and four different types of algorithms after using calibration points. As observed, K-NN utilising QR calibration gives the worst results of all algorithms while K-NN+Kalman filter utilising QR calibration shows some improvement in overall accumulated accuracy. Two out of four scenarios give the best accumulated accuracy with the third algorithm, which is EWKNN+Bayesian estimation utilising QR calibration. The last algorithm, which is EWKNN+Bayesian estimation + a Kalman filter utilising QR calibration, has better accuracy in the second and last scenario with the direction from point S to point R on both Wi-Fi chipsets. The difference between the third and fourth algorithms in R to S direction is not much. As explained in previous results, the last algorithm did sometimes improve overall accuracy, but sometimes not. It has some advantages even though it does not give a significant improvement in accuracy. The implementation of a Kalman filter did work to prevent errors from soaring sharply. This could avoid the position of a user from being estimated not in one room but in another four or five rooms away at the end of the pathway. If the pattern of location error shows some gradual decrease, the fourth algorithm shows slight changes in the error gradient.

Figure 5.19 shows the CDFs performance comparison of location estimation errors for various algorithms based on all scenarios in Table 5.16. The K-NN combined with QR calibration gives location error of less than 5m for just 48% of the time. When K-NN plus Kalman filter includes the QR calibration point, this algorithms gives location error of less than 5m for 51% of the time. This shows that when QR calibration is implemented along the path with deterministic basic algorithm, the improvement is 3% when compared to the results in Figure 4.25. Implementation of integrated EWKNN, Bayesian estimation with localisation region, combined with QR calibration point along the path movement shows drastic improvement with location error of less

than 5m for 70% of the time. The same algorithm when combined with some modification of Kalman filter process during calibration, the implementation of QR calibration point along the path movement shows some promising improvement by another 8%. The result shows the best achievement with location error of less than 5m for 78% of the time.

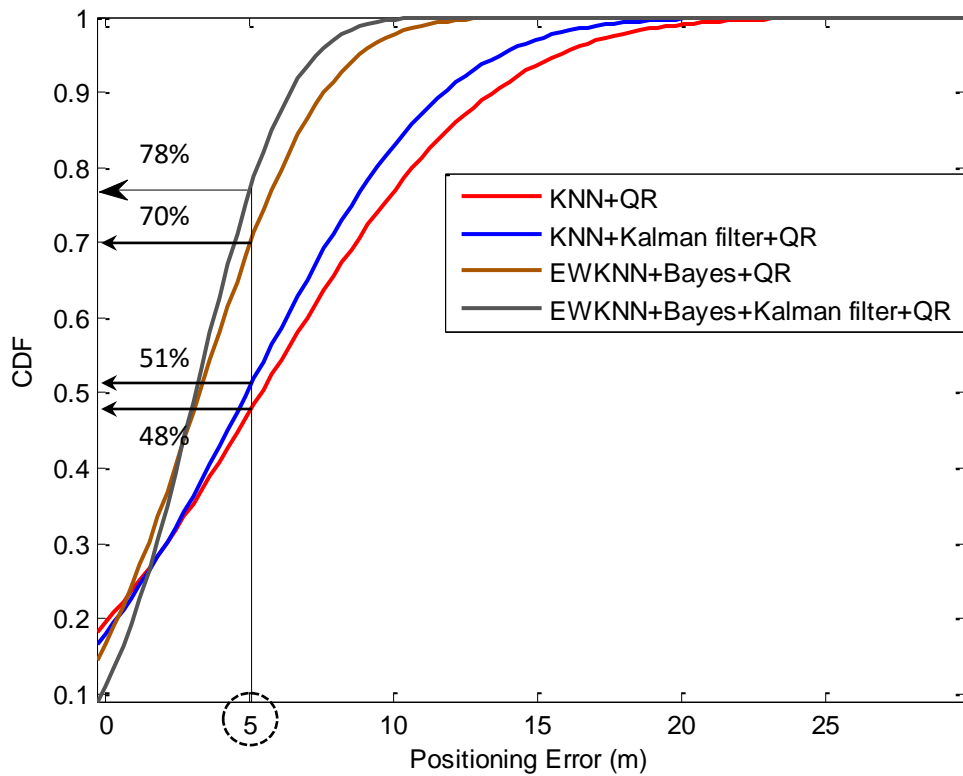


Figure 5.19: Performance positioning error comparison between the proposed algorithm and several location estimation algorithms with QR calibration.

## 5.4 Summary

The chapter discusses on the implementation of integrated positioning algorithm that was designed to suit the calibration point technique. The Wi-Fi fingerprinting algorithm was chosen as positioning method which is an integration of EWKNN and Bayesian estimation. This location based calibration algorithm that works on dynamic localisation region and QR calibration has shown significant improvement to the overall accumulated accuracy. The error distribution and accumulated accuracy help to identify which area should consider locating the QR calibration point instead of putting it everywhere. In the last part, it has been shown that modification on Kalman filter during calibration point helps to improve and smooth up the user location. The result of CDF improvement was up to 30% for location error of less than 5m compared to KNN with QR calibration. The used of QR code as dynamic coefficient to correct the user location is not considered here because out of scope. It is discussed in Future work section.

## CHAPTER 6: Conclusion

### 6.1 Summary

The problem of GPS signals not effectively reaching all parts of a building has prompted interest in developing alternative solutions for Indoor Location Based services. In this thesis, the integrated indoor positioning algorithm utilising QR calibration has been tested and investigated. A Wi-Fi fingerprinting technique was chosen as the main focus due to its availability and accuracy in various building geometries.

To test and evaluate the performance of the proposed algorithms, simulation tools are needed; Vistumbler and Matlab were chosen for this task. The measurement vectors of real RSSIs were sampled with Vistumbler before all data were transferred into Matlab to test the algorithms. Several scenarios were taken into account when collecting RSSI vectors and in algorithm development. These include the path direction of the user, the number of sampled RSSI vectors, and the Wi-Fi chipset manufacturer. The effects of each parameter were investigated and an algorithm which can cope to these factors was developed.

A deterministic technique was chosen in this research to get the right balance between accuracy and complexity. The integration of several layers of location estimation algorithm has been proposed. New algorithm has been developed with interconnection between EWKNN and iterative Bayesian estimation, and the location is smoothed with Kalman filter. The technique utilizes *dynamic localisation region* which selects the adjacent RP location before the algorithm estimates the user location.

This technique controls the location error from rising dramatically due to several factors like different Wi-Fi chipsets and movement directions.

To further improve the accumulated accuracy, QR calibration point has been introduced. The positioning error distribution and accumulated accuracy help to identify the critical area or zone to place the QR code instead of placing it everywhere. The earlier designed algorithms that can suit the QR calibration help to reduce and control location error. Comparisons have been made to other deterministic algorithms by analysing the accumulated accuracy and CDF graphs.

The performance of previously designed algorithm with QR calibration is enhanced with Kalman filter. Modification on Kalman filter at calibration point helps to improve the accumulated accuracy hence increasing the percentage of location error below 5m. This combined package of new algorithm did improve the CDF of location error of less than 5m with 30% compare to conventional deterministic technique with calibration point.

## **6.2 Future Work**

There is still plenty of room for research that can be done by extending the findings of this thesis. Research into indoor location-based services has caught the interest of many researchers and academicians recently. The following section outlines suggestions for future research work in this area.

### **6.2.1 Applying Other Distance Calculation with Statistical information**

In this thesis, Euclidean distance is used to find the nearest match between vectors in the on-line and off-line phases. Euclidean distance is based on an average vector data. To get more accurate results in distance calculations, it is suggested to analyse the statistical information of RSSI vectors. Here, several other distance calculations which utilise statistical information, such as Mahalanobis distance, Bhattacharya distance, and Spearman distance can be considered [99]. This extra information can be used as a dynamic coefficient on QR code to correct the user location in the case of inter-devices calibration.

### **6.2.2 Integration between Localisation Region and Clustering Techniques**

In our algorithm, the *localisation region* has been applied in implementing the Bayesian estimation to prevent error estimation from rising sharply. With certain building geometries, there is the possibility that errors become too large due to similar pattern combinations of RSSI readings in another place. To address this problem, another layer of clustering techniques can be added. Clustering can analyse and group similar patterns of RSSIs in the off-line phase. When RSSI vectors are measured in the on-line phase, the algorithms try their best to match to the data in the off-line phase. If the current location is known, it is possible to prevent a return distance match from jumping to another group of clusters. This will avoid errors from rising drastically between TPs. Several examples of clustering is affinity propagation clustering, hierarchical clustering, and evolving clustering [108], [111]. Combination with clustering techniques helps improve processing time in searching for adjacent RPs.

### **6.2.3 Integrated Fingerprint with Triangulation Technique Utilising QR**

#### **Calibration**

In this research, the work started with a deterministic K-NN algorithm to estimate user location. This was done by calculating the “distance” between vector samples in the on-line phase and a database during the off-line phase. The vector of the nearest distance is kept in the matrix for further calculations to determine user position. The granularity of the fingerprint technique is still the main influence in position estimation. The small scale of RPs will give more accurate results, but labour cost will be the biggest problem.

To reduce the effect of RPs’ granularity, it is suggested to add another layer-positioning algorithm by utilising distance previously calculated. If we know the coordinates of APs and the distances from APs to user, based on the deterministic matching algorithm used in this thesis, a trilateration method to estimate user position can be applied. By applying MMSE (minimum mean square error), the user position in three dimensions (3D) can be resolved. In a trilateration method, there must be at least three base stations, so the equation will be non-linear. Therefore, the algorithm with a non-linear Kalman filter can be integrated, which is called an Extended Kalman filter [112]. By utilising QR calibration points and information about different Wi-Fi chipsets, the output of the trilateration can be compared to the actual position and the parameter values can be adjusted to correct user position.

## References:

- [1] S. A. Zekavat and R. B. Michael, *Handbook of Position Location, Theory, Practice, and Advances*. John Wiley & Sons, Inc. Publication, IEEE Press, 2012.
- [2] F. Jaoa and F. Simone, *Mobile Positioning and Tracking, From Conventional to Cooperative Techniques*. John Wiley & Sons, Inc. Publication, 2010.
- [3] A. H. Sayed, A. Tarighat, and N. Khajehnouri, "Network-based wireless location: Challenges faced in developing techniques for accurate wireless location information," *IEEE Signal Process. Mag.*, vol. 22, no. 4, pp. 24–40, 2005.
- [4] A. Hossein and A. Salmasi, "A Hybrid TOA / AOA Hardware-Oriented Algorithm for Mobile Positioning," in *International Conference on Broadband and Wireless Computing, Communication and Applications*, 2011.
- [5] A. De Gante and M. Siller, "A Survey of Hybrid Schemes for Location Estimation in Wireless Sensor Networks," *Procedia Technol.*, vol. 7, pp. 377–383, Jan. 2013.
- [6] C. Li and Z. Weihua, "Hybrid TDOA/AOA mobile user location for wideband CDMA cellular systems," *IEEE Trans. Wirel. Commun.*, vol. 1, no. 3, pp. 439–447, 2002.
- [7] C. Wann, Y. Yeh, and C. Hsueh, "Hybrid TDOA/AOA Indoor Positioning and Tracking Using Extended Kalman Filters," *Proceeding IEEE 63rd Veh. Technol. Conf.*, vol. 0, no. c, pp. 1058–1062, 2006.
- [8] S. Gezici, "A Survey on Wireless Position Estimation," in *Wireless Personal Communications*, vol. 44, no. 3, 2007, pp. 263–282.
- [9] H. Liu and H. Darabi, "Survey of wireless indoor positioning techniques and systems," *IEEE Trans. Syst. Man, Cybernetics*, vol. 37, no. 6, pp. 1067–1080, 2007.
- [10] G. Sun, J. Chen, W. Guo, and K. J. R. Liu, "Signal Processing Techniques in Network-Aided Positioning," *IEEE Signal Process. Mag.*, no. July, pp. 12–23, 2005.
- [11] G. Deak, K. Curran, and J. Condell, "A survey of active and passive indoor localisation systems," *Comput. Commun.*, vol. 35, no. 16, pp. 1939–1954, Sep. 2012.
- [12] B. Li, J. Salter, A. Dempster, and C. Rizos, "Indoor positioning techniques based on wireless LAN," in *First IEEE International Conference on Wireless Broadband and Ultra Wideband Communications*, 2006, pp. 13–16.
- [13] E. Navarro, B. Peucker, M. Quan, A. C. Clark, and J. Jipson, "Wi-Fi Localization Using RSSI Fingerprinting," in *California Polytechnic State University 1 Grand Avenue, San Luis Obispo*, 2010, pp. 1–6.
- [14] D. Liu, B. Sheng, F. Hou, W. Rao, and H. Liu, "From Wireless Positioning to Mobile Positioning: An Overview of Recent Advances," *IEEE Syst. J.*, pp. 1–11, 2014.
- [15] I. Guvenc and C.-C. Chong, "A Survey on TOA Based Wireless Localization and NLOS Mitigation Techniques," *IEEE Commun. Surv. Tutorials*, vol. 11, no. 3, pp. 107–124, 2009.
- [16] J. Yoon, J. Kim, W. Lee, and D. Eom, "A TDoA-Based Localization Using Precise Time-Synchronization," in *Conference on Advanced Communication Technology (ICACT), 2012*

*14th International*, 2012, pp. 1266–1271.

- [17] A. A. M. Isa, M. M. Hud, M. H. Othman, M. S. M. Isa, M. S. I. M. Zin, N. Z. Haron, and A. S. Jaafar, "Analysis of WiMAX Positioning Using Received- Signal-Strength Method," vol. 5, no. 2, pp. 19–26, 2013.
- [18] J. Xu, M. Ma, and C. L. Law, "AOA Cooperative Position Localization," no. M1, pp. 1–5, 2008.
- [19] J. Prieto, S. Mazuelas, A. Bahillo, R. M. Lorenzo, P. Fern, and E. J. Abril, "NLOS Mitigation prior to Range Estimation Smoothing for Wireless Location Systems," in *IEEE ICC*, 2010.
- [20] X. Li, "An Iterative NLOS Mitigation Algorithm for Location Estimation in Sensor Networks," 2006.
- [21] M. A. Soleimani and A. R. Sharafat, "A Novel Geometric Approach for Mitigating NLOS Effects in Wireless Location Estimation," in *Conference on Electrical Engineering (ICEE), 2011 19th Iranian*, 2011.
- [22] Y. Qi, H. Kobayashi, and H. Suda, "On time-of-arrival positioning in a multipath environment," *IEEE Trans. Veh. Technol.*, vol. 55, no. 5, pp. 1516–1526, 2006.
- [23] S.-S. W. S.-S. Woo, H.-R. Y. H.-R. You, and J.-S. K. J.-S. Koh, "The NLOS mitigation technique for position location using IS-95CDMA networks," *Veh. Technol. Conf. Fall 2000. IEEE VTS Fall VTC2000. 52nd Veh. Technol. Conf. (Cat. No.00CH37152)*, vol. 6, pp. 2556–2560, 2000.
- [24] B. Thorbjornsen, N. M. White, a D. Brown, and J. S. Reeve, "Radio frequency (RF) time-of-flight ranging for wireless sensor networks," *Meas. Sci. Technol.*, vol. 21, no. 3, p. 35202, 2010.
- [25] T. Kagawa, H. Li, and R. Miura, "A UWB Navigation System Aided by Sensor-Based Autonomous Algorithm - Deployment and Experiment in Shopping Mall -," no. c, pp. 613–617, 2014.
- [26] F. Gong and X. Zhang, "Hybrid GPS / TDOA location algorithm in non-line-of- sight environment," in *International Conference on Computer Science and Network Technology Hybrid*, 2012, pp. 2033–2036.
- [27] P. D. Groves, *Principle of GNSS, Inertial, and Multisensor Integrated Navigation Systems*. ARTECH HOUSE INC, 2008.
- [28] S. Zhao, Y. Chen, H. Zhang, and J. A. Farrell, "Differential GPS aided Inertial Navigation : a Contemplative Realtime Approach," no. 2010, pp. 8959–8964, 2014.
- [29] B.-G. C. B.-G. Cho, J.-K. K. J.-K. Koo, B.-J. Y. B.-J. Yoon, and B.-W. K. B.-W. Kim, "The research of dead reckoning stabilization algorithm using different kinds of sensors," in *International Conference on Control Automation and Systems (ICCAS), 2010*, 2010, pp. 1089–1092.
- [30] H. Sternberg and M. Fessele, "Indoor navigation with Low-Cost Inertial Navigation Systems," *2009 6th Work. Positioning, Navig. Commun.*, vol. 2009, pp. 1–4, Mar. 2009.
- [31] R. Karlsson and F. Gustafsson, "The Future of Automotive Localization Algorithms," *IEEE Signal Processing Magazine*, no. March, 2017.

- [32] J. Ševčík, "Pedestrian Localization in Closed Environments," *IFIP Adv. Inf. Commun. Technol.*, vol. 413, pp. 679–687, 2013.
- [33] W. Xu, Wu, Daneshmand, Liu, "Mobility enhanced localization in outdoor environments," *Wirel. Commun. Mob. Comput.*, no. February 2015, pp. 421–430, 2015.
- [34] J. Bojja, M. Kirkko-Jaakkola, J. Collin, and J. Takala, "Indoor Localization Methods Using Dead Reckoning and 3D Map Matching," *J. Signal Process. Syst.*, pp. 1–12, 2013.
- [35] J. F. Vasconcelos, C. Silvestre, and P. Oliveira, "INS/GPS aided by frequency contents of vector observations with application to autonomous surface crafts," *IEEE J. Ocean. Eng.*, vol. 36, no. 2, pp. 347–363, 2011.
- [36] L. U. Smartphones, B. Zhou, S. Member, Q. Li, Q. Mao, and W. Tu, "Activity Sequence-Based Indoor Pedestrian," vol. 45, no. 5, pp. 1–13, 2014.
- [37] M. Kourogi and T. Kurata, "A method of pedestrian dead reckoning for smartphones using frequency domain analysis on patterns of acceleration and angular velocity," in *Record - IEEE PLANS, Position Location and Navigation Symposium*, 2014, pp. 164–168.
- [38] Q. Tian, Z. Salcic, K. I. K. Wang, and Y. Pan, "A Multi-Mode Dead Reckoning System for Pedestrian Tracking Using Smartphones," *IEEE Sens. J.*, vol. 16, no. 7, pp. 2079–2093, 2016.
- [39] B. Huang, G. Qi, X. Yang, L. Zhao, and H. Zou, "Exploiting cyclic features of walking for pedestrian dead reckoning with unconstrained smartphones," *Proc. 2016 ACM Int. Jt. Conf. Pervasive Ubiquitous Comput. - UbiComp '16*, pp. 374–385, 2016.
- [40] M. S. Eng, M. Kamil, P. M. Haid, T. Chobtrong, and D. E. Günes, "Hybrid Indoor and Outdoor Positioning with MEMS-based Inertial Motion Sensors," in *Sensoren und Messsysteme*, 2014, pp. 3–7.
- [41] F. Caron, E. Duflos, D. Pomorski, and P. Vanheeghe, "GPS/IMU data fusion using multisensor Kalman filtering: Introduction of contextual aspects," *Inf. Fusion*, vol. 7, no. 2, pp. 221–230, 2006.
- [42] S. Tanathong and I. Lee, "Using GPS/INS data to enhance image matching for real-time aerial triangulation," *Comput. Geosci.*, vol. 72, pp. 244–254, Nov. 2014.
- [43] X. Chen, C. Shen, W. Zhang, M. Tomizuka, and Y. Xu, "Novel hybrid of strong tracking Kalman filter and wavelet neural network for GPS / INS during GPS outages," *Measurement*, vol. 46, no. 10, pp. 3847–3854, 2013.
- [44] D. Bhatt, P. Aggarwal, V. Devabhaktuni, and P. Bhattacharya, "A novel hybrid fusion algorithm to bridge the period of GPS outages using low-cost INS," *Expert Syst. Appl.*, vol. 41, no. 5, pp. 2166–2173, 2014.
- [45] P. Kim, *Kalman Filter for Beginners, with MATLAB Examples*. A-JIN Publishing, 2011.
- [46] *Kalman Filtering : Theory and Practice Using MATLAB California State University at Fullerton*, vol. 5. 2001.
- [47] J. Cheng, L. Yang, Y. Li, and W. Zhang, "Seamless outdoor/indoor navigation with WIFI/GPS aided low cost Inertial Navigation System," *Phys. Commun.*, Jan. 2014.
- [48] I. P. Alonso, D. F. Llorca, M. Gavilán, S. Á. Pardo, M. Á. García-garrido, L. Vlacic, and M.

- Á. Sotelo, "Accurate Global Localization Using Visual Odometry and Digital Maps on Urban Environments," vol. 13, no. 4, pp. 1535–1545, 2012.
- [49] H. Guan, L. Li, and X. Jia, "Multi-Sensor Fusion Vehicle Positioning Based on Kalman Filter," no. 1, pp. 0–3, 2013.
- [50] A. M. Kamel, V. Renaudin, J. Nielsen, and G. Lachapelle, "INS Assisted Fuzzy Tracking Loop for GPS-Guided Missiles and Vehicular Applications," *Int. J. Navig. Obs.*, vol. 2013, pp. 1–17, 2013.
- [51] H. Hile and G. Borriello, "Positioning and Orientation in Indoor Environments Using Camera Phones," in *IEEE Computer Graphics and Applications*, 2008, pp. 1–13.
- [52] N. Rajakaruna, C. Rathnayake, K. Y. Chan, and I. Murray, "Image Deblurring for Navigation Systems of Vision Impaired People Using Sensor Fusion Data," in *IEEE Conference on Intelligent Sensors, Sensor Networks and Information Processing (ISSNIP)*, 2014, no. April, pp. 21–24.
- [53] R. Jafri, S. Abid, and A. Hamid, "Computer vision-based object recognition for the visually impaired in an indoors environment : a survey," *Springer*, 2013.
- [54] S. Kaushik, "Strength of Quick Response Barcodes and Design of Secure Data Sharing System," *Int. J. Adv. Comput. Sci. Appl.*, vol. 2, no. 11, pp. 28–32, 2011.
- [55] S. Alghamdi, R. Van Schyndel, and A. Alahmadi, "Indoor Navigational Aid Using Active RFID and QR-Code For sighted and Blind People," in *IEEE Eight International Conference on Intelligent Sensors, Sensor Networks and Information Processing*, 2013, pp. 18–22.
- [56] B. W. Stephen and K. B. Vijay, *Reed Solomon Codes and Their Applications*. New York: IEEE PRESS, 1999.
- [57] Denso Wave Incorporated, "<http://www.qrcode.com/en/>," 2017. .
- [58] R. Want, A. Hopper, V. Falcão, and J. Gibbons, "The active badge location system," *ACM Trans. Inf. Syst.*, vol. 10, no. 1, pp. 91–102, 1992.
- [59] A. Mike, S. Hodges, and A. Hopper, "Implementing a Sentient Computing System," *Location Aware Computing*, pp. 50–56, 2001.
- [60] P. D. Groves, L. Wang, D. Walter, H. Martin, K. Voutsis, and Z. Jiang, "The four key challenges of advanced multisensor navigation and positioning," *2014 IEEE/ION Position, Locat. Navig. Symp. - PLANS 2014*, no. May, pp. 773–792, May 2014.
- [61] P. D. Groves, "The PNT Future Trends in Integrated Navigation," *InsideGNSS*, pp. 44–49, 2013.
- [62] V. Moghtadaiee, S. Lim, and A. G. Dempster, "System-Level Considerations for Signal-of-Opportunity Positioning," pp. 1–7, 2010.
- [63] V. Moghtadaiee, A. G. Dempster, and S. Lim, "Indoor localization using FM radio signals: A fingerprinting approach," *2011 Int. Conf. Indoor Position. Indoor Navig.*, pp. 1–7, Sep. 2011.
- [64] A. K. M. Mahtab Hossain, Y. Jin, W. S. Soh, and H. N. Van, "SSD: A robust RF location fingerprint addressing mobile devices' heterogeneity," *IEEE Trans. Mob. Comput.*, vol. 12, no. 1, pp. 65–77, 2013.

- [65] S. Feldmann, "An indoor Bluetooth-based positioning system: concept, implementation and experimental evaluation," *Int. ...*, 2003.
- [66] A. Matic, A. Popleteev, V. Osmani, and O. Mayora-Ibarra, "FM radio for indoor localization with spontaneous recalibration," *Pervasive Mob. Comput.*, vol. 6, no. 6, pp. 642–656, Dec. 2010.
- [67] a. Mandal, C. V. Lopes, T. Givargis, a. Haghighat, R. Jurdak, and P. Baldi, "Beep: 3D indoor positioning using audible sound," *Second IEEE Consum. Commun. Netw. Conf. 2005. CCNC. 2005*, pp. 348–353, 2005.
- [68] D. Carrillo, V. Moreno, B. Úbeda, and A. Skarmeta, "MagicFinger: 3D Magnetic Fingerprints for Indoor Location," *Sensors*, vol. 15, no. 7, pp. 17168–17194, 2015.
- [69] M. H. Afzal, V. Renaudin, and G. Lachapelle, "Magnetic field based heading estimation for pedestrian navigation environments," in *2011 International Conference on Indoor Positioning and Indoor Navigation*, 2011, pp. 1–10.
- [70] C. Steiner, S. Member, and A. Wittneben, "Low Complexity Location Fingerprinting With Generalized UWB Energy Detection Receivers," vol. 58, no. 3, pp. 1756–1767, 2010.
- [71] F. Manzoor and K. Menzel, "Indoor Localisation for Complex Building Designs using Passive RFID Technology 2 . Proposed Algorithm," pp. 0–3, 2011.
- [72] A. Koch and A. Zell, "RFID-Enabled Location Fingerprinting Based on Similarity Models from Probabilistic Similarity Measures," in *IEEE International Conference on Robotics and Automation (ICRA)*, 2016, pp. 4557–4563.
- [73] R. Hansen, R. Wind, C. S. Jensen, and B. Thomsen, "Seamless Indoor/Outdoor Positioning Handover for Location-Based Services in Streamspin," *2009 Tenth Int. Conf. Mob. Data Manag. Syst. Serv. Middlew.*, pp. 267–272, 2009.
- [74] A. Abusara, M. S. Hassan, and M. H. Ismail, "Reduced-complexity fingerprinting in WLAN-based indoor positioning," *Telecommun. Syst.*, 2016.
- [75] J. Yim, S. Jeong, K. Gwon, and J. Joo, "Improvement of Kalman filters for WLAN based indoor tracking," *Expert Syst. Appl.*, vol. 37, no. 1, pp. 426–433, Jan. 2010.
- [76] P. Torteeka, X. I. U. Chundi, and Y. Dongkai, "Hybrid Technique for Indoor Positioning System based on Wi-Fi Received Signal Strength Indication."
- [77] T. Roos, P. Myllymäki, H. Tirri, P. Misikangas, and J. Sievänen, "A Probabilistic Approach to WLAN User Location Estimation," *Int. J. Wirel. Inf. Networks*, vol. 9, no. 3, pp. 155–164, 2002.
- [78] I. Lee, M. Kwak, and D. Han, "A Dynamic  $k$ -Nearest Neighbor Method for WLAN-Based Positioning Systems," *J. Comput. Inf. Syst.*, vol. 56, no. 4, pp. 295–300, 2016.
- [79] P. Torteeka and X. Chundi, "Indoor positioning based on Wi-Fi Fingerprint Technique using Fuzzy K-Nearest Neighbor," *Proc. 2014 11th Int. Bhurban Conf. Appl. Sci. Technol. Islam. Pakistan, 14th - 18th January, 2014*, pp. 461–465, 2014.
- [80] P. Bahl and V. N. Padmanabhan, "RADAR: an in-building RF-based user location and tracking system," in *Proceedings IEEE INFOCOM 2000. Conference on Computer Communications. Nineteenth Annual Joint Conference of the IEEE Computer and Communications Societies (Cat. No.00CH37064)*, 2000, vol. 2, no. c.

- [81] J. H. Anton, *Bayesian Estimation and Tracking: A Practical Guide*. John Wiley & Sons, Inc. Publication, 2012.
- [82] M. Bshara, U. Orguner, F. Gustafsson, and L. Van Biesen, "Fingerprinting localization in wireless networks based on received-signal-strength measurements: A case study on wimax networks," *IEEE Trans. Veh. Technol.*, vol. 59, no. 59, pp. 283–294, 2010.
- [83] L. Koski, T. Perälä, and R. Piché, "Indoor positioning using WLAN coverage area estimates," *2010 Int. Conf. Indoor Position. Indoor Navig. IPIN 2010 - Conf. Proc.*, no. September, pp. 15–17, 2010.
- [84] V. Honkavirta, T. Perälä, S. Ali-Löyty, and R. Piché, "A comparative survey of WLAN location fingerprinting methods," *Proc. - 6th Work. Positioning, Navig. Commun. WPNC 2009*, vol. 2009, pp. 243–251, 2009.
- [85] Y. Kim, H. Shin, and H. Cha, "Smartphone-based Wi-Fi pedestrian- tracking system tolerating the RSS variance problem," in *Proc. IEEE PerCom*, 2012, pp. 11–19.
- [86] Y. Jiang, "Hallway based automatic indoor floorplan construc- tion using room fingerprint," in *Proc. Pervasive UbiComp*, 2013, pp. 315–324.
- [87] N. Patwari, J. N. Ash, S. Kyperountas, A. O. Hero, R. Moses, and N. S. Correal, "Locating the Nodes: Cooperative Localization in Wireless Sensor Networks," *IEEE Signal Process. Mag.*, vol. 22, pp. 54–69, 2005.
- [88] D. Rodionov, K. Bushminkin, and G. Kolev, "A Cooperative Localization Technique for Tracking in Hospitals and Nursing Homes," *2013 IEEE Int. Conf. Healthc. Informatics*, pp. 471–475, Sep. 2013.
- [89] M. Werner, M. Kessel, and C. Marouane, "Indoor positioning using smartphone camera," in *International Conference on Indoor Positioning and Indoor Navigation*, 2011, pp. 1–6.
- [90] H. Lee, J. Kim, S. Lee, S. Lee, and T. Lee, "Vision-based absolute indoor point positioning in the hallway without image database," in *2013 IEEE International Conference on Consumer Electronics (ICCE)*, 2013, no. 3, pp. 284–285.
- [91] G. Lui, T. Gallagher, B. Li, A. G. Dempster, and C. Rizos, "Differences in RSSI readings made by different Wi-Fi chipsets: A limitation of WLAN localization," in *2011 International Conference on Localization and GNSS, ICL-GNSS 2011*, 2011, pp. 53–57.
- [92] F. Dong, Y. Chen, J. Liu, Q. Ning, and S. Piao, "A calibration-free localization solution for handling signal strength variance," in *Springer-Verlag*, 2009, pp. 79–90.
- [93] L.-H. Chen, E. H.-K. Wu, M.-H. Jin, and G.-H. Chen, "Intelligent Fusion of Wi-Fi and Inertial Sensor-Based Positioning Systems for Indoor Pedestrian Navigation," *IEEE Sens. J.*, vol. 14, no. 11, pp. 4034–4042, Nov. 2014.
- [94] "Vistumbler, A Wireless Network Scanner," 2015. [Online]. Available: <https://www.vistumbler.net/>.
- [95] Z. Farid, R. Nordin, W. Muhamad, A. Wan, and S. Z. Hasan, "Leveraging Existing WLAN Infrastructure for Wireless Indoor Positioning Based On Fingerprinting and Clustering Technique."
- [96] L. Jacob, D. Hutchinson, and J. Abawajy, "Wi-fi security : Wireless with confidence,"

*ASIC 2011 Proc. 4th Aust. Secur. Intell. Conf.*, pp. 88–96, 2011.

- [97] S. Gupta, B. S. Chaudhari, and B. Chakrabarty, "Vulnerable network analysis using war driving and security intelligence," *2016 Int. Conf. Inven. Comput. Technol.*, pp. 1–5, 2016.
- [98] F. Yu, M. Jiang, J. Liang, X. Qin, M. Hu, T. Peng, and X. Hu, "5 G WiFi Signal-Based Indoor Localization System Using Cluster k -Nearest Neighbor Algorithm," *Int. J. Distrib. Sens. Networks*, vol. 2014, 2014.
- [99] Y. Xie, Y. Wang, A. Nallanathan, and L. Wang, "An Improved K-Nearest-Neighbor Indoor Localization Method Based on Spearman Distance," *IEEE Signal Process. Lett.*, vol. 23, no. 3, pp. 351–355, 2016.
- [100] T. Jaffr, G. Pierre-Mickael, P. Stylianos, and E. Peytchev, "On the efficacy of WiFi indoor positioning in a practical setting," in *IEEE Symposium on Computers and Communications (ISCC), 2013*, 2013, pp. 699–704.
- [101] B. Li, a. G. Dempster, and Y. K. Tan, "Using two global positioning system satellites to improve wireless fidelity positioning accuracy in urban canyons," *IET Commun.*, vol. 5, no. 2, pp. 163–171, Jan. 2011.
- [102] S. Boonsriwai and A. Apavatjrut, "Indoor WIFI localization on mobile devices," *2013 10th Int. Conf. Electr. Eng. Comput. Telecommun. Inf. Technol. ECTI-CON 2013*, 2013.
- [103] H. Lin, Y. Zhang, M. Griss, and I. Landa, "Enhanced Indoor Locationing in a Congested Wi-Fi Environment," in *MRC-TR-2009*, 2009, no. March, pp. 1–16.
- [104] T. D. Le, H. M. Le, N. Q. T. Nguyen, D. Tran, and N. T. Nguyen, "Convert Wi-Fi signals for fingerprint localization algorithm," in *7th International Conference on Wireless Communications, Networking and Mobile Computing, WiCOM 2011*, 2011, pp. 0–4.
- [105] B. S. -, J. H. L. -, T. L. -, and H. S. K. -, "Enhanced Weighted K-Nearest Neighbor Algorithm for Indoor Wi-Fi Positioning Systems," *Int. J. Networked Comput. Adv. Inf. Manag.*, vol. 2, pp. 15–21, 2012.
- [106] J. Yim, J. Kim, G. Lee, and K. Shim, "Kalman filter vs. particle filter in improving K-NN indoor positioning," in *Lecture Notes in Computer Science (including subseries Lecture Notes in Artificial Intelligence and Lecture Notes in Bioinformatics)*, vol. 6882 LNAI, no. PART 2, 2011, pp. 203–213.
- [107] J. Yim, C. Park, J. Joo, and S. Jeong, "Extended Kalman Filter for wireless LAN based indoor positioning," *Decis. Support Syst.*, vol. 45, pp. 960–971, 2008.
- [108] Z. Tian, X. Tang, M. Zhou, and Z. Tan, "Fingerprint indoor positioning algorithm based on affinity propagation clustering," *EURASIP J. Wirel. Commun. Netw.*, vol. 2013, no. 1, p. 272, 2013.
- [109] F. Maly, P. K. B, and M. Jedlicka, "Room-Level Indoor Localization Based on Wi-Fi Signals," in *Springer International Publishing Switzerland*, 2016, pp. 209–218.
- [110] J. Ma, X. Li, X. Tao, and J. Lu, "Cluster filtered KNN: A WLAN-based indoor positioning scheme," *2008 IEEE Int. Symp. A World Wireless, Mob. Multimed. Networks, WoWMoM2008*, 2008.
- [111] L. Mengual, O. Marbán, and S. Eibe, "Clustering-based location in wireless networks,"

*Expert Syst. Appl.*, vol. 37, no. 9, pp. 6165–6175, Sep. 2010.

- [112] Z. A. Deng, Y. Hu, J. Yu, and Z. Na, “Extended Kalman filter for real time indoor localization by fusing WiFi and smartphone inertial sensors,” *Micromachines*, vol. 6, no. 4, pp. 523–543, 2015.